Delft University of Technology

Master Thesisproject
LM3901

Master Thesis

A step towards economically viable biodegradable rubber: improving medium chain length PHA production using medium chain fatty acids and mixed cultures

---

Author:
Lena Depaz (4540778)

In partial fulfillment of the MSc Life Science and Technology.

August 21, 2021

Composition committee:

Prof. dr. R. Kleerebezem,	Technische Universiteit Delft
Prof. dr. A. Wahl,	Technische Universiteit Delft
Prof. dr. D. Weissbrodt,	Technische Universiteit Delft

Abstract

Rubber is currently produced in either a biological way or a chemical way. The *Hevea brasilienis* is one of the only commercial rubber producing plants and is susceptible to various biological threats. On the other hand, the chemical production of rubber requires petrochemicals and does not yield rubber with all the desired properties. An alternative is therefore needed, which could be provided by micro-organisms. Medium chain length polyhydroxyalkanoate (mcl-PHA) is a form of polyhydroxyalkanoate (PHA) which has properties similar to the desired rubber properties. However, mcl-PHA is not as extensively studied as other forms of PHA, like polyhydroxybutyrate. The majority of the research has been focused on pure cultures with artificial substrates, both of which increase the cost of the production to economically unviable levels. This is especially the case since the biological and the chemical production are very cheap. To reduce the costs, a mixed culture could be used. By investigating which conditions lead to high mcl-PHA production with a mixed culture, a step can be taken towards an economically viable biodegradable rubber replacement.

To develop a culture which was able to produce mcl-PHA, an enrichment was first performed in a sequential batch reactor with a feast-famine regime to select for PHA producers. Additional selection pressures like substrate selection, pH, oxygen flow rate and time between carbon source addition and nitrogen source addition were imposed on the culture. After the culture reached pseudo-steady state, an accumulation was done.

The substrate was one of the most important selection pressures. Using octanoate as sole carbon and energy source, the microbial community was successfully enriched in a feast-famine regime with the capacity to produce mcl-PHA. The use of octanoate with a pH of 7 and no reduced oxygen flow resulted in mcl-PHA weight percentages of 26.62 wt% polyhydroxyoctanoate (PHO) and 5.15 wt% polyhydroxyhexanoate (PHH) during the cycle. This was raised to 30.44 wt% PHO and 9.54 wt% PHH during the accumulation. During the second enrichment, the carbon source and the oxygen flow of the first enrichment were maintained, but the pH was increased to 8. This led to an increase in mcl-PHA production, to 33.42 wt% PHO and 7.24 wt% PHH during the cycle and 44.21 wt% PHO and 9.24 wt% PHH during the accumulation. Two other condition changes were also investigated: lowered oxygen flow and uncoupling the system. For the lowered oxygen flow, the oxygen flow rate was reduced to 5% of the original flow rate and the increased pH of 8 of the second enrichment was kept. This resulted in similar values as the enrichment with only increased pH. It is therefore unclear whether the lowered oxygen flow rate could be attributed to the high mcl-PHA production or that the culture performed well despite the lowered oxygen flow. The uncoupled system was a system where the nitrogen source was added 2 hours after addition of the carbon source. Based on the oxygen profile and preliminary results of the enrichment, the culture mainly grew after the addition of carbon and little mcl-PHA was produced. However, scl-PHA production was quite high, with a total of 51 wt% PHB.

This work proves that high levels of mcl-PHA could be produced from mixed cultures. This is a good step towards producing an economically viable, biodegradable rubber replacement.

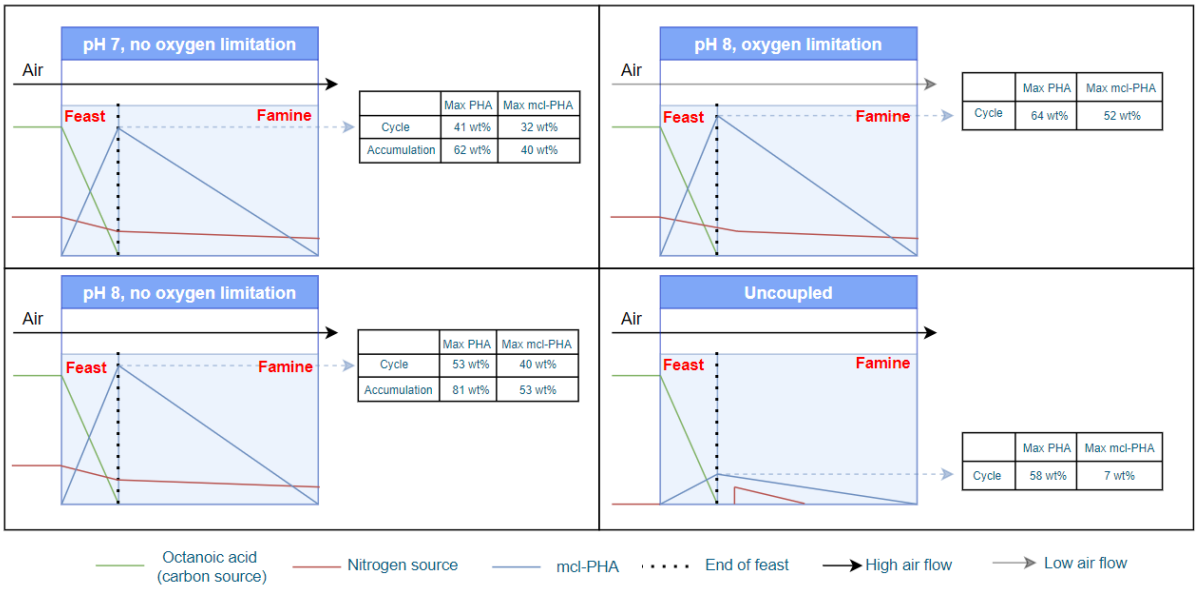

Figure 1: Visual summary of the evolution of the compounds during the various enrichments and the maximum obtained PHA content and mcl-PHA content during the cycle (analysis) and the accumulation of each enrichment.

Preface

This thesis was written during an unprecedented pandemic in modern times. As a result of that, various compromises for our safety and our health were made, including but not limited to the time we could spend in the lab. Luckily, I have never been forced to compromise on the amount of support and help I received during this project. Although at times the support could not be face to face, it was there nonetheless and for that I am extremely grateful. I would therefore like to start off this thesis by thanking my daily supervisor, Chris Vermeer, and my supervisor professor Robbert Kleerebezem. I would also like to thank my committee members, professor Aljosha Wahl and professor David Weissbrodt. This project would not have been as successful -or even possible- without their unwavering support. Next, I would like to thank Emily Van den Berg, who has been my lab partner and my colleague for the last 8 months. Without her, the work would have not been nearly as fun as it was. Furthermore, I would like to thank everyone in the Environmental Biotechnology department with a special mention for the lab safety coordinators.

Although the time that was available in the lab has been reduced, I am very proud to present the results that I have obtained. I do not think that their quality is diminished compared to other years in any way.

I enjoyed my time as a Master student in the Environmental Biotechnology department tremendously. The work we did was exciting and relevant and we were surrounded by people who also were passionate about their work and who were more than willing to talk about their research. I have gained valuable experience as a researcher and I am looking forward to more opportunities to use my gained knowledge.

Lena Depaz,
August 21, 2021

Contents

1 Introduction

Rubber is a polymer with various interesting applications owing to its intrinsic structure, its high molecular weight and ill-defined contributions of minor components, such as proteins, minerals, carbohydrates and lipids. The difficulty recreating these characteristics using petrochemical reactions results in a preference for the biological process of harvesting rubber from rubber trees instead of chemical reactions which rely on petroleum to produce rubber. Although 2500 rubber plants are known, the *Hevea brasilienis* is almost the only commercial rubber plant [1]. Various problems have therefore arisen which could threaten the rubber production.

- The first issue is that due to low genetic variety in the commercial use of *H. brasilienis*, the species is particularly susceptible to various bacterial and fungal diseases. No mutant of *H. brasilienis* has been identified and/or created which can withstand the most important biological threats to the species [1].
- Another issue is that the high labor intensity (up to 4-5 hours of continuous tapping on the tree trunks each day) and the high up front costs for the processing of the latex from the tree into rubber has caused farmers to opt for more economically favorable crops, like palm oil [2]. This increased land competition could potentially cause a shortage in the rubber supply. This is aggravated by the fact that *H. brasilienis* can only be cultivated in lowland rain forests or in warm areas with a lot of rainfall [3]. This diminishes the potential land area considerably.
- A final issue with natural rubber is the increase in latex allergies [4]. These allergic reactions are thought to be caused by plant-specific proteins of *H. brasilienis*, potentially in combination with endotoxins of bacteria which can grow during the processing during the latex processing.

Because of these issues, alternatives will be needed. No other rubber plants have proven as commercially viable and the chemical reactions have not yet been able to recreate the required characteristics of rubber so that it can be used for all applications rubber is used nowadays [5]. A potential solution could be rubber production from bacterial origin in the form of medium chain length poly-hydroxyalkanoates (mcl-PHA) due to its mechanically and chemically similar characteristics .

Poly-hydroxyalkanoates (PHA) are a type of biopolymer which can be made by various micro-organisms as a storage compound for carbon and energy. PHA accumulation is usually promoted when an essential nutrient for growth is present in limited amount in the cultivation medium, whereas carbon is in excess. Due to similar characteristics as plastic and rubber and due to its biodegradability, PHA has become an interesting alternative for these compounds [6]. There are two major categories of PHA compositions: short chain length PHA (scl-PHA) and medium chain length PHA (mcl-PHA). Scl-PHA have monomers between three and five carbons. They are produced by most micro-organisms to some degree and have properties similar to plastic. [6]. It has therefore already been extensively studied [7], [8], [6], [9]. Mcl-PHA have monomers between 6 and 14 carbons. Mcl-PHA is more similar to rubber in properties [10] but the ability to produce mcl-PHA is more limited in terms of which organism can do it. Due to the similarity in properties between rubber and mcl-PHA, mcl-PHA could be a biodegradable rubber replacement.

The applicability of mcl-PHA is currently limited due to its low rate of crystallizing and due to the narrow temperature range in which it displays similar properties to rubber [5]. Some research groups have attempted to overcome this challenge. One promising way is using cross-linking. When radiating mcl-PHA containing 15% unsaturated monomers, the mcl-PHA became cross-linked. This resulted in a more thermostable mcl-PHA with rubber properties over a larger temperature range. This greatly improves its applicability. On top of that, the biodegradability was maintained [10]. Other ways of cross-linking would be through the use of chemicals but this would be less environmentally friendly [11].

However, the applicability is not only limited by these aforementioned intrinsic qualities. At present, mcl-PHA is also limited by its cost of production due to the high costs of the substrate and the limited number of micro-organisms which can (exclusively) produce mcl-PHA [12]. To circumvent these problems, a waste stream could be used together with an enriched culture. This would lower the costs of the production significantly but introduces another set of challenges. For example, the applicability is lowered due to the fact that the composition of the PHA cannot be guaranteed if waste streams, which will undoubtedly have changing compositions, are used.

1.1 mcl-PHA cultivation

The composition of the mcl-PHA is depended on the substrate and the micro-organism. At present, mcl-PHA production seems to be almost exclusively done *Pseudomonas spp.*, *Comamomas spp.* and some *Bacillus spp.* [5]. The ability to produce mcl-PHA is due to the presence of a class II phaC gene. Class I, III and IV have not shown the ability to produce mcl-PHA [13]. The genus *Pseudomonas* can inhabit a wide variety of environments owing to their wide genomic variety [14]. While this could be an advantage for enriching for *Pseudomonas*, it can also present a disadvantage since it can mean that essentially all conditions could result in *Pseudomonas* but not necessarily in mcl-PHA producing *Pseudomonas*.

The production of mcl-PHA from pure cultures, which is mainly done by strains of *Pseudomonas spp.*, has already been studied in a lot of detail before both with synthetic substrates [15], [16] [17], [18] as with non-synthetic substrates like wastewater [19], [20], [21]. Like scl-PHA, mcl-PHA production is depended on the conditions, the organism and the substrate used. Some conditions, organisms and substrates have already been studied and proven suitable for mcl-PHA production. Suitable substrates for mcl-PHA include alkanoic acids, sugars, and sometimes other simple carbon sources depending on which pathways are available to the organism under the used conditions [22].

Caprylic acid, a C8 alkanoic acid also known as octanoic acid, is an alkanoic acid which has been shown in literature to be a suitable substrate for potential mcl-PHA producers [23], [16], [24]. This would be advantageous since mixtures of carpyolate acid and caprylic acid are less expensive than other typically used synthetic substrates, like nonanoic acid and decanoic acid [23]. However, the reduction in price would still not be sufficient for an economically viable process. Therefore, caprylic acid as a component of a wastestream was also investigated. Although caprylic acid does not occur often during a regular fermentation process, it can become a big part of the waste stream if chain elongation occurs during the fermentation due to the presence of ethanol [25], [6]. If caprylic acid is a big part of the waste stream, the price of mcl-PHA production could be lowered significantly. It is therefore an interesting substrate for the production of mcl-PHA and will be used for that reason during the experiments. However, since octanoic acid is not a significant portion of waste streams if there are no chain elongators, hexanoic acid was also investigated as a potential substrate since hexanoic acid is often present in more significant amounts after fermentation of waste streams [26], [27]. Hexanoic acid is in theory capable of producing mcl-PHA but in practice seems to produce more often scl-PHA [28]. For that reason, octanoic acid is better suited as a selection pressure during the enrichment but hexanoic acid could be an interesting substrate for the accumulation of mcl-PHA after the enrichment.

Various reactor conditions and reactor regimes have also been tested using pure cultures. For the reactor regimes, fed-batch has been the most used in literature [29]. Fed-batch regimes are generally stable, well-reproducible and can be easily adjusted in terms of feeding required, like nitrogen limitation. This has made them attractive for both pilot and industrial scale productions of PHA. Batch reactors do not yield high biomass production when nitrogen limitation is applied and completely functioning continuous reactors for mcl-PHA production have not yet been achieved on a scale larger than lab scale [30], [29]. A fed-batch reactor will therefore be used in this experiment to produce the mcl-PHA. The variety in physiology in the Pseudomonas species has allowed for many different conditions in the bioreactor: the temperature range in which the subspecies can grow is large and the presence of *Pseudomonas spp.* in many different environments is an attest to its variety in metabolisms [31], [32].

The production of mcl-PHA from mixed cultures is a more recent interest in the scientific community due to the costs associated with pure cultures with synthetic substrates. However, the recency of the interest does not mean that there are no proven methods to produce mcl-PHA using mixed cultures. In general, the culture is first enriched for mcl-PHA producers using sequential batch reactors (SBR) with a feed-famine regime and then mcl-PHA is produced in a fed-batch [33], [23], [12], [34] [35]. The SBR with feed-famine regime gives an advantage to PHA producers since they can in theory absorb the nutrients more quickly and will not die during an extended famine phase. The SBR cycle in general consists therefore of a feeding phase, a reaction phase during which feast and famine occur, and an effluent withdrawal phase. The cycle times range from 8 hours to 24 hours.

1.2 Selective advantages of mcl-PHA production over scl-PHA production for bacteria

The exclusiveness of mcl-PHA production compared to scl-PHA production begs the question what the advantages are of mcl-PHA production over scl-PHA production. This question has not been solved yet at the time

of writing this report, so some speculation about the potential reasons for preferring mcl-PHA over scl-PHA will be presented.

Redox balance during oxygen limitation The first potential reason is based on the metabolic pathways available to the micro-organisms. PHA production can be done using three different pathways, as seen in Figure 2.

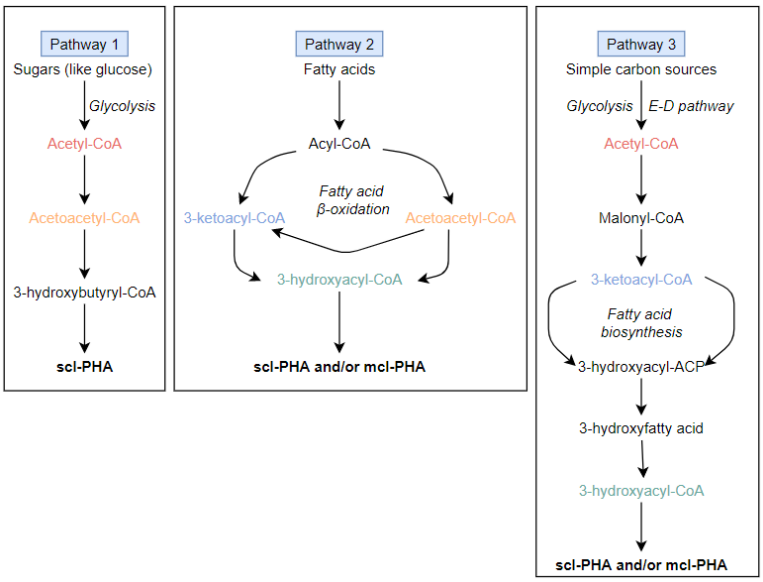

Figure 2: Simplified portrayal of the pathways to produce PHA, based on [22]. All three pathways can make scl-PHA and pathway 2 and 3 can mcl-PHA. Whether scl-PHA or mcl-PHA is made in pathways 2 and 3 depends on which substrate is available. The names in the same color are intermediates which are present in multiple pathways. The terms in italics are the pathways involved in the reaction(s).

The first pathway, which has sugars as its substrate and relies on glycolysis, is predominantly present in scl-PHA producing organisms. The second pathway, which uses fatty acids as its substrate and relies on fatty acid β-oxidation, is present in mcl-PHA producing organisms but can also produce scl-PHA depending on the length of the fatty acid. The third pathway, which uses simple carbon sources and relies on glycosysis, the Enthner-Doudoroff pathway and fatty acid de novo biosynthesis, is present in mcl-PHA producing organisms but can also produce scl-PHA.

The production of PHA is linked to the central carbon metabolism since it can be used as a carbon source during starvation. Furthermore, it also has an important role as a sink for reducing equivalents [22]. The production of PHA is therefore controlled by the redox state of the cell and the intracellular levels of reducing equivalents like NADH, NADPH and acetyl-CoA. High ratio's of [NADH]/[NAD] and high levels of [3-hydroxyacyl-CoA]/[CoA] lead to high production of PHA. This could provide an indication as to why mcl-PHA could be preferred: during periods of limited oxygen availabilty, mcl-PHA production from intermediates of the β-oxidation pathway like fatty acids requires only one oxidation step since they are highly reduced. This can be visualised by looking at Figure 3. Appendix A.3 also shows the full reaction steps of each process. During this step, the acyl-CoA monomers are oxidized to enoyl-CoA monomers using FAD as the electron acceptor. The storage of these monomers as mcl-PHA generate fewer reduced electron carriers compared to being further oxidized to a fatty acyl-CoA which is shortened by two carbons and potentially later stored as scl-PHA [36]. These reduced electron carriers, namely NADH and NADPH, can therefore not accumulate any further if mcl-PHA are made instead of scl-PHA. scl-PHA production in this case would lead to a greater redox imbalance.

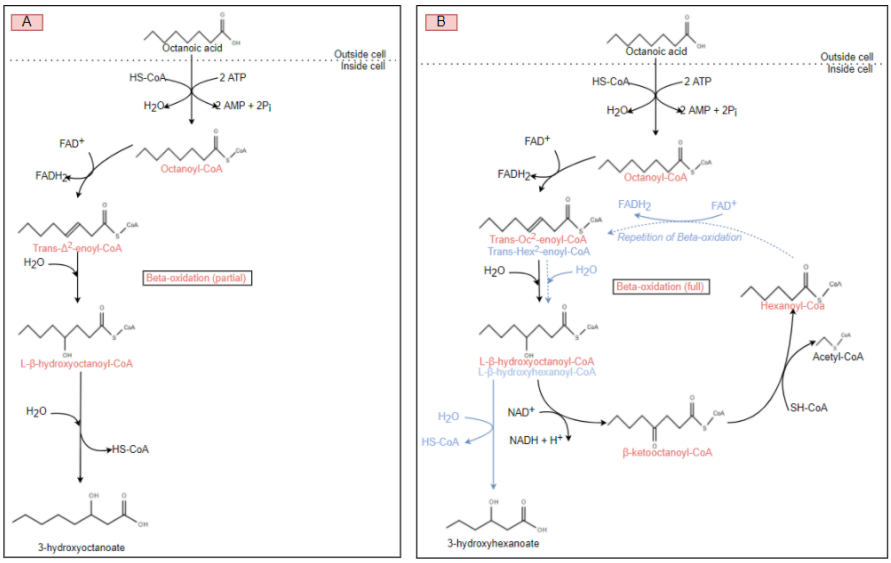

Figure 3: Full and partial β-oxidation of the fatty acid octanoic acid. The names in red indicate that the molecule is a precursor of a first β-oxidation cycle. The names indicated in blue show that the molecules is a precursor of a second β-oxidation cycle. A. The partial β-oxidation of octanoic acid yields 3-hydroxyoctanoate. B. The full β-oxidation of octanoic acid can yield 3-hydroxyhexanoate. The blue arrows indicate the partial completion of a second β-oxidation cyclus to yield a PHA molecule.

Electron balance during oxygen or nitrogen limitation Similar to the first reason, the preference of mcl-PHA over scl-PHA could be to maintain metabolic balance during nutrient or electron acceptor limitations. The production of mcl-PHA could be a mechanism for storing electrons to maintain a balanced redox state during oxygen limitation since the completion of the β-oxidation pathway requires NAD^+ and the subsequent oxidation of acetyl-CoA, a product of the β-oxidation pathway, generates an additional 3 NADH and 1 $FADH_2$ [36]. The completion of the β-oxidation pathway, which would result in the production of scl-PHA, would thus result in a redox imbalance in which a surplus of electrons are released. Therefore, an incomplete β-oxidation pathway which would yield mcl-PHA could be preferred.

The surplus of electrons which is released when producing scl-PHA is in times of abundant nutrients and electron carriers/donors not an issue, since they can be channeled towards the production of biomass if a nitrogen source is present [37]. Therefore, the production of mcl-PHA could be favored over scl-PHA if the nitrogen source is supplied after the carbon source has been depleted since the production of mcl-PHA would not result in an electron imbalance.

The balance in the electron balance and the redox balance during oxygen limitation and nitrogen limitation could give organisms producing mcl-PHA an ecological advantage since they can theoretically withstand these conditions better than scl-PHA producers or non-PHA producers and therefore grow better.

1.3 Focus of this research

Research question The first focus of this research will be on the production of mcl-PHA from less expensive substrates, like C8 fatty acids and waste water streams. A second focus will be on improving the amount of mcl-PHA by adjusting the conditions of the sequential batch reactor and the fed-batch reactor. The research question is therefore:

"Which bioreactor conditions select for a microbial community with the highest mcl-PHA production capacity when using octanoic acid as a substrate?"

General set-up The enrichment for mcl-PHA producers will combine knowledge from established pure cultures and mixed cultures which produce mcl-PHA. First, an SBR with a feed-famine regime will be run to enrich for mcl-PHA producing organisms. After reaching a semi-steady state in the SBR based on the length of the feast phase, the biomass in the bioreactor will be used to inoculate a fed-batch reactor with nitrogen limitation. The enriched culture should produce mcl-PHA during this process. The scheme for the whole process can be seen in Figure 4.

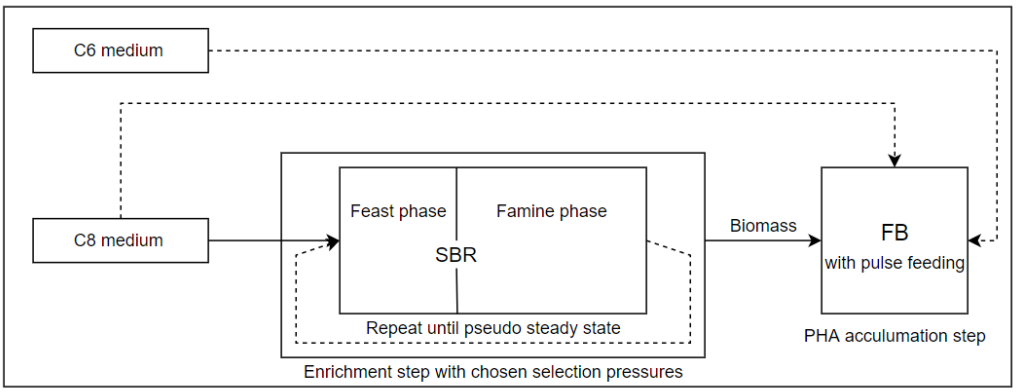

Figure 4: General overview of the mcl-PHA producing process. The enrichment is done by a sequential batch reactor (SBR) with octanoic acid (C8 medium) as substrate. The SBR is run until a pseudo steady state is achieved. The biomass from this final cycle of the SBR is used for an accumulation with pulse feeding. For the accumulation with the fed-batch regime (FB) either octanoic acid (C8 medium) or hexanoic acid (C6) medium was used.

Potential ways to select for mcl-PHA producers As mentioned before, the production of mcl-PHA can be favored over the production of scl-PHA based under certain conditions. These conditions could therefore prove to be valuable selection pressures and will therefore be tested in this report:

- Micro-aerophilic conditions
- Uncoupled nitrogen source from carbon source

2 Materials and methods

2.1 Sequential batch reactor for enrichments

2.1.1 Reactor set-up

The enrichment was based on the enrichment performed by Larissa Bons [**?**]. For the enrichment, a 1.5L sequential batch reactor was operated with 1.4L working volume (Applikon Biotechnology, The Netherlands). The bioreactor was equipped with a six-bladed stirrer to ensure ideal mixing. The bioreactor was controlled by a hardware abstraction layer (HAL; TU Delft, the Netherlands) which was in turn controlled by a PC with a custom scheduling software (D2I; TU Delft, the Netherlands). The D21 was a central controller for the pH, the stirrer, the airflow and the pumps for the nutrients, water, effluent removal. The D21 was also used for measuring the pH, the DO, the temperature, the pH adjustments, the composition of the in- and off-gas and the balances of the water and the feed. The air flow rate was regulated by a mass flow controller (MX4/4, DASGIP , Eppendorf, Germany). The temperature in the reactor was regulated to 30° C ±1. The stirrer (269872, Maxon Motor, Switzerland) was set to a stirring speed of 800 rpm (TC4SC4, DASGIP, Eppendorf, Germany). The pH of the reactor was controlled by the addition of 1M HCl and 1M NaOH using an integrated revolution counter (MP8, DASGIP, Eppendorf, Germany).

2.1.2 Inoculum and substrate

The inoculum was aerobic activated sludge collected from a wastewater treatment plant (AWZI Harnaschpolder Delfluent, The Netherlands). The nutrient medium was based on the medium used by Johnson et al. [35] and consisted of 67.5 mM NH_4Cl, 24.9 mM KH_2PO_4, 5.55 mM $MgSO_4.7H_2O$, 7.2 mM KCl 15 mL/L trace elements solution and 100 mg/L allyl thiourea. This last one is added to prevent nitrification since it targets the active site of the ammonium monooxygenase action, thereby inhibiting it [38]. The trace metal solution was prepared according to Vishniac and Sander [39] and consisted of 50 grams of $C_{10}H_{16}N_2O_8$, 22.0 grams of $ZnSO_4.7H_2O$, 5.54 grams of $CaCl_2$, 5.06 grams of $MnCl_2.7H_2O$, 4.99 grams of $FeSO_4.7H_2O$, 1.10 grams of $(NH_4)_6Mo_7O_{24}.4H_2O$, 1.57 grams of $CuSO_4.5H_2O$, 1.61 grams of $CoCl_2.6H_2O$ and 1000 mL of H_2O. The trace metal solution was adjusted to pH 6.0 with KOH. The completed nutrient medium solution was adjusted to pH 5.7 to avoid precipitation of the phosphate. The carbon source was prepared separately and consisted of 4.75 mM $C_8H_{15}NaO_2$. The pH of the carbon medium was adjusted to pH 7.8 to avoid protonation of the octanoic acid, which would cause it to precipitate. For the uncoupled system, the carbon medium was combined with the nutrient medium with the exception of the nitrogen source, which was prepared separately. All compounds retained their original concentration in the medium. The amount of nitrogen during the uncoupled enrichment was regulated by adding less of the nitrogen source.

2.1.3 Regime

After one day of acclimation, the reactor was operated as a non-sterile SBR. The acclimation day consisted of filling the reactor with 1160 mL of water, 35.0 grams of 20 times concentrated nutrient medium and 35.0 grams of 20 times concentrated carbon medium and inoculating the reactor. No other pulses of nutrient medium and/or carbon medium were provided during the acclimation day. After the acclimation day, the contents of the SBR were subjected to a feast-regime with a 24 minute filling phase, a 690 minute reaction phase, and a 6 minute biomass removal phase for a total cycle time of 12 hours. During the filling phase, 610 grams of water, 35.0 grams of 20 times concentrated nutrient medium and 35.0 grams of 20 times concentrated carbon medium are added. During the biomass removal phase, half of contents of the reactor (700 mL) are removed. The solids retention time of the reactor is therefore equal to 24 hours. The biomass which remained in the reactor was used as inoculum for the next batch, which started immediately after the previous batch. Twice a week, the reactors were cleaned at the end of a cycle. The contents of the bioreactor were stored during the cleaning process in an open container. During this time, there was no stirring or supplementation of oxygen. The main objective of the cleaning was to remove biofilms from the bioreactor walls, the metal parts of the reactor and probes. This ensured that all biomass was subjected to the feast-famine regime.

2.1.4 Different enrichments

An overview of the enrichments can be seen in Figure 5.

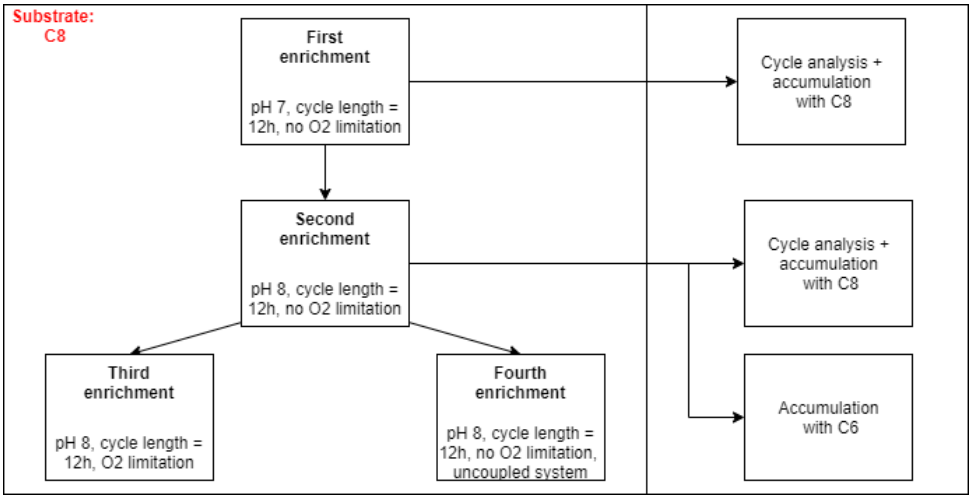

Figure 5: Overview of the conditions of the different enrichments performed and of the various cycle analysis and accumulation performed. The enrichments and the subsequent cycle analysis were always done with octanoic acid (C8) as the substrate and the accumulations were done with either octanoic acid or hexanoic acid (C6)

The first enrichment was operated at a pH of 7 with an airflow of 200 mL/min. A cycle analysis and an accumulation using octanoic acid were performed after this enrichment. The second enrichment was operated at a pH of 8 with an airflow of 200 mL/min. A cycle analysis, an accumulation using octanoic acid and an accumulation using hexanoic acid were performed after this enrichment. The third enrichment was done with a final airflow of 10 mL/min and a pH of 8. The fourth enrichment was done with a pH of 8, an airflow of 200 mL/min and an uncoupled system. The time between addition of the carbon source and the nitrogen source was 2 hours. 48.6% of the amount of nitrogen source was added compared to previous enrichments to ensure that all ammonia was depleted before starting the cycle. No cycle analysis or accumulation were performed after the third and fourth enrichment.

2.1.5 Cycle analysis

Cycle analysis' were performed after obtaining quasi-steady state of the SBR. This was defined by the time required for the feast phase. If this stayed relatively constant, a pseudo-steady-state was assumed. Before the cycle started, a sample for NGS and microscopy was taken. During the cycle, PHA samples, VFA samples, NH4-N samples and TSS/VSS samples were taken at critical moments. These moments were defined by a sudden change in the O_2 and CO_2 profile and the DO profile. The PHA samples, TSS/VSS samples, NH4-N and the NGS samples were treated as described in the analytical methods. The DO, pH, temperature, acid/base dosage and the composition of the off-gas and the in-gas were monitored online.

2.2 Fed-batch regime during accumulation

After enriching using specific reactor conditions and achieving pseudo-steady-state, a fed-batch regime was used to determine the maximum production of PHA.

2.2.1 First enrichment

After the first enrichment, the accumulation was done by giving twice as much C-medium as during a normal cycle, combined with the normal amount of nutrient medium as described above with the exception of the presence of the nitrogen-source. On top of that, the acid regulation was done by the C-medium so that the carbon source would not be depleted during the accumulation. The accumulation experiment lasted 12 hours and 12 samples were taken.

2.2.2 Second enrichment

Similar to the first enrichment, the accumulation after the second enrichment was done by initially giving twice the amount of C-medium compared to the normal cycle combined with the normal amount of nutrient medium as described above with the exception of the presence of the nitrogen-source. The acid regulation was done

by the C-medium so that the carbon source would not be depleted during the accumulation and 6 hours after starting the accumulation, 10% of the initial amount of octanoic acid was added every 2 hours.

2.3 Analytical methods

2.3.1 PHA analysis using gas chromatography

Samples were taken for the analysis of PHA using gas chromatography (GC) two times a week after the famine phase had started. This was determined based on the DO and the O2 profile. For the samples, 15 mL of broth from the reactor was taken and centrifuged for 15 min at 4760 rpm. The supernatant was removed and the pellet was stored in the freezer at -20 degrees Celcius until it could be analysed using the GC. During the first enrichment, no formaldehyde was added to the PHA samples. Starting from the first cycle analysis, three drops of formaldehyde were added to prevent degradation of the PHA. This was done during all subsequent enrichments and analyses. Before analyzing the samples for the GC, the samples were taken out of the -20 degrees Celcius freezer and covered in parafilm which had holes pricked in it. The samples were then kept for at least 5 minutes in the freezer at -80 degrees Celcius. The samples were then freeze-dried for at least a whole night or until completely dry.

The GC was calibrated with an internal standard and using pure standards for hydroxy-butyrate (HB), hydroxy-hexanoate (HH) and hydroxy-octanoate (HO). The pure standards for HB, HH and HO were bought from (CAS: 80181-31-3, Sigma-Aldrich, USA). The values for the calibration and the extensive method used for the GC can be seen in Appendix A.1. To summarize the method, the freeze-dried samples were transferred to glass tubes and weighted. 100 μL of internal standard, 1.5 mL of the solvent H_2SO_4 and 1.5 mL dicholoroethane were added to the glass tubes with the pellet. These tubes were heated for 3 hours at 100 degrees Celcius during which they were shaken every 30 minutes. The samples were brought to room temperature and subsequently 3 mL of milli-Q was added. The samples were shaken and thereafter centrifuged at 4700 rpm to separate the organic and inorganic phase. 1 mL of the organic phase was filtered and put into GC vials.

2.3.2 Community analysis using Next Generation Sequencing

Samples for next generation sequencing (NGS) were taken three times a week at the end of the famine phase before the new cycle would start. If cleaning of the reactor was scheduled that day, the sample would be taken before the cleaning. 2 mL of broth was taken from the reactor and centrifuged for 15 minutes at 4760 rpm. The supernatant was removed and the pellet was stored in the freezer at -20 degrees Celcius until further analysis. The defrosted pellet was treated with the DNeasy UltraClean Microbial Kit (Qiagen, The Netherlands) following the instructions of the manufacturer to extract the genomic DNA. Two deviations from the manual were made: the samples were incubated for 5 minutes at 65 degrees Celcius in a warm water bath before beating the samples and the subsequent beating was done for 5 minutes instead of 10 minutes at maximum speed with a Mini-Beadbeater-24 (Biospec, U.S.A.). The DNA quantification was done using the Qubit® dsDNA Broad Range Assay Kit (Thermo Fisher Scientific, U.S.A.).

The 16S-rRNA amplicon sequencing of the samples was done by Novogene (Novogene, Hongkong). The V3-4 region of the 16S-rRNA gene was amplicon sequenced on an Illumina paired-end platform. The raw reads were quality filtered: chimeric sequences were removed and OTU's were generated on the base of more than 97% identity. The microbial community analysis was performed by Novogene using the Mothur Qiime software(V1.7.0). The phylogenetical determination was done using the most recent SSURef database from Silva (http://www.arb-silva.de/).

For the sake of representation in this report, only the genus which had more than 5% relative abundance in the sample were shown. If the genus had less than 5% relative abundance in the sample, it was counted under 'Other'. For some organisms, the genus was unknown. In that case, the most specific last known taxonomic rank was used. These organisms are noted by the letter of their taxonomic rank followed by an underscore followed by the name of the organism. Therefore, names beginning with $'f_'$ indicate that the name is the name of the family, names with o indicate that the name is the name of the order and so on.

2.3.3 TSS/VSS analysis using thermogravimetric analysis

The samples for the TSS/VSS analysis were taken like the PHA samples with the exception that no formaldehyde was used. Similarly, the pellet was kept at -20 degrees Celsius until the analysis could be performed. Before analysis, the samples were taken out of the -20 degrees Celcius freezer and covered in parafilm which had holes pricked in it. The samples were then kept for at least 5 minutes in the freezer at -80 degrees Celcius. The

samples were then freeze-dried for at least a whole night or until completely dry. The pellet was then weighted separately before being analyzed by a thermogravimetric analyzer (TGA).

The Perkin Elmer TGA 8000 (Perkin Elmer, United Kingdom) was used to analyze the amount of total suspended solids (TSS), volatile suspended solids (VSS) and the ash content. The TGA measures the weight of the sample over time while the temperature is changed linearly to evoke temperature reactions [**?**]. This is also referred to as dynamic thermogravimetry. The sample is weighted using a precision scale and a balance pin located in the TGA itself.

Since the biomass was quite porous and light, a small amount of the biomass was put in the TGA. The TGA then heated up from 30 degrees Celcius to 104 degrees Celcius at a rate of 10 degrees Celcius per minute. The sample was kept at 104 degrees Celcius for 150 minutes to ensure that all water and other volatile contamination in the pores would be eliminated and so that only the true total suspended solids were left behind. Next, the sample was heated up from 104 degrees Celcius to 550 degrees Celcius at a rate of 10 degrees Celcius per minute. The sample was kept at 550 degrees Celcius for 30 minutes. This ensures that only the ash remained in the sample. The VSS is then calculated by substracting the ash content from the TSS content. After the analysis of the second enrichment, another step was added: the sample was heated up quickly to 900 degrees Celcius at the end. This was to prevent contamination of the TGA chamber.

However, the TGA broke after 1.5 uses so afterwards the TSS and VSS were determined solely on the weight of the pellet after freeze-drying and an estimate of the ash content and the evaporated sample. Based on the first use of the TGA, the TSS is approximately 91% of the whole sample after freezedrying and the ash content is approximately 13% of the TSS.

$$\text{TSS } [mg/L] = 0.91 * pellet_{\text{after freezedrying}}[mg] * \frac{1L[L]}{Sample_{broth}[mg] - Sample_{\text{empty tube}}[mg]} \tag{1}$$

$$\text{Ash } [mg/L] = 0.13 * TSS[mg/L] \tag{2}$$

$$VSS[mg/L] = TSS[mg/L] - Ash[mg/L] \tag{3}$$

$$\text{Active biomass } [mg/L] = \text{VSS } [mg/L] - \text{total PHA } [mg/L] \tag{4}$$

2.3.4 NH4-N and (volatile) fatty acids measurements

The VFA samples and NH4-N samples were obtained by filtering the supernatant of the TSS/VSS samples with a 45 μm filter (PVDF membrane, Millipore, Ireland). This was done to minimise the volume that had to be taken out of the reactor. This filtered supernatant was then frozen until further analysis. The analysis was performed using a Discrete Analyzer (DA) (Gallery Discrete Analayzer, Thermo Fisher Scientific, USA) for the NH4-N and a high-performance liquid chromatographer (HPLC) for the other VFA's. The HPLC was equipped with a column (BioRad Aminex HPX-87H, USA), a UV/RI detector, a pump and auto sampler (2489/2414, 515 and 717 plus, respectively, Waters Chromatography, The Netherlands). The mobile phase had a flow rate of 0.6 mL/min, a temperature of 59° C and consisted of 1.5mM phosphoric acid in Milli-Q. These measurements were only done during the cycle analysis and the accumulation experiments. 120 μL of each sample was added in vials for the GC.

2.3.5 Online measurements

During the experiments, the DO, pH, temperature, acid/base dosage and the composition of the off-gas and the in-gas were monitored online. The online measurements were performed by the hardware and software mentioned before. A mass spectrometer (MS) (PRIMA BT Benchtop, Thermo Fisher Scientific, USA) was used to analyse the composition of the off-gas and the in-gas. For the models, the average composition per minute was taken. If no data was known for a particular minute, it is assumed that the composition is the same as the previous known (average) composition. Outliers due to sampling were manually adjusted to exclude said outliers.

2.4 Model

2.4.1 Metabolic model

The metabolic model was made using MATLAB [40] and the kinetic model was made using Microsoft Excel (Microsoft Excel v.16, 2021).

To investigate which PHA monomers would be produced under certain conditions, a model was build to calculate the consumption rates and the production rates of the important compounds. It was also used to calculate relevant yields. This model considered the metabolic and kinetic parameters for a mcl-PHA producing organism. The model was based on the model of Marang et at. [41]. An overview of the reactions in the metabolic model can be seen in Figure 6.

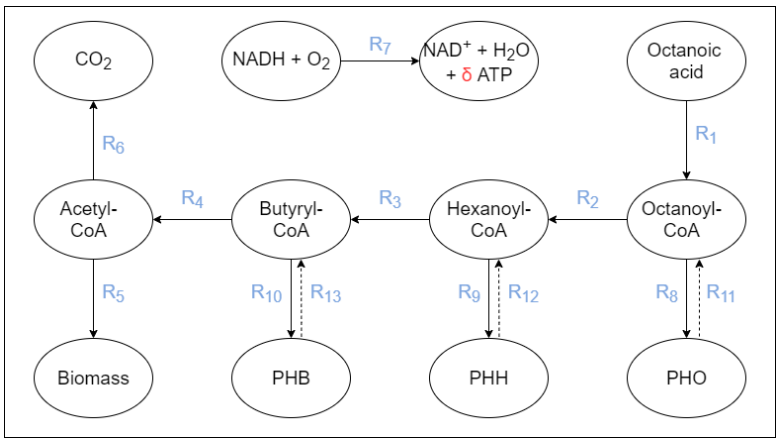

Figure 6: Overview of the considered reactions in the metabolic model. The degradation reactions are indicated with broken arrows.PHO = poly-hydroxy-octanoate, PHH = poly-hydroxy-hexanoate, PHB = poly-hydoxy-butyrate.

The reactions can be found in Appendix A.3. In this model, several assumptions are made. This metabolic model assumes that the phosphorylation will yield 2 ATP ($\delta = 2$). It is also assumed that the uptake of octanoic acid requires 3 ATP per mole of octanoic acid: 1 ATP for the actual uptake and 2 ATP for the activation of the octanoic acid to octanoyl-CoA. $FADH_2$ is assumed to be a $NADH_2$ equivalent. Due to its difference in ATP yield during the oxidative phosphorylation, next models should not consider those two equivalent. It is therefore not considered a separate compound but is considered in the $NADH_2$ cost or production in these reactions. The degradation of PHO, PHH and PHB is assumed to cost 1 ATP per mole monomer. The $NADH_2$ production and/or consumption for the degradation and production of the different types of PHA was calculated using the degree of reduction.

The metabolic model consists of 5 phases:

1. Growth in the feast phase
2. Storage compound production in the feast phase
3. Catabolism in the feast phase
4. Growth on the storage compound during famine phase
5. Catabolism during famine phase

For each parts, the reactions which take place are noted and a bootstrap is determined. A linear regression using the conserved moieties of the reactions is done to obtain a vector with variables which describes how many times each reactions will be run during the part so that the bootstrap condition is met. This is to ensure normalization of the reactions for 1 specific reaction. Equations 5 and 6 show the general mathematical equation for the calculation of the variables.

$$\begin{pmatrix} A_{1,1} & A_{1,2} & \dots & A_{1,N} \\ A_{2,1} & A_{2,2} & \dots & A_{2,N} \\ \vdots & \vdots & \vdots & \vdots \\ A_{M,1} & A_{M,2} & \dots & A_{M,N} \end{pmatrix} \begin{pmatrix} x_1 \\ x_2 \\ \vdots \\ x_N \end{pmatrix} = \begin{pmatrix} b_1 \\ b_2 \\ \vdots \\ b_N \end{pmatrix} \tag{5}$$

$$\begin{pmatrix} x_1 \\ x_2 \\ \vdots \\ x_M \end{pmatrix} = \begin{pmatrix} A_{1,1} & A_{1,2} & \dots & A_{1,N} \\ A_{2,1} & A_{2,2} & \dots & A_{2,N} \\ \vdots & \vdots & \vdots & \vdots \\ A_{M,1} & A_{M,2} & \dots & A_{M,N} \end{pmatrix} \setminus \begin{pmatrix} b_1 \\ b_2 \\ \vdots \\ b_M \end{pmatrix} \tag{6}$$

The matrix A contains the conserved moieties of each reaction participating in each part. The conserved moieties considered in this model are ATP, $NADH_2$, acetyl-CoA, butyryl-CoA, hexanoyl-CoA and octanoyl-CoA, represented by the rows (M). The columns represent the reactions (N). The vector b contains the bootstrap reaction which ensures normalization of the yields. The vector x contains the variables.

Next, the yield of relevant compounds is determined using this obtained multiplicator and the stoichiometry of the compounds in the reactions. The mathematical reactions for the determination of the yield can be found in Appendix A.3. The reactions participating in each part will be described briefly. For a more thorough understanding of the metabolic model, please refer to A.3.

During growth in the feast phase, the uptake, the catabolism, the anabolism and oxidative phosphorylation are performed. The bootstrap for this reaction is the uptake.

During storage compound production in the feast phase, the reactions to make acetyl-Coa from the substrate, the PHO/PHH/PHB productions reactions, the oxidative phosphorylation and the anabolism reaction are happening. The bootstrap for this reaction is the uptake.

During catabolism in the feast phase, the uptake, the catabolism , and the oxidative phosphorylation are happening. The bootstrap for this reaction is the uptake. In this part, the ATP production and consumption has not been considered a conserved moieties which needs to be zero since catabolism inherently will produce energy.

During growth during famine phase, oxidative phosphorylation, catabolism , anabolism and degradation of storage compounds is happening. The bootstrap for this reaction is the degradation of PHA.

During catabolism during famine phase, oxidative phosporylation, catabolism and degradation reactions occur. The bootstrap for this reaction is the degradation of PHA. In this part, the ATP production and consumption has not been considered a conserved moieties which needs to be zero since catabolism inherently will produce energy.

For the yields which contain PHA, the yield of the individual PHA's was multiplied by the maximum fraction of the PHA during the experiment. This value is therefore data-depended. To illustrate this, the yield of CO2 over PHA in the feast for the cycle analysis of the first enrichment is shown in equation

$$Y_{CO2/PHA} = \frac{f_{PHB}}{f_{PHA}} \times Y_{CO2/PHB} + \frac{f_{PHH}}{f_{PHA}} \times Y_{CO2/PHH} + \frac{f_{PHO}}{f_{PHA}} \times Y_{CO2/PHO} \tag{7}$$

$$Y_{CO2/PHA} = -0.1220 \frac{Cmol}{Cmol} \times \frac{21.5wt\%}{60.4wt\%} - 0.0244 \frac{Cmol}{Cmol} \times \frac{9.5wt\%}{60.4wt\%} + 0.0244 \frac{Cmol}{Cmol} \times \frac{30.4wt\%}{60.4wt\%} \tag{8}$$

$$Y_{CO2/PHA} = -0.03436 \frac{Cmol}{Cmol} \tag{9}$$

2.4.2 Kinetic model

The kinetic model is based on Herbert-Pirt kinetics. The formulas for the necessary kinetic parameters can be found in Appendix A.4, equations 45 until 60. These kinetic parameters are used in a set of ordinary differential equations. These equations are given by the following formulas:

$$\frac{dS}{dt} = [X] \times q_s \tag{10}$$

$$\frac{dX}{dt} = [X] \times (q_{X/PHA} + q_{X/S}) \tag{11}$$

$$\frac{dPHB}{dt} = \frac{f_{PHB}}{f_{PHA}} \times X \times (q_{PHB}^{prod} + q_{PHB}^{con}) \tag{12}$$

$$\frac{dPHH}{dt} = \frac{f_{PHH}}{f_{PHA}} \times X \times (q_{PHH}^{prod} + q_{PHH}^{con}) \tag{13}$$

$$\frac{dPHO}{dt} = \frac{f_{PHO}}{f_{PHA}} \times X \times (q_{PHO}^{prod} + q_{PHO}^{con}) \tag{14}$$

$$\frac{dNH_4^+}{dt} = \frac{dX}{dt} \times Y_{N/X}^{feast} \tag{15}$$

2.5 Element balances and electron balances

The carbon balances and the electron balances were calculated using both the online and offline data and using the model for each cycle analysis and fed-batch accumulation experiment. For the electron balance, the oxidation state (OS) as seen in Table 1 was used.

Table 1: Relevant compounds and their oxidation state per (carbon) mole.

CO_2	0	e-mol/Cmol
O_2	-4	e-mol/mol
OA	5.5	e-mol/Cmol
HA	5.33	e-mol/Cmol
PHO	5.25	e-mol/Cmol
PHH	5	e-mol/Cmol
PHB	4.5	e-mol/Cmol
$NH4^+$	0	e-mol/mol
Biomass	4.2	e-mol/Cmol

The carbon balance was calculated as seen in equation 16 and the electron balance was calculated using equation 18. In these equations, all compounds are expressed in Cmol unless otherwise noted and all oxidation states (OS) are expressed in e-mol/(C)mol.

$$C - balance[\%] = \frac{100}{OA_{begin}} * (cum.OA \ - (cum.\ PHA \ + cum.CO_2 + cum.\ X\ )) \tag{16}$$

$$cum.\ PHA\ [e\text{-}mol/cmol] \ = cum.\ PHO\ * OS\ PHO + cum.\ PHH\ * OS\ PHH + cum.\ PHB\ * OS\ PHB \tag{17}$$

$$e{-}balance[\%] = \frac{100}{OA_{begin} * OS\ OA} * (cum.OA * OS\ OA - (cum.PHA[\frac{e-mol}{cmol}] + cum.X * OS\ X + cum.O_2 * OS\ O_2)) \tag{18}$$

For the kinetic model, the online data was processed using a MATLAB script, which returned the average online data per minute. For the gas data, both the inflow of gas and the outflow of gas, the average per sampling moment was taken and this value was copied until the next sampling moment. Outliers were manually adjusted.

2.6 Plating of the micro-organisms

For plating, 4 different agar media were used. The first one was two times concentrated media that was used for the reactor, combined with the same amount of agar. The second one was also two times concentrated media from the reactor, but with added vitamins. The third plates were with pre-made LB agar media. The fourth plates were with pre-made SM agar media.

The agar media was heated to a minimum of 80 degrees before being poured on to the plates. This also ensured that micro-organisms residing in the agar would die. A dilution series of the sample was made, ranging from 10^{-4} to 10^{-8}. 20 μL of a dilution of the sample was taken and spread out on the plate. The plates were kept at 30° C and were kept in parafilm.

3 Results and discussion

3.1 Metabolic model

The stoichiometric parameters of the metabolic model based on the assumptions and equations described in the material and methods can be found in Table 2.

Table 2: Stoichiometric parameters of metabolic model in the feast phase and in the famine phase

Stoichiometry feast			**Stoichiometry famine**		
Growth equation			Metabolic equation		
$Y^{feast}_{CO2/X}$	0.24	Cmol/Cmol	$Y^{famine}_{CO2/X\ O}$	0.24	Cmol/Cmol
$Y^{feast}_{O2/X}$	-0.66	mol/Cmol	$Y^{famine}_{CO2/X\ H}$	0.32	Cmol/Cmol
$Y^{feast}_{X/S}$	-0.81	Cmol/Cmol	$Y^{famine}_{CO2/X\ B}$	0.50	Cmol/Cmol
$Y_{N/X}$	-0.20	Nmol/Cmol	$Y^{famine}_{CO2/X}$	0.29	Cmol/Cmol
PHA production			$Y^{famine}_{O2/X\ O}$	-0.58	Cmol/Cmol
$Y^{feast}_{CO2/PHO}$	0.02	Cmol/Cmol	$Y^{famine}_{O2/X\ H}$	-0.59	Cmol/Cmol
$Y^{feast}_{CO2/PHH}$	-0.02	Cmol/Cmol	$Y^{famine}_{O2/X\ B}$	-0.63	Cmol/Cmol
$Y^{feast}_{CO2/PHB}$	-0.12	Cmol/Cmol	$Y^{famine}_{O2/X}$	-0.61	mol/Cmol
$Y^{feast}_{O2/PHO}$	-0.10	mol/Cmol	$Y^{famine}_{X/PHO}$	-0.81	Cmol/Cmol
$Y^{feast}_{O2/PHH}$	-0.09	mol/Cmol	$Y^{famine}_{X/PHH}$	-0.76	Cmol/Cmol
$Y^{feast}_{O2/PHB}$	-0.08	mol/Cmol	$Y^{famine}_{X/PHB}$	-0.67	Cmol/Cmol
$Y^{feast}_{PHO/S}$	-0.98	Cmol/Cmol	$Y_{N/Xm}$	-0.20	Nmol/Cmol
$Y^{feast}_{PHH/S}$	-1.03	Cmol/Cmol	Catabolic equation		
$Y^{feast}_{PHB/S}$	-1.14	Cmol/Cmol	$Y^{famine}_{CO2/PHO}$	-1.00	Cmol/Cmol
Catabolic equation			$Y^{famine}_{CO2/PHH}$	-1.00	Cmol/Cmol
$Y^{feast}_{CO2/S}$	-1.00	Cmol/Cmol	$Y^{famine}_{CO2/PHB}$	-1.00	Cmol/Cmol
$Y^{feast}_{O2/S}$	1.38	mol/Cmol	$Y^{famine}_{O2/PHO}$	1.31	mol/Cmol
$Y^{feast}_{ATP/S}$	-5.13	mol/Cmol	$Y^{famine}_{O2/PHH}$	1.25	mol/Cmol
			$Y^{famine}_{O2/PHB}$	1.13	mol/Cmol
			$Y^{famine}_{ATP/PHO}$	-5.13	mol/Cmol
			$Y^{famine}_{ATP/PHH}$	-4.83	mol/Cmol
			$Y^{famine}_{ATP/PHB}$	-4.25	mol/Cmol

A point of note is the negative value of the parameters $Y^{feast}_{CO2/PHH}$ and $Y^{feast}_{CO2/PHB}$. The parameter $Y^{feast}_{CO2/PHO}$ has a positive value, as expected. The negative value of these parameters could indicate that a reverse TCA cycle is used if the whole flux through the catabolic reaction seen in Equation 24 is negative. This could mean that another set of reactions is required to generate sufficient $NADH_2$. In literature, no evidence for another source of $NADH_2$ was found or evidence for a zero flux through the catabolism. Another possibility is that the production of PHO generates sufficient energy to compensate for the production of PHB and PHH. This would mean that the flux through the catabolic reaction is positive and generates the necessary $NADH_2$. This of course raises the question why the energy-requiring compounds PHB and PHH would be produced when PHO does not require this energy cost. A third possibility is that the initial assumption for the delta, which dictates the efficiency of the phosphorylative oxidation, of 2 was wrong. While a value of 2 has been used in previous models for other substrates, a delta value of 0.75 is the maximum to ensure that both $Y^{feast}_{CO2/PHH}$ and $Y^{feast}_{CO2/PHB}$ have a positive value. [35], [42], [43] This would indicate that the efficiency of the phosphorylative oxidation is quite low. Since the delta has a large influence on the stoichiometric parameters, parameters which rely on the stoichiometric parameters and the data could have been affected. A most notable example of this is the correct ATP maintenance requirements. A better understanding of the efficiency of the oxidative phosphorylation would improve this model therefore tremendously.

3.2 First enrichment: Establishing a baseline

To obtain mcl-PHA, the activated wastewater sludge first needed to be enriched for mcl-PHA producing organisms. This was done by selecting for PHA producers using the feast-famine regime and by using a medium-chain length fatty acid as substrate. The solid retention time was equal to the hydraulic retention time, namely 24 hours. The pH was 7, the cycle time was 12 hours and the temperature was 30 degrees Celcius. After inoculating the bioreactor, a lag phase was observed of approximately 12 hours. After this lag phase, a CO_2 spike was observed and the carbon source was depleted. The first cycle was started approximately 12 hours later. The reactor ran for 89 cycles during which the feast times were observed using the oxygen profile and the DO profile.

3.2.1 Evolution during the enrichment

The evolution of the length of the feast times can be seen in Appendix A.5. During the enrichment, PHA samples and NGS samples were taken and analysed. The evolution of these samples can be seen in Figure 7a and 7b.

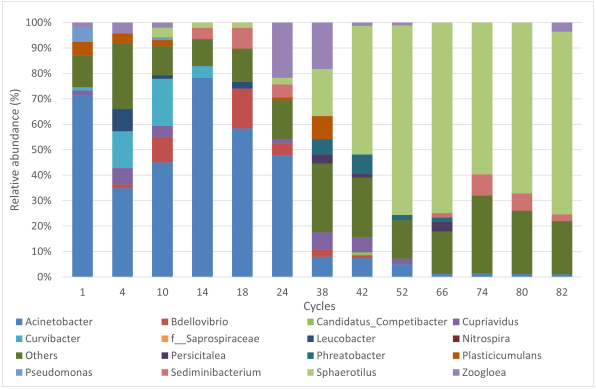

(a) Evolution of the relative abundance of the organisms in the community during the first enrichment.

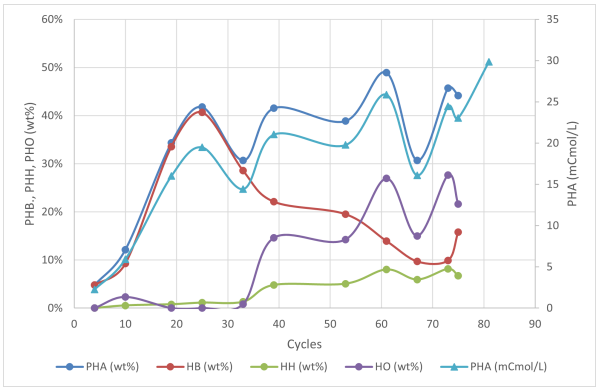

(b) Evolution of the PHA content during the first enrichment.

Figure 7: Evolution of the relative abundance of the organisms and the PHA content during the first enrichment.

As can be seen in Figure 7b, there was little to no PHO during the first 40 cycles of the enrichment but the PHB content did increase. After 39 cycles, the PHO weight percentage started to increase. The highest PHO content is terms of weight percentage was observed after 75 cycles, with a PHO content of 28 wt%, a PHH content of 8 wt% and a PHB content of 10 wt%. The total PHA content was therefore 46 wt%. It is remarkable that despite the high PHO content, no significant amount of *Pseudomonas* and *Comammoma*, the species most known to produce mcl-PHA, were found using NGS. This could indicate that another organism is able to produce mcl-PHA. In the NGS results, there is a correlation between the increase in PHO content and the increase in the abundance of the genus *Sphaerotilus*. The abundance of this organism has also been observed in microscopy samples, as can be seen in Figure 8. This image was taken from the 52nd cycle and shows the characteristic shape of the *Sphaerotilus*.

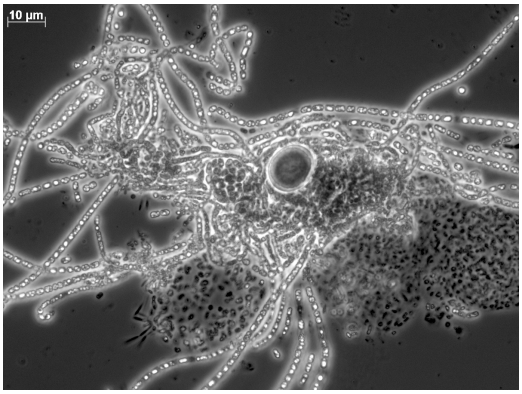

Figure 8: Microscopy image of the 52nd cycle of the first enrichment. The characteristic shape of *Sphaerotilus*, namely the long cable-like shape, can be clearly seen.

This organism is a proteobacteria which is linked to waste water [44]. It is known to enjoy oxygen limited environments and environments with an excess of nutrients in relation to the activated sludge concentration [45]. It has not been previously identified as a potential mcl-PHA producer and does not seem to have been previously grown on octanoic acid specifically. It is also not a species known to flourish in feast-famine regimes, as the species is not a great PHA producers and does not prefer the low nutrient levels during the famine [45]. To prove that the *Sphaerotilus* were responsible for the mcl-PHA production, a sample of cycle 81 of the first enrichments was used to inoculate a reactor with the same conditions as during this first enrichment. After being in cold storage for 4 months, there were few *Sphaerotilus* still present in the bioreactor as seen with microscopy (data not shown). However, the *Sphaerotilus* did become more prevalent in the reactor after 22 cycles. This is similar to the NGS data of the first enrichment, where *Sphaerotilus* needed 24 cycles to become a significant organism in the reactor.

After 40 cycles, a sample was taken and plated on 4 different agar media as described in the material and methods with 4 different dilutions ranging from 1E-4 to 1E-6. This was to isolate and further characterize the *Sphaerotilus*. This was only an attempt to prove or disprove that the *Sphaerotilus* could produce mcl-PHA when using octanoic acid as a carbon source. After 10 days, no *Sphaerotilus* were found using microscopy. It is possible that since *Sphaerotilus* prefers oxygen limitation that the plates were non-ideal for the organism to grow on [46] [44]. It is also possible that since *Sphaerotilus* prefers an excess of nutrients that it was unable to grow [45]. Further isolation and characterization of this organism will therefore be needed to prove that *Sphaerotilus* is indeed a mcl-PHA producer. However, if this organism does prove to be able to produce mcl-PHA, this would mean that more organisms than previously thought are capable of producing mcl-PHA. This could potentially be a breakthrough in the production of mcl-PHA.

3.2.2 Cycle analysis

After 73 cycles, a cycle analysis was performed. Figure 9 shows the evolution of the most important compounds: the overall PHA content, the cumulative CO_2 production, the cumulative O_2 consumption, the octanoic acid concentration and the ammonium concentration.

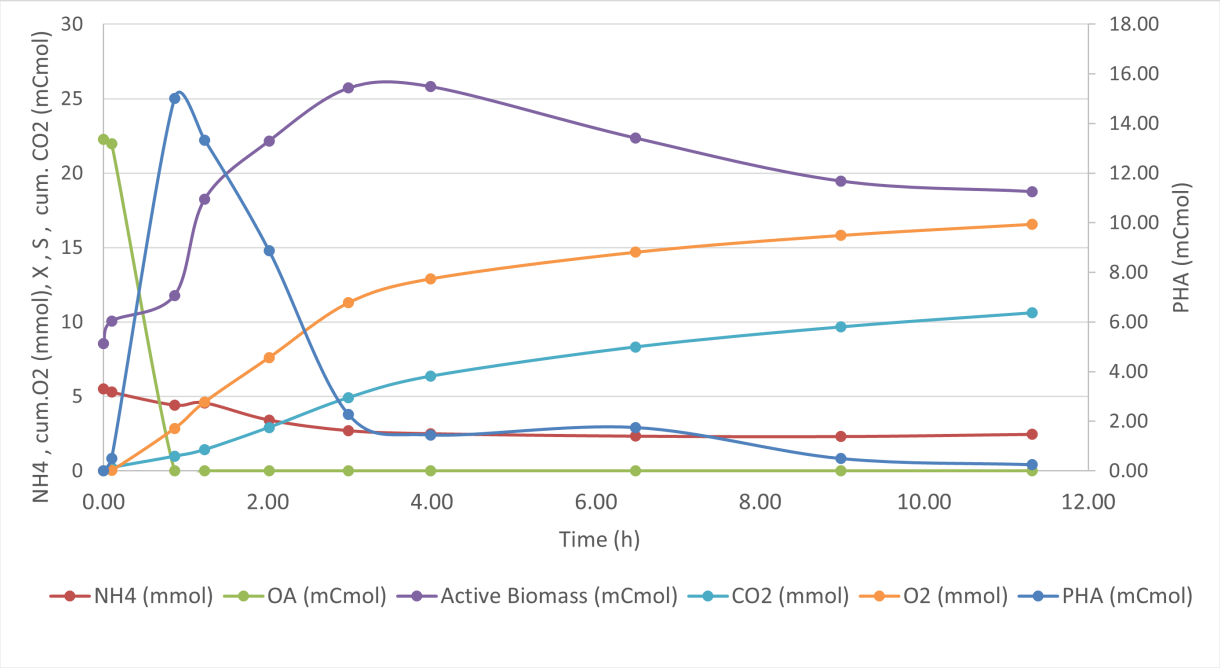

Figure 9: Evolution of the most important compounds during a cycle analysis performed after 73 cycles.

The highest concentration of PHA (13.3 mCmol) was obtained 74 minutes after adding the carbon source. At this point, the carbon source in the medium has been depleted for at least 22 minutes and the nitrogen source is still freely available in the medium. A maximum HO content of 27 wt% is obtained at that point, with a PHH content of 5 wt% and a PHB content of 9 wt% for a total PHA content of 41 wt%. Especially the total PHA content is on the low side compared to the week leading up to the cycle analysis, when PHA content was between 40 wt% and 50 wt%. A back-up of the sample point at 74 minutes was analysed with the GC. This sample yielded a PHA content of 56 wt%, with a HO content of 36 wt%, a PHH content of 8 wt% and a HB content of 11 wt%. This one is comparatively higher than the average obtained for the week prior but since no further back-ups were available, a full rerun of the cycle analysis could not be performed. For that reason, this cycle analysis was only used for qualitative reasons and not for quantitative reasons.

Of the ammonia that was consumed during the cycle, 36 % was consumed during the feast and 64% was consumed during the famine. This indicates that there is still a significant amount of growth during the feast phase of the cycle. 28% of the oxygen is consumed in the feast. Despite some growth during the feast, the majority of growth occurs during the famine as intended. The carbon balance of the data closes with 1.65% off at the end of the cycle and the electron balance closes with 8.71% off at the end of the cycle.

The average biomass specific consumption rates, the average biomass specific production rates and the important yields during the cycle were calculated using a model for both the feast and the famine. This can be seen in Table 3. The relevant parameters of the model were chosen to fit the data obtained during the cycle analysis and can likewise be seen in Table 3. The carbon balance of the model closed with on average -3% off.

Table 3: Summmary of the model-derived rates of consumption, rates of production and the yields determined by the model of the cycle analysis of the first enrichment

	Variable	Values	Unit
Feast	q_{PHB}	0.49	[Cmmol/Cmmol/h]
	q_{PHH}	0.22	[Cmmol/Cmmol/h]
	q_{PHO}	0.69	[Cmmol/Cmmol/h]
	q_S	2.05	[Cmmol/Cmmol/h]
	$Y_{PHA/S}$	0.68	[Cmol/Cmol]
	$Y_{X/S}$	0.26	[Cmol/Cmol]
	$Y_{CO2/S}$	0.07	[Cmol/Cmol]
	$Y_{O2/S}$	0.25	[mol/Cmol]
Famine	q_{PHB}	-0.03	[Cmmol/Cmmol/h]
	q_{PHH}	-0.01	[Cmmol/Cmmol/h]
	q_{PHO}	-0.04	[Cmmol/Cmmol/h]
	$Y_{X/PHA}$	3.06	[Cmol/Cmol]
	$Y_{CO2/X}$	1.67	[Cmol/Cmol]

3.2.3 Accumulation

14 cycles after performing the cycle analysis, a fed-batch accumulation experiment was performed. The goal of this experiment was to determine the highest content of PHA obtainable. Figure 10 in shows the evolution of the most important compounds during the accumulation.

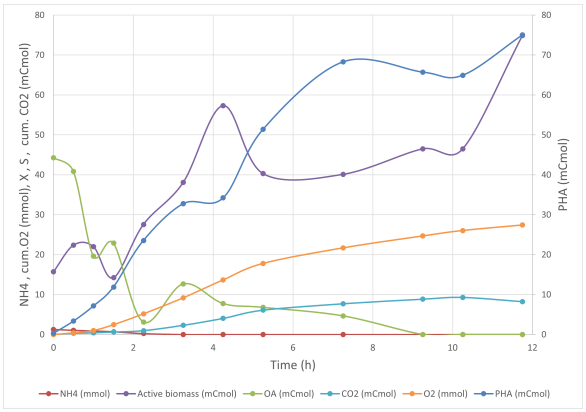

(a) Evolution of compounds during the accumulation of the first enrichment performed after 87 cycles

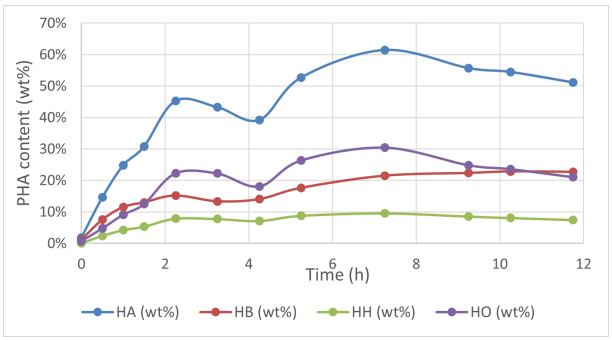

(b) Evolution of the PHA content during the accumulation of the first enrichment performed after 87 cycles

Figure 10: Evolution of the relevant compounds and the PHA content during the accumulation with octanoic acid of the first enrichment done after 87 cycles.

The highest content of PHA obtainable during the accumulation was determined to be 61.5 wt%, with a HO content of 30.4 wt%, a HH content of 9.5 wt% and a HB content of 21.5 wt%. This results in a production of 26 mCmol/L HO, 7.6 mCmol/L HH and 15.1 mCmol/L HB. However, the highest production of PHA is not at this moment due to the fact that the total amount of biomass kept increasing. Due to this, the highest PHA production was 24.2 mCmol/L HB, 7.9 mCmol/L HH and 21.5 mCmol/L HO. The weight percentages at this point are respectively 22.7%, 7.4% and 21.1%. Therefore, it is possible that the accumulation experiment did not last long enough to obtain the highest productivity, despite reaching the highest weight percentage. On top of these observations, there are another 2 noteworthy observations. The first is that the substrate was depleted after 9 hours, despite the fact that octanoic acid was coupled to the acid regulator and that the pH stayed constant. This could point to another acid potentially being formed. The second interesting observation is that the nitrogen source was depleted after 5.25 hours but the active biomass concentration continued to increase.

3.3 Second enrichment: An increase in pH increases the mcl-PHA production

During the enrichment at pH 7, a substantial amount of biofilm was observed. Since this biofilm could escape the selection pressures and since it would become a hinder for future potential industrial applications and could be an indicator for metabolic stress, the pH was increased to pH 8 in an attempt to de-stress the cells slightly. It was expected that this would increase both the weight percentage of PHA and the overall production, since higher pH would lower the toxicity of the substrate and therefore improve the metabolic speed. On top of that, the potential decrease in biofilm is an advantage for future industrial applications. The second enrichment was therefore ran for 99 cycles at pH 8 with the same airflow as the first enrichment, 200 mL/min. The enrichment was run for in total 140 cycles. After the first 100 cycles, the enrichment was halted and the biomass was stored in cold storage (-4° C). After 20 days, the stored biomass was re-introduced in the reactor and the reactor was run for another 40 cycles.

3.3.1 Evolution during the enrichment

Figure 11 shows the evolution of the PHA content at the end of the feast phase during the second enrichment at pH 8.

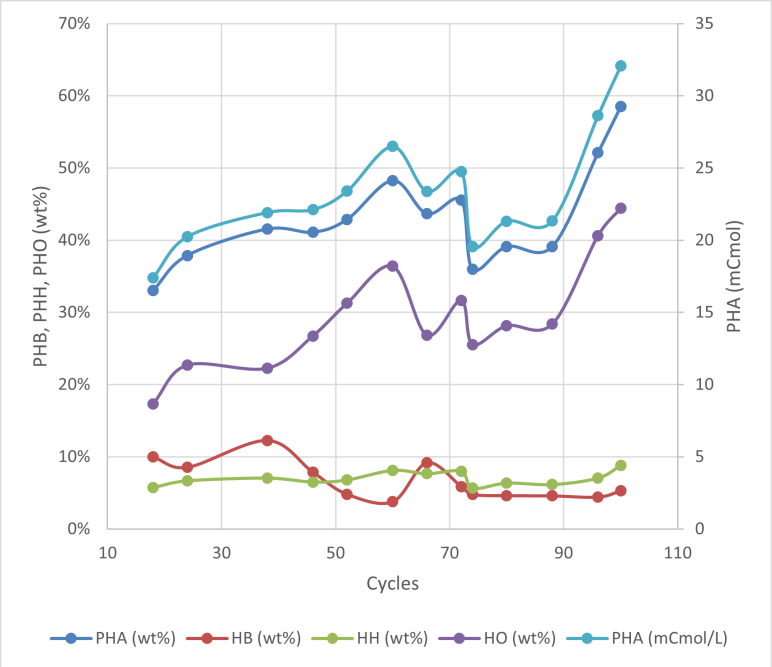

Figure 11: Evolution of the PHA concentration and the weight percentages obtained during the second enrichment at pH 8.

As shown, the weight percentage increases to an overall PHA weight percentage of 63%, with a weight percentage of 49% for HO, a weight percentage of 9% for HH and a weight percentage of 6% for HB. The highest productivity goes up compared to the first enrichment: from a total HA of 29.9 mCmol/L to 32.1 mCmol/L. On top of that, the original goal of reduced biofilm formation was obtained while surpassing the obtained yields.

3.3.2 Cycle analysis

After 99 cycles, a cycle analysis was performed. During the cycle analysis, the maximum concentration of PHA was 16.95 mCmol. This corresponds with a weight percentage of 48 wt% PHO, with a total PHA yield of 62 wt%. PHB and PHH had weight percentages of 5 wt% and 8 wt% at their peaks respectively. This is the highest obtained weight percentage of mcl-PHA during the enrichment. To save time, the accumulation of this experiment was performed 40 cycles after the cycle analysis but the biomass had been in cold storage for 20 days between the end of the cycle analysis and the start of the 40 cycles. The time in the fridge combined with multiple mechanical crashes of the system resulted in drastic changes to the PHA levels observed. During this accumulation, the maximum weight percentage of PHO did not go above 8.5 wt%, with a maximum total PHA weight percentage of 74.2 wt%. To explain that result, four possible reasons will be discussed. First of

all, it is possible that due to the prolonged time in the fridge, the organisms responsible for the high PHO content had died and/or become inactive. If *Sphaerotilus* was still present in the culture at this point and time and was responsible for the production of mcl-PHA, this is the most likely explanation since *Sphaerotilus* has been reported to be unable to stand cold storage for prolonged periods of time [46]. Another possible reason could be that the numerous mechanical failures resulted in unstable conditions which favored another organism and applied an unforeseen and unintended selection pressure on the community. Another possible explanation could be that the accumulation conditions were detrimental to the organisms producing mcl-PHA. It is possible that the higher octanoic acid concentration was fatal to the organism producing mcl-PHA. However, given the success of the re-done accumulation, this seems unlikely. A final reason for the unexpected results of the accumulation could be due to instability of the pH probe at pH 8. While the probe was regularly calibrated at pH 4 and pH 8, the probe later proved to behave more erratic at higher pH's including pH 8. Due to this, it is expected that the actual pH leading up to the accumulation was higher than the intended pH 8. This could have provided a selection pressure for organisms other than the mcl-PHA producing organism, although it is unclear which organisms exactly would have been selected for due to this higher pH.

Due to the unexpected results during the accumulation, back-up biomass from around 46 cycles into the second enrichment was taken out of cold storage and was again enriched until similar results compared to the second enrichment were obtained. This revival of the second enrichment was used to perform a new cycle analysis and two accumulations: one with octanoic acid and one with hexanoic acid. The new cycle analysis was used to verify that the batches behaved similarly. The goal of the accumulation with hexanoic acid was to establish whether it is possible to obtain mcl-PHA using the more industrially relevant hexanoic acid and to obtain a broader understanding of the mcl-PHA production process.

Figure 12 shows both the cycles of the second enrichment for comparison.

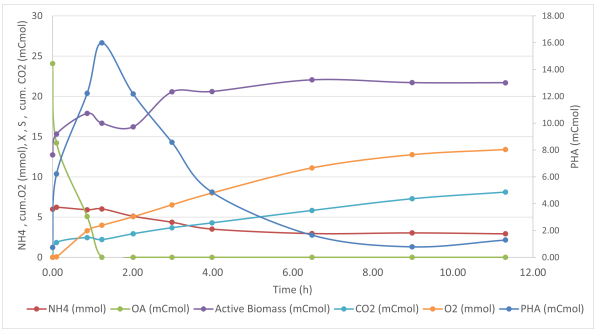

(a) Evolution of compounds during the cycle of the original second enrichment

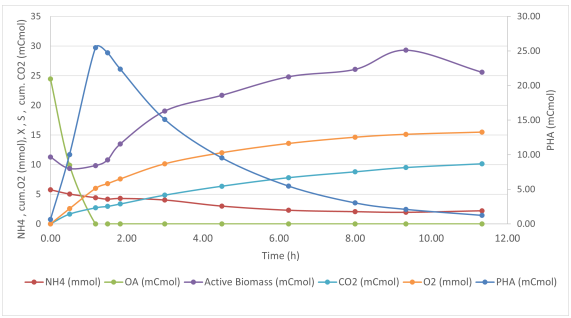

(b) Evolution of compounds during the cycle of the redone second enrichment

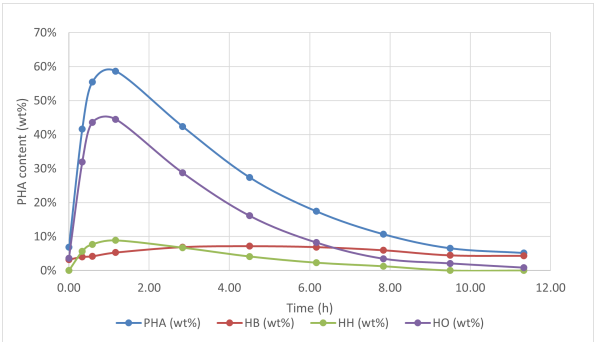

(c) PHA content during the cycle of the redone second enrichment

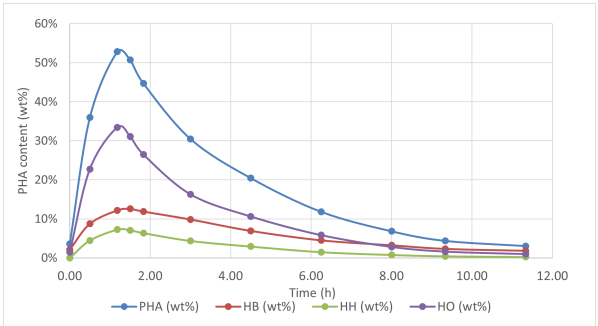

(d) PHA content during the cycle of the redone second enrichment

Figure 12: Comparison of the evolution of the compounds during the cycle analysis and the PHA content during the cycle.

As can be seen in Figure 12, there is an increase in the amount of PHA and biomass in mCmol in the second cycle compared to the first cycle. The other compounds (octanoic acid, ammonium, CO_2 and O_2) stay relatively the same. The PHA content in wt% decreases in the second cycle compared to the first, with a maximum PHO content of 44 wt% in the first cycle compared to 33 wt% in the second cycle. It is possible that if the second

cycle had been run for a longer period of time, the culture would have fully recovered to the levels of the first cycle of the second enrichment.

During the re-done cycle, 38% of the nitrogen source was consumed during the feast and 62 % was consumed during the famine. This is slightly more than during the first cycle analysis, which had 36% and 64% respectively. This is also reflected in the oxygen consumption, where 33% of the oxygen consumed was consumed in the feast, while the cycle analysis of enrichment 1 had 28% oxygen consumed in the feast despite having less mcl-PHA production. However, this is likely due to the underestimation of the mcl-PHA production during the cycle analysis of the first enrichment.

The average consumption rates, the average production rates and important yields during the repeated cycle were calculated using a model. This can be seen in Table 4. The relevant parameters of the model were chosen to fit the data obtained during the cycle analysis. The carbon balance of the model closes with -9% off.

Table 4: Summary of the model-derived rates of consumption, rates of production and the yields for the model of the second cycle for the second enrichment

	Variable	Values	Unit
Feast	q_{PHB}	0.50	[Cmmol/Cmmol/h]
	q_{PHH}	0.29	[Cmmol/Cmmol/h]
	q_{PHO}	1.33	[Cmmol/Cmmol/h]
	q_S	2.13	[Cmmol/Cmmol/h]
	$Y_{PHA/S}$	0.97	[Cmol/Cmol]
	$Y_{X/S}$	0.03	[Cmol/Cmol]
	$Y_{CO2/S}$	0.01	[Cmol/Cmol]
	$Y_{O2/S}$	0.12	[mol/Cmol]
Famine	q_{PHB}	-0.03	[Cmmol/Cmmol/h]
	q_{PHH}	-0.02	[Cmmol/Cmmol/h]
	q_{PHO}	-0.08	[Cmmol/Cmmol/h]
	$Y_{X/PHA}$	2.84	[Cmol/Cmol]
	$Y_{CO2/X}$	1.44	[Cmol/Cmol]

3.3.3 Accumulation with octanoic acid

The re-enriched culture was used to do two accumulations. First, an accumulation with octanoic acid was performed in the exact same way as the previous accumulation was performed. The evolution of the most important compounds can be seen in Figure 13.

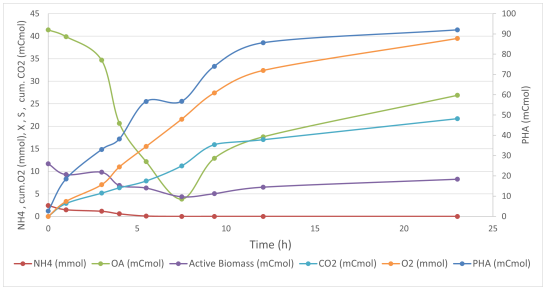

(a) Evolution of important compounds during the accumulation using octanoic acid as the substrate.

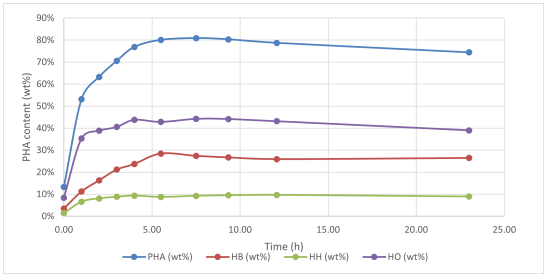

(b) PHA content during the accumulation using octanoic acid as substrate.

Figure 13: Comparison of the evolution of the compounds during the cycle analysis and the PHA content during the cycle.

As seen in Figure 13b, the PHO content reaches its maximum level, namely 44 wt%, in 2 to 3 hours. The PHO content stays stable for the rest of the accumulation. Since a PHO content of 44 wt% was also the maximum obtained level during the cycle, it is possible that this is the biological limit of the organism under these conditions. While the PHO content reaches its peak quickly, the PHB content takes about 5.5 hours to reach its peak of 28 wt%. It is possible that two different organisms responsible are for the accumulation of PHO

and PHB, since the PHO accumulator seems to be much faster at the production of PHO and presumably at the uptake of the substrate while the PHB accumulator seems to really flourish when the PHO accumulator has reached its peak. In this case, the halt in PHO accumulation could be due to a lack of available storage space in the organism. In the case that the PHO accumulator and the PHB accumulator are the same organism, the organism would stop accumulating PHO at 44 wt% and continue increasing the PHB content until the N-source is depleted, which is at around 5.5 hours. However, this is not in line with the expectations, since for the production of scl-PHA like PHB the depletion of the nitrogen source is a stimulans to produce more scl-PHA [22]. It is possible that the depletion of the nitrogen source and the halting of the PHB accumulation is a coincidence, and the reason for the halted PHB production is simply due to lack of space in the organism. The reason for the 'limit' at 44 wt% PHO and the halted PHB accumulation at 5.5 hours is therefore in the last case less clear. The PHH content stays stable at around 9 wt% during the whole accumulation and can therefore not be attributed to either theory.

The oxygen consumption rate of the first 5 hours is significantly higher than during the subsequent 19 hours. In the first 5 hours, 20 mmol of the total 65 mmol oygen is consumed or 30%. The average oxygen consumption rate in the first 5 hours is equal to 0.07 mmol oxygen per minute, compared to 0.04 mmol oxygen per minute in the subsequent 19 hours. This is in line with the expectations, since accumulation of all compounds has then reached its platform. In the first hour, when only PHO increases dramatically, only 3.3 mmol of the total 65 mmol oxygen is consumed, or 5.1%. The average consumption rate of the first hour is also more similar to the average consumption rate of the subsequent 23 hours, with the first hour average oxygen consumption rate 0.055 mmol oxygen per minute and the subsequent 23 hours 0.046 mmol oxygen per minute. Figure 34 in Appendix A.8 shows the evolution of the oxygen consumption rate for the accumulation with octanoic acid.

It should be noted that for this accumulation, the expected initial value of substrate is lower than expected. This is likely due to problems during the addition of the carbon source.

3.3.4 Accumulation with hexanoic acid

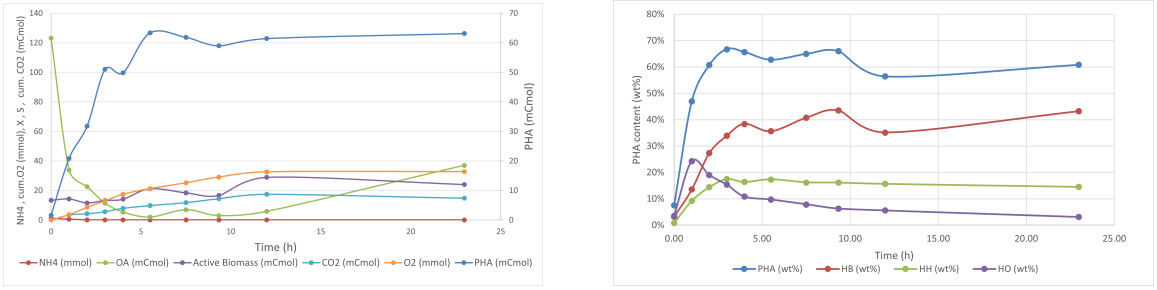

(a) Evolution of important compounds during the accumulation using hexanoic acid as the substrate.

(b) PHA content during the accumulation using hexanoic acid as substrate.

Figure 14: Comparison of the evolution of the compounds during the cycle analysis and the PHA content during the cycle.

The PHA content shown in Figure 14b shows an interesting trend: in the first hour of the accumulation, there is a relatively large peak of 24 wt% PHO. The reaction to go from hexanoate to PHO is a reduction, which means that electrons are required. This is confirmed by the fact that the average oxygen consumption during the first hour is three times higher than during rest of the accumulation: 0.062 mmol/min in the first hour compared to 0.02 mmol/min during the rest of the accumulation. 11% of all oxygen is consumed during this first hour, compared to 89% during the following 23 hours. On top of that, the majority of the ammonia is also consumed during the first hour of the accumulation: 0.674 mmol of the total 1.2 mmol or 56% of the total ammonia. It is possible that in the first hour there is an excess of electrons which require an electron sink in the form of PHO. The production of PHO mostly likely occurs through a reverse β-oxidation pathway. After the first hour of the accumulation, there seems to be less of a need for an electron sink and the accumulation of PHO therefore decreases. In terms of PHO in mCmol in the bioreactor, the PHO content only decreases after 5.5 hours.

During the first 4 hours, when PHB production reaches a platform, 16.4 mmol of the whole 31.8 mmol oxygen is consumed, or 52%. The average oxygen consumption rate for the first 4 hours is equal to 0.07 mmol per minute, while the average oxygen rate for the subsequent 20 hours is equal to 0.01 mmol per minute. Most

of the respiration therefore takes place during the first 4 hours. This can be seen in Figure 35 in Appendix A.8.

In theory, PHH should be the most readily produced product from hexanoic acid since it only requires to go through the β-oxidation pathway 0.5 times, while the production of PHB goes through the β-oxidation pathway 1.5 times. On top of that, the production of PHH instead of PHB should result in lower NADH output, which would be beneficial since the ammonia is depleted fast which means that the electrons cannot be channeled into the biomass production. However, this does not seem to be the case. Instead, the PHB continues to be the most popular product after the first hour of the accumulation. This could be due to the fact that class I phaC genes prefer shorter-chain substrates, like butyryl-CoA. This could therefore indicate that there are two different organisms at work: one organism with a class II phaC gene which produces PHO and another organism or other organisms which produce the PHB. However, it is also possible that the organism which usually makes PHO and/or PHH needed time to adjust to hexanoic acid and therefore started producing PHB later.

It should be noted that the initial amount of substrate in this experiment is higher than expected. However, since the carbon balance closes with only 0.5% off, it is assumed that a mistake was made during the preparation of the medium and not that there was a measuring mistake with the HPLC.

3.4 Third and fourth enrichment: O_2 limitation and uncoupling did not result in higher mcl-PHA production

In line with the original literature study, the third enrichment was done using oxygen limitation. For this enrichment, the reactor was inoculated with biomass from the second enrichment after having been in cold storage for half a month. Based on the production of mcl-PHA from hexanoic acid [47], the airflow was set to 10 mL/min. This system was run for 77 cycles. The evolution of the PHA production during the oxygen limitation can be seen in Figure 15.

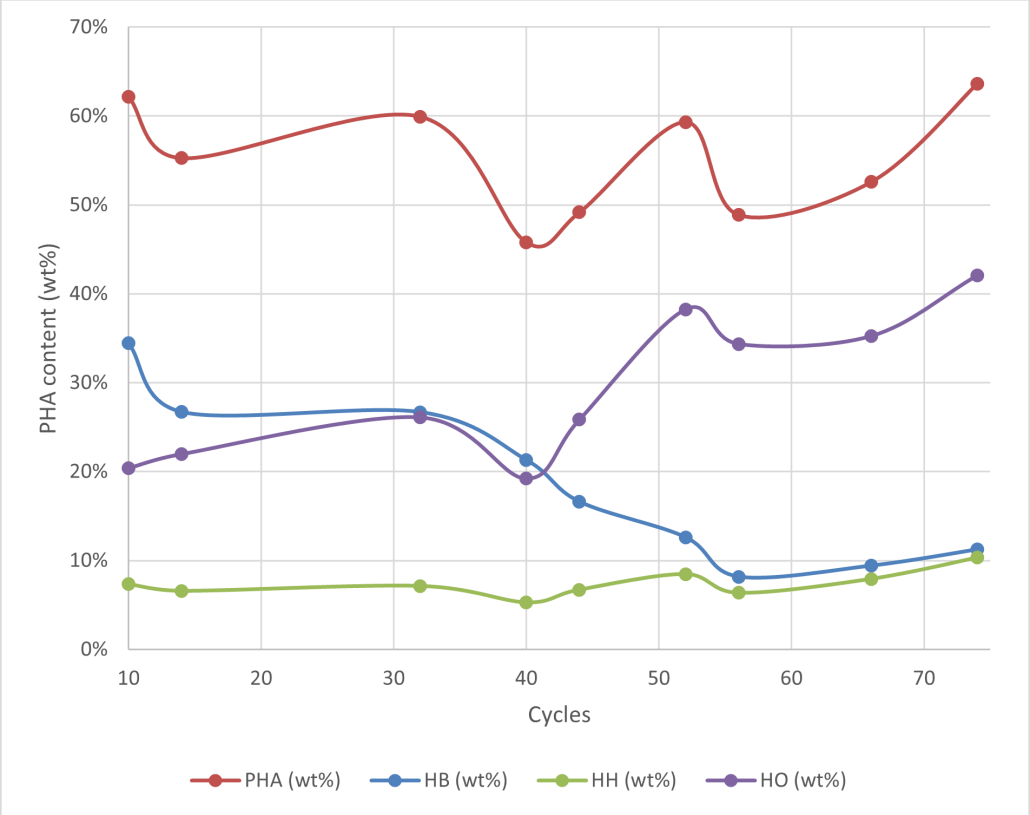

Figure 15: Evolution of the PHA productivity and the weight percentages obtained during the third enrichment with oxygen limitation.

The PHA content and the mcl-PHA content specifically is quite similar to the (mcl-)PHA content of the second enrichment, with a maximum PHO content of 42 wt% and a maximum PHA content of 64 wt%. It is therefore

unclear whether the relatively high PHO content is due to the oxygen limitation, as expected according to literature search, or despite the oxygen limitation. Follow-up research could focus on oxygen limitation with different pH's for the reactor, notably pH 7 and pH 8 as seen in this work. If the mcl-PHA content is more affected by the differences in pH compared to difference in oxygen flow rate, it could indicate that the pH was the deciding factor and not the lower oxygen flow rate. However, the high PHO content with oxygen limitation is a benefit for future industrial applications since this would require less aeration and would therefore cut back on costs. It should be noted that since only one condition was tested, 10 mL/min, that it is possible that other conditions would lead to an improved mcl-PHA production since it is not certain that 10 mL/min is the ideal scenario for the organisms in the reactor. Other conditions were not tested due to limitations in time but should be considered in follow-up research.

The fourth enrichment using an uncoupled system was only run for 26 cycles. The experiment was therefore terminated after 26 cycles. It should be noted that only 2 conditions, with a τ of 1.5 hours and a τ of 2 hours was tried. For both cases, the cycle length of 12 hours was maintained. It was terminated based on the oxygen profile, which can be seen for a τ of 1.5 hours in Figure 16 after 12 cycles. For a comparison with other gas profiles, please refer to Appendix A.7

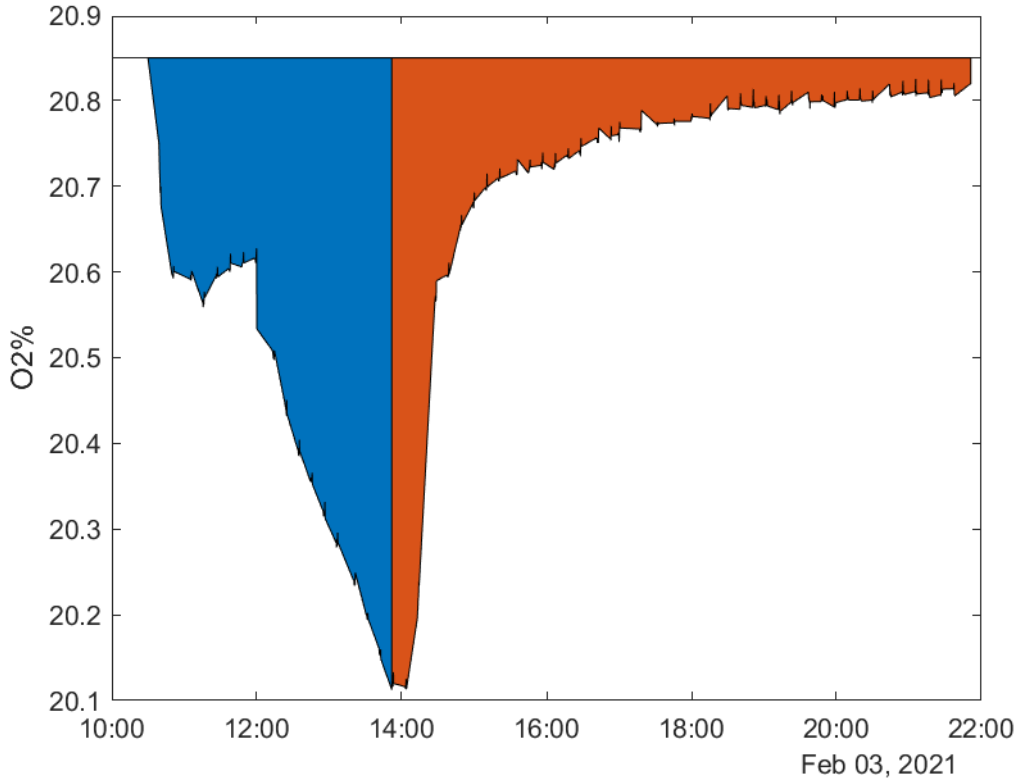

Figure 16: Gas profile enrichment 4 after 12 cycles. In blue, the feast is shown and in orange, the famine is shown. The end of feast was at 13:42, with an oxygen consumption of 52% in the feast. This was 1h42 minutes after N-source addition, which was at 12:00.

During those 90 minutes of the carbon addition and the absence of a nitrogen source, the organisms seem to take up the substrate and then remain inactive until the addition of ammonia. It is assumed that the substrate is not yet consumed during this time based on the growth profile but this was unfortunately not verified. After the addition of ammonia, mainly growth can be seen in the oxygen profile. During the feast, 52% of total oxygen consumed is consumed. Despite almost no mcl-PHA production (2% of PHH and 5% of PHO), there is high PHB production, with a weight percentage of 52%. This is reinforced by the fact that during the famine, no characteristic camel-like or wave-like profile is shown as seen in Appendix A.7, Figure 25b and 26b respectively. The camel-like profile and wave-like profile seem to be excellent indicators of high mcl-PHA production.

The mcl-PHA content decreased further when a τ of 2 hours was used, for a PHO content of 5 wt%, a PHH content of 2 wt% and a PHB content of 51 wt%, for a total PHA content of 58 wt%. It should be noted that the longer τ was only maintained for 14 cycles and only 1 PHA samples was taken. It is therefore potentially not representative of the actual performance of the culture and had potentially not enough time to fully enrich

for a culture which used from the uncoupled system to make more mcl-PHA. It is also is possible that a longer τ in combination with a longer cycle length would lead to higher mcl-PHA production. This should therefore still be considered in follow-up research.

4 General discussion

4.1 Comparison of the enrichments

To get a better understanding of the difference between the enrichments, Table 5 shows the biomass specific consumption rates, biomass specific production rates and the yields of relevant compounds for the cycle analysis of the first and the re-done second enrichment.

Table 5: Comparison of the average biomass specific consumption rate, the average production rates and the yields during the cycle analysis of the first enrichment and the repeat of the second enrichment. These values were calculated using the metabolic and kinetic model.

	Variable	Unit	Enrichment 1	Enrichment 2
Feast	q_{PHB}	[Cmmol/Cmmol/h]	0.49	0.50
	q_{PHH}	[Cmmol/Cmmol/h]	0.22	0.29
	q_{PHO}	[Cmmol/Cmmol/h]	0.69	1.33
	q_S	[Cmmol/Cmmol/h]	2.05	2.13
	$Y_{PHA/S}$	[Cmol/Cmol]	0.68	0.97
	$Y_{X/S}$	[Cmol/Cmol]	0.26	0.03
	$Y_{CO2/S}$	[Cmol/Cmol]	0.07	0.01
	$Y_{O2/S}$	[mol/Cmol]	0.25	0.12
	fraction N consumed in feast		0.36	0.38
Famine	q_{PHB}	[Cmmol/Cmmol/h]	-0.03	-0.03
	q_{PHH}	[Cmmol/Cmmol/h]	-0.01	-0.02
	q_{PHO}	[Cmmol/Cmmol/h]	-0.04	-0.08
	$Y_{X/PHA}$	[Cmol/Cmol]	0.45	0.66
	$Y_{CO2/X}$	[Cmol/Cmol]	0.55	0.35
	fraction N consumed in famine		0.64	0.62
	C-balance (%)		1.65	-2.45
	e-balance (%)		8.71	9.53
	ratio O2 feast/famine		28%	33%

The values shown in Table 5 show a significant difference between the first and the second enrichment. For starters, the values for the yield of O2 over substrate in the feast ($Y_{O_2/S}$) in the first and second enrichment are 0.25 mol/Cmol and 0.12 mol/Cmol respectively or respectively 18% and 9% of the theoretical maximum. This decrease of more than 50% of the amount of oxygen consumed per substrate is at least partly due to the fact that an overestimation of the oxygen consumption in the feast is made with the model for the first enrichment and an underestimation is made for the second enrichment, as seen in Figure 36 and Figure 38. Similarly, the values for the yield of CO2 over substrate in the feast ($Y_{CO_2/S}$) in the first enrichment and the second enrichment are 0.07 and 0.01 Cmol/Cmol respectively or 7% and 1% of the theoretical maximum. Again, an underestimation of the CO_2 production is made for the second enrichment in the model. For the first enrichment, the produced CO_2 is however very in line with the data. It should therefore be noted that the model is not good at predicting the O_2 consumption and at times the CO_2 production compared to the actual production and consumption, as seen in Figure 36 and Figure 37 in Appendix A.9. This is likely related to the difficulty with balancing the delta, or the efficiency of the phosphorylative oxidation, and the ATP maintenance requirement. Since these values directly impact the predicted O_2 consumption and CO_2 production, further works should include a more thorough sensitivity analysis of all fitted parameters and should include a sensitivity analysis of the delta.

The obtained $Y^{feast}_{PHA/S}$ is 0.68 Cmol/Cmol for the first enrichment. This is 67% of the theoretical maximum. The second enrichment had a yield of 0.97 Cmol/Cmol of PHA over substrate in the feast for the second enrichment, equal to 93% of the theoretical maximum. This proves that the second enrichment obtained better results than the first enrichment since more of the substrate went towards the production of PHA. This mainly goes at the expense of biomass, since in the first enrichment the obtained $Y^{feast}_{X/S}$ is equal to 0.26 Cmol/Cmol, while in the second enrichment the value is equal to 0.03 Cmol/Cmol. Both are decidedly less than the theoretical maximum, which is 0.81 Cmol/Cmol. The first enrichment reached 32% of the theoretical maximum, while the second enrichment reached barely 3.8%. This is likely due to the fact that during the second enrichment an apparent dip in the biomass concentration was noted in the feast, while in the first enrichment there was an increase in the amount of biomass during the feast. Despite that, the fraction of N consumed in the feast is practically the same, indicating that while the organisms in the second enrichment did not grow, they did consume the nitrogen

source. This could be an issue of trying to fit a model to uncertain biomass or nitrogen measurements. Since the biomass data for the second enrichment was based on assumptions since the TGA was unavailable, it is possible that the growth during the feast was underestimated and therefore an incorrect yield of biomass over substrate was obtained in the feast was obtained. On the other hand, the O_2 consumption, the CO_2 production, the nitrogen consumption and the active biomass could be fitted to the model quite well for the second enrichment, as can be seen in Figure 38. On the other hand, this is less true for the first enrichment: while the model could be fitted quite well to the O_2 consumption, the CO_2 production and the nitrogen consumption, the model could not be fitted very well to the active biomass concentration. So while it is true that the actual biomass in the second enrichment was likely not the actual concentration in the reactor, it seems that the biomass in the first enrichment was also not completely true to the reactor conditions or the model either. This could also potentially be linked to a wrong assumption for the efficiency of the oxidative phosphorylation and therefore also the ATP maintenance needed.

In the famine, the yield of biomass over PHA ($Y_{X/PHA}^{famine}$) is equal to 0.45 Cmol/Cmol for the first enrichment, 58% of the theoretical maximum, and 0.66 Cmol/Cmol for the second enrichment, or 84% of the theoretical maximum.

The biomass-specific production rate for PHB remained relatively stable during the first and second enrichment, with a value of 0.49 Cmol/Cmol/h in the first enrichment and a value of 0.5 Cmol/Cmol/h in the second enrichment. For PHH and PHO especially, the difference is moch more significant. For PHH, the biomass specific production rate was 0.22 Cmol/Cmol/h in the first enrichment and 0.29 Cmol/Cmol/h in the second enrichment, or an increase of 32%. For PHO, the biomass specific production rate went from 0.69 Cmol/Cmol/h in the first enrichment to 1.33 Cmol/Cmol/h in the second enrichment, or an increase of 92%. At the same time, the biomass specific consumption rate in the famine stays constant for PHB, at a value of 0.03 Cmol/Cmol/h, while the biomass specific consumption rates of PHH and PHO double, from 0.01 Cmol/Cmol/h to 0.02 Cmol/Cmol/h and from 0.04 Cmol/Cmol/h to 0.08 Cmol/Cmol/h respectively. This means that while the production and consumption of PHB remained stable compared to the biomass, the production of PHH and PHO was more rapid but so was the consumption.

The PHA content at the highest PHO content for the different enrichments can be seen in Table 6. For the enrichment 1 and 2, the values from the cycle analysis and the accumulation experiment were taken. Since no cycle analysis or accumulation was performed for enrichment 3, which had oxygen limitation, the highest value during the enrichment was taken. It should be noted however that it is not known whether this sample was taken at the exact moment that the PHA content was at its highest and should therefore be taken with a grain of salt. Since enrichment 4 with an uncoupled system was terminated based on its oxygen profile, no values for this enrichment are known.

Table 6: Comparisons of the highest obtained PHO content during the cycle analysis and accumulation of enrichment 1 and enrichment 2 and one of the cycles during enrichment 3.

		Enrichment 1 pH 7, no O_2 lim.		Enrichment 2 pH 8, no O_2 lim.		Enrichment 3 pH 8, O_2 lim.	
		wt%	mol%	wt%	mol%	wt%	mol%
Cycle	PHB content at highest PHO content	9.21	31.52	12.18	32.15	11.23	25.25
	PHH content at highest PHO content	5.15	13.29	7.24	14.42	10.32	17.50
	Maximum PHO content	26.62	55.19	33.42	53.43	42.06	57.24
	PHA content at highest PHO content	40.97	100.00	52.84	100.00	63.61	100.00
Accumulation	PHB content at highest PHO content	21.48	45.59	27.42	44.83		
	PHH content at highest PHO content	9.54	15.27	9.24	11.40		
	Maximum PHO content	30.44	39.14	44.21	43.77		
	PHA content at highest PHO content	61.45	100.00	80.87	100.00		

The maximum PHO content was found in the original cycle analysis of enrichment 2, with a PHO content of 44%. However, since the system experienced system failure shortly afterwards, enrichment 3 with oxygen limitation had the highest PHO content during the cycle, with a PHO content of 42.06 wt%. This is close to the maximum obtained PHO content of 44.21 wt%, which was obtained during the re-done second enrichment. Since the cycle analysis of the re-done second enrichment did not reach the same PHO content as the original cycle of enrichment 2, it is difficult to say whether a higher weight percentage of PHO could be obtained or whether the 44 wt% is a biological limit of the culture. If 44 wt% is not a biological limit, further research

should try to emulate the conditions of the original second enrichment and should establish whether the oxygen limitation was beneficial to the mcl-PHA producers or whether the third enrichment only performed well due to the higher pH of 8. To do that, NGS data and metagenomic data should be done of the culture during the second enrichment and of the oxygen limitation enrichment.

In terms of mole percentage, all three PHA's remained relatively stable with PHB at around 30 mol%, PHH 15 mol% and PHO 55 mol% during the cycles. This indicates that mainly the amount in terms of weight percentage increased and not the ratio between the different PHA's. During the accumulation, PHO has a slight increase in mol%, while PHH has a decrease in mol%.

For the accumulation, the re-done second enrichment performed notably better than the first enrichment and the original second enrichment, although this should be taken with a grain of salt due to the system failure.

In general, whether a culture will produce mcl-PHA can be anticipated based on the oxygen profile as seen in Appendix A.7. Low ratio's of oxygen consumed in the feast over oxygen consumed in the famine are in this work indicative of high mcl-PHA production and a high mcl-PHA production over PHA production. The lowest ratio, observed around the original cycle analysis of the second enrichment, was equal to 0.0153 and represented a PHO content of 41 wt%, PHH content of 7 wt% and PHB content of 4 wt%, for a total PHA content of 52 wt%. This can be seen in Figure 25b. The oxygen consumption in the feast over the oxygen consumption in the famine can be plotted against the mcl-PHA produced. This can be seen in Figure 17. The highest ratio's of mcl-PHA over PHA production were obtained when the oxygen consumption in the feast was between 22 and 32% of the total oxygen consumption in the cycle. It should be noted that not all PHA samples were taken at their optimal moment so this could lead to inaccuracies in the actual mcl-PHA content. Low oxygen consumption rates being indicative of high mcl-PHA production could be only for octanoic acid, since similar trends were not observed during enrichments with hexanoic acid as performed by [47], seen in Figure 28 in Appendix A.7. The oxygen consumption in the feast over the mcl-PHA production in wt% can also be found in Appendix A.7. Figure 29b shows the enrichments with octanoic acid and Figure 29a shows both the enrichments with octanoic acid and hexanoic acid.

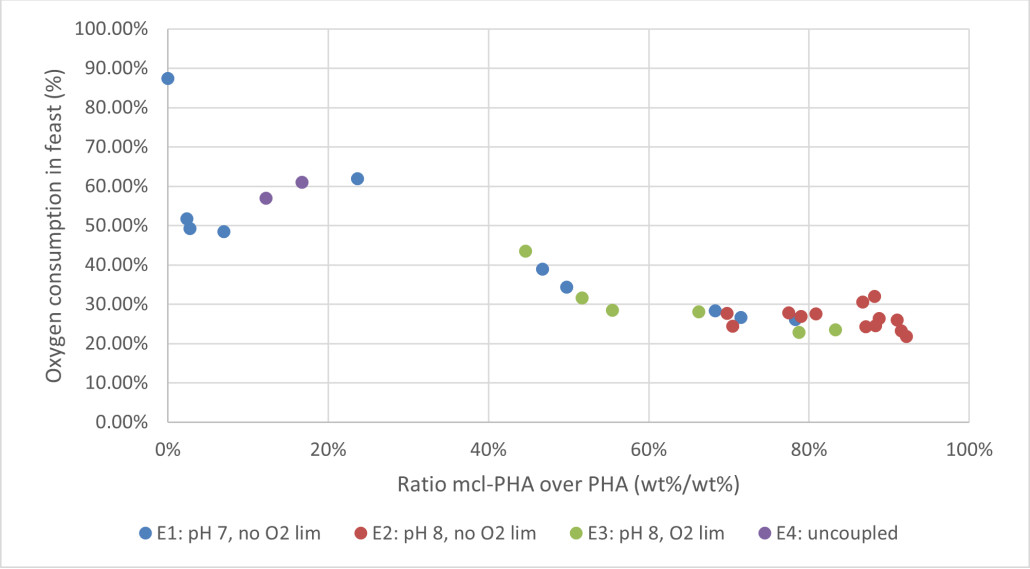

Figure 17: Oxygen consumption in the feast over total oxygen consumption in the cycle plotted against the ratio of mcl-PHA over total PHA production for each enrichment.

4.2 Comparison with literature

In literature, octanoic acid has been used as a substrate for mcl-PHA production. While most of the research has been done using pure cultures, some information is available of mcl-PHA production from mixed cultures. A comparison of literature values and the values obtained in this report can be seen in Table 7.

Table 7: Comparison of PHA content in terms of weight percentage and mole percentage reported in literature and in this report. All values are for experiments with pure octanoic acid. For each experiment, the used organism, the aeration rate, the temperature, the pH and the initial substrate for the accumulation is stated.

Organism	Substrate	Aeration [L/min]	T °C	pH -	$[S]_{init}$ [mM]	PHA [wt%]	PHB [mol%]	PHHx [mol%]	PHO [mol%]	Productivity [mg/L]	Source
MCC	C8	2	30	7	6.2	17.02	60.02	5.22	34.76	427.2	[23]
MCC	C8	2	30	7	12.5	31.09	57.54	6.24	35.92	1125.5	[23]
MCC	C8	2	30	7	18.7	38.1	85.95	2.84	10.87	1570.8	[23]
MCC	C8	2	30	7	12.5	34.07	39.45	8.8	51.74	1366.4	[23]
P. oleovorans NRRL B- 778	C8	2	30	no[1]	-		99	0	<1	250	[16]
P. putida BM01	C8	yes	30	-	40	58.1	-	7	88	2180	[48]
P. citronellolis ATCC 13674	C8	yes	30	-	40	28.6	-	12	85	610	[48]
P. aeruginosa ATCC 29347	C8	yes	30	-	40	27.3	-	7	90	650	[48]
P. aeruginosa ATCC 27583	C8	yes	30	-	40	21.3	-	10	86	390	[48]
P. fluorescens BM07	C8	yes	30	-	40	27.7	-	8	86	790	[48]
P. oleovorans	C8	yes	31	7	10		-	9.6	86.1	-	[49]
P. putida Bet001	C8	yes	30	7	10	49.7	-	8.1	76.2	-	[50]
MCC	C8	0.2	30	7	9.5	61.45	45.59	15.27	39.14	-	This work
MCC	C8	0.2	30	8	9.5	80.87	44.83	11.4	43.77	-	This work

The mole percentages of PHB, PHH and PHO can differ wildly. A pure culture with a pure substrate, namely octanoic acid, can result in high mole percentages of PHO [48], [49], [50]. For a pure culture, up to 90% of the PHA can be PHO [48]. Mixed cultures appear to have much lower mole percentages of PHO, with mole percentages of around 35%. While the first enrichment, with a pH of 7, only reached a mole percentage of 39% PHO, the second enrichment with a pH of 8 was able to reach a mole percentage of 44% PHO. The mole percentage of mcl-PHA in this research are slightly higher compare to the mole percentages obtained by Chen, who also used a mixed culture, and far below the levels obtained using pure cultures. However, the obtained PHA content in terms of weight percentage obtained in this report are far better than previously reported values. In the research of Chen, it was shown that the time until accumulation had a large impact on the mole percentage of mcl-PHA. For an aeration of 2 L/min, a temperature of 30°C, a pH of 7 and an initial substrate concentration of 12.5, the mole percentage shifted from 35.9% if the sequential batch was run for 2 months before accumulation to a mole percentage of 51.7% if the sequential batch was run for 4 months before accumulation. The influence of the pH become therefore less certain since the enrichment at pH 8 was started by inoculating the reactor with biomass from the end of the enrichment at pH 7. Perhaps the stark increase in mcl-PHA can be at least partially attributed to an increased enrichment time. Since Chen saw a shift in the microbial community between the enrichment of 2 months and the enrichment of 4 months, analysing the microbial community for the second enrichment would be recommended. Another observation is the difference in the initial substrate concentration used in previous research. In general, higher initial concentrations of substrate seems to lead to a decline in the PHA content in terms of weight percentage based on the limited amount of information presented in Table 7. This could be due to the potential toxicity of the octanoic acid. This is however disputed by *P. putida BM01*, which had a an initial substrate concentration of 40 mM and had a PHA content of 58 wt%.

A point of note is the absence of some of the bioreactor-specific parameters, like the SRT. Since the SRT can vary wildly in literature, the SRT could potentially still have an important role in the mcl-PHA production and selecting for mcl-PHA producers.

4.3 Mcl-PHA producers

During the first enrichment, the *Sphaerotilus* were the dominant organism. This was confirmed with both NGS data and microscopy data, as seen in Figure 7a and Figure 8. However, *Sphaerotilus* are not known to produce mcl-PHA and have not been shown to posses the class II phaC gene, a requisite for the production of mcl-PHA. On top of that, *Sphaerotilus* is mainly present in streams with low oxygen concentrations, an excess of nutrients in relation to the active biomass concentration or in streams with a high carbohydrate to nitrogen ratio [45], none of which applies to the conditions during the first enrichment. On the other hand, *Sphaerotilus* has not been investigated with specifically octanoic acid as a substrate before. Potentially *Sphaerotilus* flourishes with medium chain length fatty acids as substrate, although it has been reported that caprate and caprylate do not support PHB accumulation and cell growth is almost completely inhibited by these substrates [46]. To fully

[1]No pH control was performed.

confirm the *Sphaerotilus* as the mcl-PHA producers and understand the conditions which lead to enriching for this organism, metagenomics data and/or isolation of this organism and analysis of the pure culture should be performed. The metagenomics data should reveal whether an organism in the culture has the required class II phaC gene. If *Sphaerotilus* does not possess this gene, either there is another, closely related gene which could produce mcl-PHA or another organism is responsible for the production of mcl-PHA. If *Sphaerotilus* does possess the class II phaC gene, this would be the first noted occurrence of that. Isolating the *Sphaerotilus* was unsuccessful with plates, presumably at first due to the death/inactivity of the cells due to cold storage which they are sensitive to [51]. However, despite re-growing the culture and confirming the return of *Sphaerotilus* after 28 cycles, the *Sphaerotilus* were not able to grow on any of the plates. This could potentially be due to the fact that there is a preference for low oxygen concentration or due to the preference for high nutrient levels [44], [45].

During the second enrichment, the mcl-PHA content increased as seen in Table 6. Despite that, the *Sphaerotilus* suspected of being the main mcl-PHA producers in the first enrichment have slowly disappeared, as confirmed with microscopy (data not shown). This was also seen in the biofilm production: the characteristic 'fluffy' biofilm of the first enrichment was no longer present during the second enrichment. This could be due to the fact that at higher pH, *Sphaerotilus* has a decrease in PHB production but also a decrease in growth rate [51], [44]. Since no information is known about a *Sphaerotilus* producing mcl-PHA, it is possible that the decrease in PHB potentially combined with a decrease in mcl-PHA production caused the cells to be outcompeted by an organism which was not bothered by the increased pH or even preferred the higher pH. However, NGS data is necessary to say anything about that. It should be noted that according to [44], *Comamonas testosteroni* has a 90.7% similarity with *Sphaerotilus* in terms of 16S rDNA sequence. *Comamonas testosteroni* is a known mcl-PHA producer [52]. Perhaps the similarity included the phaC genes and *Sphaerotilus* is able to produce mcl-PHA or the organism was mistakenly identified for *Sphaerotilus* during the analysis of the NGS samples and no new information was gained about the mcl-PHA producing capacities of *Sphaerotilus* with this work.

For the oxygen limitation enrichment, *Sphaerotilus* should have an advantage since it prefers oxygen limited environments but the increased pH could still obstruct the organism. NGS should be performed to say anything conclusively about the culture during the oxygen limited enrichment.

4.4 PHA preference of the organism

It was expected that octanoic acid would mainly result in the production of PHO and some PHH with few PHB and that hexanoic acid would result in mainly PHH and some PHB [53]. However, this was under the assumption that *Pseudomonas* would be the dominant organism and this was proven not to be the case in the first enrichment. However, the accumulation with octanoate and hexanoate after the second enrichment, as seen in Figure 13 and 14 respectively, show that the inner mechanisms of the cell are not very well understood.

The accumulation with hexanoate as seen in Figure 14 begs some questions about the metabolism of the cell. In the first hour of the accumulation with hexanoate, a peak of PHO was observed. This peak was soon after overtaken by the PHB content and the PHO content slowly faded out over the course of the accumulation. Meanwhile, the production of both PHB and PHH reach a platform, albeit at different levels, at around 4 hours. Clearly, a reductive pathway and an oxidative pathway are performing at the same time although it is unclear whether those pathways are working in the same organism. On top of that, despite being fed hexanoic acid, the production of PHB reached far greater levels than the production of PHH. Since there are two types of class II phaC genes, phaC1 and phaC2, it is possible that the organisms in this culture have the phaC1 gene. This gene has a lower affinity for HH monomers [54]. This will need to be confirmed by metagenomic data.

For the accumulation with octanoates seen in Figure 13, a maximum of 44 wt% PHO is observed. This plateau was obtained very fast and was practically maintained throughout the whole accumulation. Meanwhile, PHB reached its maximum plateau of around 28 wt% rather slowly: it takes 4 hours longer to reach the PHB peak compared to the PHO peak. This begs the question whether the observed biological maximum of 44 wt% for PHO is absolute and whether there are conditions which can go beyond this observed limit. On top of that, the question remains whether 1 organism is responsible for both the PHO production and the PHB production or whether there are 2 or more different organisms at work.

4.5 Economic significance of this work

The production of scl-PHA has already been considered as a biodegradable alternative for plastic but its high production costs have also hindered a full breakthrough: for a pure culture with sugars or agricultural feedstock

as substrate, the costs of production can be five times higher than traditional plastic production. [55]. A similar issue plagues the production of mcl-PHA as a biodegradable rubber. Currently, the price of rubber is relatively high at 2.37 US dollar per kilo. [56] However, since rubber is a commodity, this is still a low price to justify the capital investment of buying fermentation equipment and the operational costs for fermentation. This is especially true since the downstream processing has not yet been investigated, which is a notoriously cost intensive process. On top that, octanoic acid as a pure substrate is 4 dollars/kg and therefore more expensive than the rubber it would produce. [57] Despite the high mcl-PHA content, both in terms of weight percentage and in terms of mole percentage, this process would not be economically viable. The high mcl-PHA content does prove that this process has potential. Potentially, coupling this process to a wastewater treating process with organisms which can do chain elongation can improve the economic prospects of this process, since octanoic acid is a potential product from the chain elongation process. [58] However, the potential uses for the rubber would be reduced since the original substrate is waste water unless the produced octanoic acid can be separated from the waste stream and purified. While this work shows that mcl-PHA production still has a long way to go, the high mcl-PHA content proves that steps in the right direction are being made.

5 Conclusion

The goal of this research was to find bioreactor conditions which led to high mcl-PHA content when using octanoic acid as a substrate. The medium chain length fatty acid octanoic acid was a successful selection pressure of itself at pH 7, and resulted in mcl-PHA weight percentages of 26.62 wt% PHO and 5.15 wt% PHH during the cycle. This was raised to 30.44 wt% PHO and 9.54 wt% PHH during the accumulation. An increase in pH from 7 to 8 also increased the mcl-PHA production, to 33.42 wt% PHO and 7.24 wt% PHH during the cycle and 44.21 wt% PHO and 9.24 wt% PHH during the accumulation. Two other condition changes were also investigated: oxygen limitation and uncoupling the system. For oxygen limitation, the oxygen flow rate was reduced to 5% of the original flow rate and the increased pH of 8 of the second enrichment was kept. This resulted in similar values as the enrichment which did not have oxygen limitation but had the higher pH. It is therefore unclear whether the lowered oxygen flow rate could be attributed to the high mcl-PHA production or that the culture performed well despite the added oxygen stress. The uncoupled system was a system where the nitrogen source was added 2 hours after addition of the carbon source. Based on the oxygen profile, this resulted in a culture which was mainly inactive until the nitrogen source was added.

Another point that remains unclear from this research is which organism(s) are responsible for the accumulation of the PHO and whether the organisms which produce high levels of PHO also produce PHB and PHH. During the first enrichment with octanoic acid the only selection pressure, the dominant organism was *Sphaerotilus* based on 16S-rRNA data. This organism is not known to produce mcl-PHA. For the enrichment with an increased pH as an additional selection pressure, the NGS data is not yet known at the time of writing. However, based on the microscopy done during the experiment, *Sphaerotilus* was not the dominating organism. Based on the NGS data, further follow-up research should be done.

Finally, this work has used a model to determine biomass specific consumption rates, biomass specific production rates and biomass specific yields. This model was constructed using metabolic data, kinetic equations and data from experiments to fit the model more precisely. This was a useful addition to the experimental data and provided a more thorough understanding of the evolution of the compounds during the cycles.

6 Recommendations

At present it is unclear whether a lower oxygen flow rate is beneficial for the mcl-PHA production. This should be investigated in more detail in a follow-up research. Since only one flow rate was investigated, follow-up research should focus on optimising the flow rate. A lowered required oxygen flow rate with similar results could be a plus for industry, since it would require less aeration for similar results.

A lot of issues with the model could have been resolved by a more thorough sensitivity analysis. A suggested approach for this sensitivity analysis would be the following based on the Matlab model: in the Matlab model, all relevant fitted parameters and the delta as a measure of the phosphorylative oxidation should be kept as a range of values. These parameters would therefore be: q_{PHA}^{max}, p, q_S^{max}, μ^{max}, K_S, m_{ATP}, k, δ and n. The ranges would be determined based on literature and expected values. The model would iterate through each value and combine it with other potential values of the other parameters. This way, a big matrix is developed so that for each combination of values for the parameters a final cycle is calculated. The obtained data for the cycle analysis can then be compared to this calculated final cycle. Using the least squares method, the difference between the obtained data and the model can be calculated. The combination of parameters which lead to the smallest deviation from the obtained data should be the optimal value for each parameter. Due to the number of values and parameters, this could be very time-consuming and optimising this would be preferred. A potential drawback of this method is that it is very reliant on the obtained data. Since there is also some uncertainty about the reliability of the biomass data from the second enrichment due to the unavailability of the TGA, this could pose a problem. However, this problem is also present in the current model.

Only two different τ were investigated during this experiment (1.5 hours and 2 hours) and neither were maintained for long enough to draw conclusive results about the effectiveness of either condition. At present, the culture seemingly preferred to remain inactive after carbon addition until the nitrogen source was added. Follow-up research should focus on determining whether this observation continues being true at higher intervals between the carbon addition and the nitrogen addition, since there could be a "breaking point" where it might no longer be a viable strategy to "wait" until the nitrogen source is added. This should likely be done in combination with longer cycle times.

According to NGS data, the dominant organism in the first enrichment at pH 7 was *Sphaerotilus*. This organism is not known in literature to produce mcl-PHA. Follow-up reseach could therefore focus on isolation this organism and analysing this organism with metagenomic data to verify whether this organism is responsible for mcl-PHA production. Since the isolation using various different plates did not work, a shake flask approach could be considered to isolate the organism from the mixed culture since this condition would have less oxygen available and nutrients could be added manually to maintain high nutrient levels. By cultivating a sample of the original culture in a shake flask, the characteristic flocs which are formed by the *Sphaerotilus* in combination with microscopic confirmation can be used to select cells for the next batch. Taken into account literature research, an excess of carbohydrates combined with a high C:N ratio and oxygen limitation could provide good conditions for the *Sphaerotilus* to grow [45]. However, it is unsure whether they would retain the ability to produce mcl-PHA if grown under these conditions. Therefore, it is also important to feed the isolated *Sphaerotilus* octanoic acid or to feed octanoic acid during the isolation process as a way to keep this selection pressure. The metagenomic data could give insight in whether this organism has the required clas II phaC gene which is defining for mcl-PHA producers. Another way to identify whether the class II phaC genes are present is through the use of a polymerase chain reaction (PCR) based on the highly conserved sequences found in the coding regions of *Pseudomonas* phaC1 and phaC2 genes [59]. This has the advantage that it can use the lysate of the genomic suspension and that it is in general more rapid, cheaper and simpler than analysing genomic data. On the negative side, if there are mutations in the highly conserves sequences, potential organisms with class II phaC gene can be overlooked.

No properties of the obtained PHA (mixtures) have been determined. It should also be noted that the GC determination of PHA content measures the monomers of the PHA. It is therefore not known whether co-polymers or separate polymers are formed. To establish the obtained PHA as a rubber replacement, the kinetic and mechanical properties should be established in follow up research, with important parameters including the unit composition, the molar mass, the mechanical properties and the thermal properties [16]. The unit compositions could be determined by GC/MS as described by [49]. Thermal properties which are of interest are the molecular weight, the melting temperature, the glass transition temperature and the degradation temperature [16],[50]. For the thermal properties, an adjusted thermogravical analysis could be performed [21]. The mechanical properties which are of interest are the tensile stress at break and the elongation (strain) at break [21]. However, these are mainly of interest for mcl-PHA films for when mcl-PHA is closer to being applied.

Before investigating the mechanical properties, downstream processing needs to be done. No downstream processing has been done during the experiment. Since this is a critical component of the cost viability, this should be investigated in new research.

Another interesting idea for follow-up research could be accumulation with various other substrates, including but not limited to butyrate and acetate. Potentially, other carbon sources like sugars could be used, likely after an enrichment with a medium chain fatty acid like octanoic acid.

List of symbols and abbreviations

Table 8: List of symbols and abbreviations used in this work.

(P)HA	(poly)hydroxyalkanoate
(P)HB	(poly)hydroxybutyrate
(P)HH	(poly)hydroxyhexanoate
(P)HO	(poly)hydroxyoctanoate
α_{PHA}	Exponent of the PHA inhibition term
δ	Efficiency of the oxidative phosphorylation
μ	Biomass specific growth rate [h^{-1}]
τ	Time between carbon addition and nitrogen addition [h]
CO_2	Carbon dioxide
f_{PHB}^{max}	Maximum fraction PHB [Cmol/Cmol]
f_{PHH}^{max}	Maximum fraction PHH [Cmol/Cmol]
f_{PHO}^{max}	Maximum fraction PHO [Cmol/Cmol]
GC	Gas chromatography
HA	Hexanoic acid
HPLC	High performance liquid chromatography
HRT	Hydraulic retention time
k_{PHA}	Rate constant for PHA degradation
K_N	Half saturation constant nitrogen source [mol/L]
K_S	Half saturation constant substrate [Cmol/L]
m_{ATP}	Specific ATP requirement for maintenance [mol/Cmol/h]
mcl-PHA	Medium-chainlength poly-hydroxy-alkanoates
NGS	Next generation sequencing
O_2	Oxygen
OA	Octanoic acid
OS	Oxidation state [e-mol/Cmol]
PHA	Polyhydroxyalkanoate
q_i	Biomass-specific production rate of compound i [(c)mol/Cmol/h]
q_i^{max}	Maximum specific uptake rate compound i [Cmol/Cmol/h]
S	Substrate
scl-PHA	Short-chainlength poly-hydroxy-alkanoates
SRT	Solid retention time
TGA	Thermogravimetric analysis
TSS	Total suspended solids
VFA	Volatile fatty acid
VSS	Volatile suspended solids
X	(Active) biomass
$Y_{i,j}$	Yield of compound i on j [(c)mol/Cmol]

References

[1] Jan B. van Beilen and Yves Poirier. Establishment of new crops for the production of natural rubber, 11 2007. ISSN 01677799.

[2] Brian Belcher, Ndan Imang, Ramadhani ACHDIAWAN Belcher, East Kalimantan, and Ramadhani Achdiawan. RATTAN, RUBBER, OR OIL PALM: CULTURAL AND FINANCIAL CONSIDERATIONS FOR FARMERS IN KALIMANTAN I. Technical report, 2004.

[3] W Gordon Whaley. Rubber-The Primary Sources For American Production Despite extensive war-time investigations of other rubber-containing latex plants, the Park rubber tree of Brazil remains, by any measure, the world's fore-most source, and only guayule and the Russian da. Technical report.

[4] B. Jean Meade, David N. Weissman, and Donald H. Beezhold. Latex allergy: Past and present, 2 2002. ISSN 15675769.

[5] Juliana B. Silva, João R. Pereira, Bruno C. Marreiros, Maria A.M. Reis, and Filomena Freitas. Microbial production of medium-chain length polyhydroxyalkanoates, 3 2021. ISSN 13595113.

[6] Constantina Kourmentza, Jersson Plácido, Nikolaos Venetsaneas, Anna Burniol-Figols, Cristiano Varrone, Hariklia N. Gavala, and Maria A.M. Reis. Recent advances and challenges towards sustainable polyhydroxyalkanoate (PHA) production, 6 2017. ISSN 23065354.

[7] Luisa S. Serafim, Paulo C. Lemos, Maria G.E. Albuquerque, and Maria A.M. Reis. Strategies for PHA production by mixed cultures and renewable waste materials, 12 2008. ISSN 01757598. URL https://link-springer-com.tudelft.idm.oclc.org/article/10.1007/s00253-008-1757-y.

[8] Martin Koller. Advances in Polyhydroxyalkanoate (PHA) Production. *Bioengineering*, 4(4):88, 11 2017. ISSN 2306-5354. doi: 10.3390/bioengineering4040088. URL http://www.mdpi.com/2306-5354/4/4/88.

[9] Rijuta Ganesh Saratale, Si Kyung Cho, Ganesh Dattatraya Saratale, Avinash A. Kadam, Gajanan S. Ghodake, Manu Kumar, Ram Naresh Bharagava, Gopalakrishnan Kumar, Dong Su Kim, Sikandar I. Mulla, and Han Seung Shin. A comprehensive overview and recent advances on polyhydroxyalkanoates (PHA) production using various organic waste streams, 4 2021. ISSN 18732976.

[10] G J M De Koning, H M M Van Bilsen, P J Lemstra, W Hazenbergt, B Witholtt, H Preusting, J G Van Der Galii˜n, A Schirmer, and D Jendrossek. A biodegradable rubber by crosslinking poly(hydroxyalkanoate) from Pseudomonas oleovorans. Technical report, 1994.

[11] Alexander Steinbüchel. Production of rubber-like polymers by microorganisms, 2003. ISSN 13695274.

[12] Sun Hee Lee, Jae Hee Kim, Debaraj Mishra, Yu Yang Ni, and Young Ha Rhee. Production of medium-chain-length polyhydroxyalkanoates by activated sludge enriched under periodic feeding with nonanoic acid. *Bioresource Technology*, 102(10):6159–6166, 5 2011. ISSN 09608524. doi: 10.1016/j.biortech.2011.03.025.

[13] Guo-Qiang Chen, Xin-Yu Chen, Fu-Qing Wu, and Jin-Chun Chen. Polyhydroxyalkanoates (PHA) toward cost competitiveness and functionality. *Advanced Industrial and Engineering Polymer Research*, 3(1):1–7, 1 2020. ISSN 25425048. doi: 10.1016/j.aiepr.2019.11.001.

[14] Mark W. Silby, Craig Winstanley, Scott A.C. Godfrey, Stuart B. Levy, and Robert W. Jackson. Pseudomonas genomes: Diverse and adaptable. *FEMS Microbiology Reviews*, 35(4):652–680, 7 2011. ISSN 01686445. doi: 10.1111/j.1574-6976.2011.00269.x. URL https://academic.oup.com/femsre/article/35/4/652/630861.

[15] Richard A Gross, Christopher Demello, Robert W Lenz, Helmut Brandi, and R Clinton Fuller. Biosynthesis and Characterization of Poly(/3-hydroxyalkanoates) Produced by Pseudomonas oleovorans. ISSN 1106-1115. URL https://pubs.acs.org/sharingguidelines.

[16] RD Ashby, Dky Solaiman, and TA Foglia. The synthesis of short- and medium-chain-length poly(hydroxyalkanoate) mixtures from glucose- or alkanoic acid-grown Pseudomonas oleovorans. *Journal of Industrial Microbiology & Biotechnology*, 28(3):147–153, 2002. ISSN 13675435. doi: 10.1038/sj/jim/7000231. URL www.nature.com.

[17] Ji Hoon Shim, Ki-Whan Chi, and Sung Chul Yoon. Swinging effect of salicylic acid on the accumulation of polyhydroxyalkanoic acid (PHA) in Pseudomonas aeruginosa BM114 synthesizing both MCL-and SCL-

PHA Rashba effect View project supramolecular coordination chemistry View project. Technical report, 2008. URL https://www.researchgate.net/publication/5683134.

[18] Zhiyong Sun, Juliana A. Ramsay, Martin Guay, and Bruce A. Ramsay. Carbon-limited fed-batch production of medium-chain-length polyhydroxyalkanoates from nonanoic acid by Pseudomonas putida KT2440. *Applied Microbiology and Biotechnology*, 74(1):69–77, 2 2007. ISSN 01757598. doi: 10.1007/s00253-006-0655-4. URL https://link.springer.com/article/10.1007/s00253-006-0655-4.

[19] D. Fernández, E. Rodríguez, M. Bassas, M. Viñas, A. M. Solanas, J. Llorens, A. M. Marqués, and A. Manresa. Agro-industrial oily wastes as substrates for PHA production by the new strain Pseudomonas aeruginosa NCIB 40045: Effect of culture conditions. *Biochemical Engineering Journal*, 26(2-3):159–167, 11 2005. ISSN 1369703X. doi: 10.1016/j.bej.2005.04.022.

[20] Justyna Mozejko and Slawomir Ciesielski. Saponified waste palm oil as an attractive renewable resource for mcl-polyhydroxyalkanoate synthesis. *Journal of Bioscience and Bioengineering*, 116(4):485–492, 10 2013. ISSN 13891723. doi: 10.1016/j.jbiosc.2013.04.014.

[21] Ana Teresa Rebocho, Joao R. Pereira, Filomena Freitas, Luisa A. Neves, Vitor D. Alves, Chantal Sevrin, Christian Grandfils, and Maria A.M. Reis. Production of medium-chain length polyhydroxyalkanoates by Pseudomonas citronellolis grown in apple pulp waste. *Applied Food Biotechnology*, 6(1):71–82, 2019. ISSN 24234214. doi: 10.22037/afb.v6i1.21793.

[22] Ryan Kniewel, Olga Revelles Lopez, and M. Auxiliadora Prieto. Biogenesis of Medium-Chain-Length Polyhydroxyalkanoates. In *Biogenesis of Fatty Acids, Lipids and Membranes*, pages 457–481. Springer International Publishing, 2019. doi: 10.1007/978-3-319-50430-8{_}29. URL https://doi.org/10.1007/978-3-319-50430-8_29.

[23] Zheng Chen, Chuanpan Zhang, Liang Shen, Heng Li, Yajuan Peng, Haitao Wang, Ning He, Qingbiao Li, and Yuanpeng Wang. Synthesis of Short-Chain-Length and Medium-Chain-Length Polyhydroxyalkanoate Blends from Activated Sludge by Manipulating Octanoic Acid and Nonanoic Acid as Carbon Sources. *Journal of Agricultural and Food Chemistry*, 66(42):11043–11054, 10 2018. ISSN 15205118. doi: 10.1021/acs.jafc.8b04001.

[24] Michele B Kellerhals, Birgit Kessler, Bernard Witholt, Alexandre Tchouboukov, and Helmut Brandl. Renewable Long-Chain Fatty Acids for Production of Biodegradable Medium-Chain-Length Polyhydroxyalkanoates (mcl-PHAs) at Laboratory and Pilot Plant Scales. 2000. doi: 10.1021/ma000655k. URL https://pubs.acs.org/sharingguidelines.

[25] Leo A. Kucek, Catherine M. Spirito, and Largus T. Angenent. High n-caprylate productivities and specificities from dilute ethanol and acetate: Chain elongation with microbiomes to upgrade products from syngas fermentation. *Energy and Environmental Science*, 9(11):3482–3494, 11 2016. ISSN 17545706. doi: 10.1039/c6ee01487a.

[26] T. I.M. Grootscholten, D. P.B.T.B. Strik, K. J.J. Steinbusch, C. J.N. Buisman, and H. V.M. Hamelers. Two-stage medium chain fatty acid (MCFA) production from municipal solid waste and ethanol. *Applied Energy*, 116:223–229, 3 2014. ISSN 03062619. doi: 10.1016/j.apenergy.2013.11.061.

[27] Kirsten J.J. Steinbusch, Hubertus V.M. Hamelers, Caroline M. Plugge, and Cees J.N. Buisman. Biological formation of caproate and caprylate from acetate: Fuel and chemical production from low grade biomass. *Energy and Environmental Science*, 4(1):216–224, 1 2011. ISSN 17545692. doi: 10.1039/c0ee00282h. URL www.rsc.org/ees.

[28] Roland Durner, Manfred Zinn, Bernard Witholt, and Thomas Egli. Accumulation of poly[(R)-3-hydroxyalkanoates] inPseudomonas oleovorans during growth in batch and chemostat culture with different carbon sources. *Biotechnology and Bioengineering*, 72(3):278–288, 2 2001. ISSN 0006-3592. doi: 10.1002/1097-0290(20010205)72:3<278::AID-BIT4>3.0.CO;2-G. URL https://onlinelibrary.wiley.com/doi/10.1002/1097-0290(20010205)72:3%3C278::AID-BIT4%3E3.0.CO;2-G.

[29] Martin Koller and Gerhart Braunegg. Potential and prospects of continuous polyhydroxyalkanoate (PHA) production, 6 2015. ISSN 23065354. URL www.mdpi.com/journal/bioengineering.

[30] Martin Koller. A review on established and emerging fermentation schemes for microbial production of polyhydroxyalkanoate (PHA) biopolyesters, 4 2018. ISSN 23115637. URL www.mdpi.com/journal/fermentation.

[31] Juan Nogales, Bernhard Palsson, and Ines Thiele. A genome-scale metabolic reconstruction of Pseudomonas putida KT2440: iJN746 as a cell factory. *BMC Systems Biology*, 2(1):1–20, 9 2008. ISSN 17520509. doi: 10.1186/1752-0509-2-79. URL https://link.springer.com/articles/10.1186/1752-0509-2-79https://link.springer.com/article/10.1186/1752-0509-2-79.

[32] S. Baumberg. Genetics and biochemistry of Pseudomonas. *Biochemical Education*, 3(3):46, 7 1975. ISSN 03074412. doi: 10.1016/0307-4412(75)90048-5. URL https://linkinghub.elsevier.com/retrieve/pii/0307441275900485.

[33] Liang Shen, Hongyou Hu, Hongfang Ji, Chuanpan Zhang, Ning He, Qingbiao Li, and Yuanpeng Wang. Production of poly(3-hydroxybutyrate-co-3-hydroxyhexanoate) from excess activated sludge as a promising substitute of pure culture. *Bioresource Technology*, 189:236–242, 8 2015. ISSN 18732976. doi: 10.1016/j.biortech.2015.04.007.

[34] Ana R. Pisco, Simon Bengtsson, Alan Werker, Maria A.M. Reis, and Paulo C. Lemos. Community structure evolution and enrichment of glycogen-accumulating organisms producing polyhydroxyalkanoates from fermented molasses. *Applied and Environmental Microbiology*, 75(14):4676–4686, 7 2009. ISSN 00992240. doi: 10.1128/AEM.02486-08.

[35] Katja Johnson, Yang Jiang, Robbert Kleerebezem, Gerard Muyzer, and Mark C.M. Van Loosdrecht. Enrichment of a mixed bacterial culture with a high polyhydroxyalkanoate storage capacity. In *Biomacromolecules*, volume 10, pages 670–676, 2009. doi: 10.1021/bm8013796. URL https://pubs.acs.org/sharingguidelines.

[36] Warren Blunt, Christopher Dartiailh, Richard Sparling, Daniel Gapes, David B Levin, and Nazim Cicek. Microaerophilic environments improve the productivity of medium chain length polyhydroxyalkanoate biosynthesis from fatty acids in Pseudomonas putida LS46. 2017. doi: 10.1016/j.procbio.2017.04.028. URL http://dx.doi.org/10.1016/j.procbio.2017.04.028.

[37] Catarina S.S. Oliveira, Carlos E. Silva, Gilda Carvalho, and Maria A. Reis. Strategies for efficiently selecting PHA producing mixed microbial cultures using complex feedstocks: Feast and famine regime and uncoupled carbon and nitrogen availabilities. *New Biotechnology*, 37:69–79, 7 2017. ISSN 18764347. doi: 10.1016/j.nbt.2016.10.008.

[38] K. Tatari, A. Gülay, B. Thamdrup, H. J. Albrechtsen, and B. F. Smets. Challenges in using allylthiourea and chlorate as specific nitrification inhibitors. *Chemosphere*, 182:301–305, 9 2017. ISSN 18791298. doi: 10.1016/j.chemosphere.2017.05.005.

[39] W. VISHNIAC and M. SANTER. The thiobacilli. *Bacteriological reviews*, 21(3):195–213, 1957. ISSN 00053678. doi: 10.1128/mmbr.21.3.195-213.1957.

[40] Matlab, 2020.

[41] Leonie Marang, Mark C.M. van Loosdrecht, and Robbert Kleerebezem. Modeling the Competition between PHA-Producing and Non-PHA-Producing Bacteria in Feast-Famine SBR and Staged CSTR Systems. Technical report, Technical University of Delft, Delft, 2015.

[42] Yang Jiang, Marit Hebly, Robbert Kleerebezem, Gerard Muyzer, and Mark C.M. van Loosdrecht. Metabolic modeling of mixed substrate uptake for polyhydroxyalkanoate (PHA) production. *Water Research*, 45(3):1309–1321, 1 2011. ISSN 0043-1354. doi: 10.1016/J.WATRES.2010.10.009.

[43] J. J. Beun, K. Dircks, M. C.M. Van Loosdrecht, and J. J. Heijnen. Poly-β-hydroxybutyrate metabolism in dynamically fed mixed microbial cultures. *Water Research*, 36(5):1167–1180, 3 2002. ISSN 0043-1354. doi: 10.1016/S0043-1354(01)00317-7.

[44] Véronique Pellegrin, Stefan Juretschko, Michael Wagner, and Gilles Cottenceau. Morphological and biochemical properties of a Sphaerotilus sp. isolated from paper mill slimes. *Applied and Environmental Microbiology*, 65(1):156–162, 1999. ISSN 00992240. doi: 10.1128/aem.65.1.156-162.1999. URL /pmc/articles/PMC90997/?report=abstracthttps://www.ncbi.nlm.nih.gov/pmc/articles/PMC90997/.

[45] Norman C. Dondero. Sphaerotilus, Its Nature and Economic Significance. *Advances in Applied Microbiology*, 3(C):77–107, 1961. ISSN 00652164. doi: 10.1016/S0065-2164(08)70507-0.

[46] M Takeda, · H Matsuoka, · H Ban, · Y Ohashi, M Hikuma, and · J-I Koizumi. Biosynthesis of poly(3-hydroxybutyrate-Co-3-hydroxyvalerate) by a mutant of Sphaerotilus natans. Technical report, 1995.

[47] Emily Van den Berg. *Eat grow and repeat.* PhD thesis, TU Delft, 2021.

[48] Mun Hwan Choi, Jong Kook Rho, Ho-Joo Lee, Jae Jun Song, Sung Chul Yoon, and Sang Yeol Lee. First-Order Kinetics Analysis of Monomer Composition Dependent Polyhydroxyalkanoic Acid Degradation in Pseudomonas spp. 2003. doi: 10.1021/bm0257199. URL https://pubs.acs.org/sharingguidelines.

[49] Helmut Brandl, Richard A Gross, Robert W Lenz, Clinton Fuller', and R. Pseudomonas oleovorans as a Source of Poly(P-Hydroxyalkanoates) for Potential Applications as Biodegradable Polyesters. Technical Report 8, 1988. URL http://aem.asm.org/.

[50] A. M. Gumel, M. S.M. Annuar, and T. Heidelberg. Growth kinetics, effect of carbon substrate in biosynthesis of mcl-PHA by Pseudomonas putida Bet001. *Brazilian Journal of Microbiology*, 45(2):427–438, 4 2014. ISSN 16784405. doi: 10.1590/S1517-83822014000200009. URL www.sbmicrobiologia.org.br.

[51] M. Takeda, H. Matsuoka, H. Hamana, and M. Hikuma. Biosynthesis of poly-3-hydroxybutyrate by Sphaerotilus natans. *Applied Microbiology and Biotechnology*, 43(1):31–34, 1995. ISSN 14320614. doi: 10.1007/BF00170618. URL https://link.springer.com/article/10.1007/BF00170618.

[52] Nehal Thakor, Ujjval Trivedi, and K. C. Patel. Biosynthesis of medium chain length poly(3-hydroxyalkanoates) (mcl-PHAs) by Comamonas testosteroni during cultivation on vegetable oils. *Bioresource Technology*, 96(17):1843–1850, 11 2005. ISSN 09608524. doi: 10.1016/j.biortech.2005.01.030.

[53] Jun Xu, Baohua Guo, Zengmin Zhang, Qiong Wu, Quan Zhou, Jinchun Chen, Guoqiang Chen, and Guodong Li. A mathematical model for regulating monomer composition of the microbially synthesized polyhydroxyalkanoate copolymers. *Biotechnology and Bioengineering*, 90(7):821–829, 6 2005. ISSN 0006-3592. doi: 10.1002/bit.20487. URL http://doi.wiley.com/10.1002/bit.20487.

[54] Valeria Mezzolla, Oscar Fernando D'Urso, and Palmiro Poltronieri. Role of PhaC type I and type II enzymes during PHA biosynthesis. *Polymers*, 10(8), 8 2018. ISSN 20734360. doi: 10.3390/polym10080910. URL /pmc/articles/PMC6403647//pmc/articles/PMC6403647/?report=abstracthttps://www.ncbi.nlm.nih.gov/pmc/articles/PMC6403647/.

[55] Emmanouela Korkakaki, Mark C.M. van Loosdrecht, and Robbert Kleerebezem. Survival of the fastest: Selective removal of the side population for enhanced PHA production in a mixed substrate enrichment. *Bioresource Technology*, 216:1022–1029, 9 2016. ISSN 0960-8524. doi: 10.1016/J.BIORTECH.2016.05.125.

[56] • Rubber price monthly 2021 | Statista. URL https://www.statista.com/statistics/727582/price-of-rubber-per-pound/.

[57] Welcome to Zauba | Zauba. URL https://www.zauba.com/.

[58] Sayalee Joshi, Aide Robles, Samuel Aguiar, and Anca G. Delgado. The occurrence and ecology of microbial chain elongation of carboxylates in soils. *The ISME Journal 2021 15:7*, 15(7):1907–1918, 2 2021. ISSN 1751-7370. doi: 10.1038/s41396-021-00893-2. URL https://www.nature.com/articles/s41396-021-00893-2.

[59] D. K.Y. Solaiman, R D Ashby, and T A Foglia. Rapid and specific identification of medium-chain-length polyhydroxyalkanoate synthase gene by polymerase chain reaction. *Applied Microbiology and Biotechnology*, 53(6):690–694, 2000. ISSN 01757598. doi: 10.1007/s002530000332.

A Appendix

A.1 GC method and calibration

A.1.1 GC method

For the determination of the PHA content of the reactor, 15 mL of broth was taken from the reactor and combined with 3 drops of formaldehyde. This formaldehyde halts the biological processes in the cells. This sample was centrifuged for at least 10 minutes and up to 20 minutes at 4700 rpm. The actual time centrifuged depended on the consistency of the pellet. If the sample could not be immediately centrifuged, it was kept on ice until it could be centrifuged. This was never longer than 30 minutes. After centrifugation, the supernatant of the sample was discarded and the pellet was stored in the freezer at -18° C until further processing. To fully dry the samples, the samples were before processing sealed with parafilm with only a few holes in the film and stored in the -80° C for at least 10 minutes. Afterwards, they were freeze dried at -60° C and at a pressure of 0.050 mbar at least overnight or until dry. After freeze drying, the samples were immediately sealed to prevent extra water weight from the air. The sample was transferred from its original container to a glass container and was weighted. Next, 100 μL of the internal, 1.5 mL of H_2SO_4 and 1.5 mL dichloroethane were added to the sample. For the esterification reaction, the sample were heated to 100° C and kept at this temperature for 3 hours and were shaken every 30 minutes. After the 3 hours, the samples were brought back to room temperature before adding 3 mL of Milli-Q. The addition of Milli-Q releases the free acids from the organic phase in the water. The water phase and the organic phase were separated by centrifugation using the same settings as mentioned before. 1 mL of the organic phase was filtered and put into GC vials. The samples were run for 120 minutes in the GC and the PHA content was determined using the calibration lines.

A.1.2 GC calibration

The GC was calibrated using 1 internal standard and 3 PHA standards: Met-HB, Met-HH and Met-HO. The standards were added to glass vials in the quantities described in Table 9.

Table 9: Quantities added of each PHA standard and internal standard for the calibration of the GC.

PHA	Met-PHA (mg)	PHA (mmol)	IS (mg)
HB	1.758	0.0149	75.62
	4.542	0.0384	78.286
	9.776	0.0828	78.03
	17.236	0.1459	77.702
HH	1.12	0.0077	76.108
	4.124	0.0282	78.784
	8.738	0.0598	78.03
	15.458	0.1057	79.064
HO	0.93	0.0053	76.33
	2.54	0.0174	76.59
	4.58	0.0313	77.62
	11.17	0.0764	74.15

1.5 mL of H_2SO_4 and 1.5 mL dichloroethane were added to the glass vials. For the esterification reaction, the sample were heated to 100∘C and kept at this temperaturefor 3 hours and were shaken every 30 minutes. After the 3 hours, the samples were brought back to roomtemperature before adding 3 mL of Milli-Q. The addition of Milli-Q releases the free acids from the organic phase in the water. The water phase and the organic phase were separated by centrifugation using the same settings as mentioned before. 1 mL of the organic phase was filtered and put into GC vials. This resulted in the calibration lines seen in Figure 18.

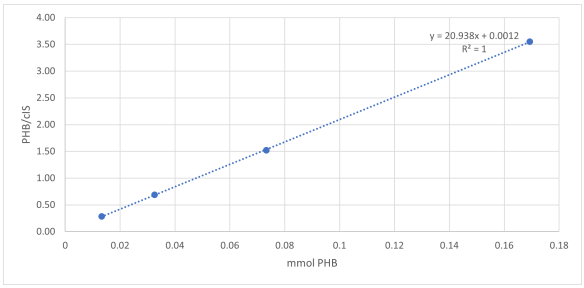

(a) Calibration HB for GC

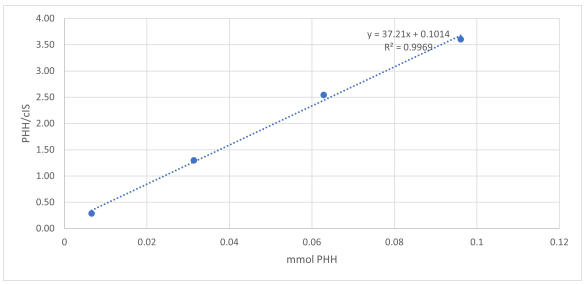

(b) Calibration HH for GC

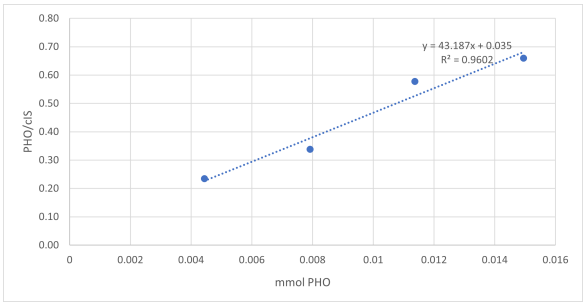

(c) Calibration HO for GC

Figure 18: Calibration lines of the GC for the three PHA standards.

A.2 HPLC calibration

Figure 19 shows the calibration lines for the HPLC for hexanoic acid and octanoic acid.

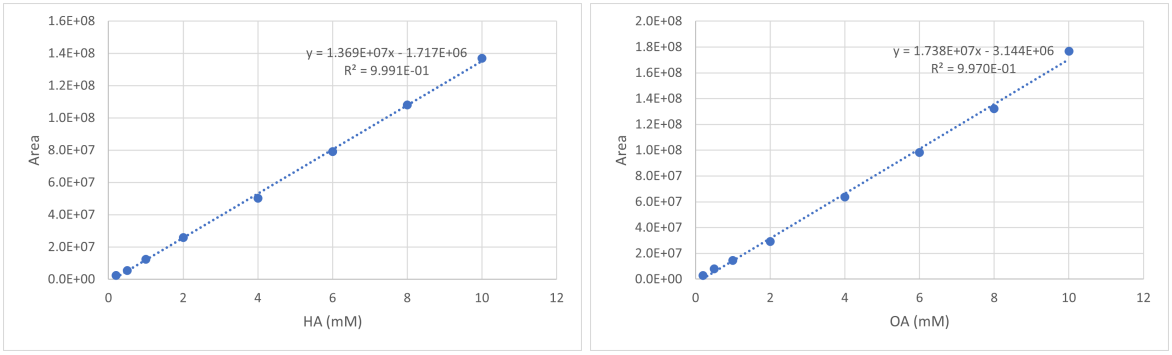

(a) Calibration hexanoic acid for HPLC

(b) Calibration octanoic acid for HPLC

Figure 19: Calibration lines of the HPLC for hexanoic acid and octanoic acid

A.3 Metabolic description

Fatty acids, like octanoic acid, can in theory be converted to both mcl-PHA and scl-PHA depending on how often the β-oxidation pathway runs. If only a partial completion of the β-oxidation pathway is done, the resulting PHA will be 3-hydroxyoctanoate. If the β-oxidation pathway is completed one time, the resulting PHA will be 3-hydroxyhexanoate. If the β-oxidation pathway is completed two times, the resulting PHA will be 3-hydroxybutyrate. This gives the following possible equations for a mcl-PHA producing organism on octanoic acid.

$$1.00\,\text{Octanoic acid} + 0.38\,\text{ATP} \longrightarrow 1.00\,\text{Octanoyl}-\text{CoA} \tag{19}$$

$$1.00\,\text{Octanoyl}-\text{CoA} \longrightarrow 0.25\,\text{NADH}_2 + 0.75\,\text{Hexanoyl}-\text{CoA} + 0.25\,\text{Acetyl}-\text{CoA} \tag{20}$$

$$1.00\,\text{Hexanoyl}-\text{CoA} \longrightarrow 0.33\,\text{NADH}_2 + 0.33\,\text{Acetyl}-\text{CoA} + 0.67\,\text{Butyryl}-\text{CoA} \tag{21}$$

$$1.00\,\text{Butyryl}-\text{CoA} \longrightarrow 0.50\,\text{NADH}_2 + 1.00\,\text{Acetyl}-\text{CoA} \tag{22}$$

$$2.16\,\text{ATP} + 1.27\,\text{Acetyl}-\text{CoA} + 0.20\,\text{NH}_3 \longrightarrow 0.43\,\text{NADH}_2 + 0.27\,\text{CO}_2 + 1.00\,\text{Biomass} \tag{23}$$

$$1.00\,\text{Acetyl}-\text{CoA} \longrightarrow 2.00\,\text{NADH}_2 + 1.00\,\text{CO}_2 \tag{24}$$

$$1.00\,\text{NADH}_2 + 0.50\,\text{O}_2 \longrightarrow 2.00\,\text{ATP} \tag{25}$$

$$1.00\,\text{Octanoyl}-\text{CoA} \longrightarrow 0.13\,\text{NADH}_2 + 1.00\,\text{3-hydroxyactoanoate} \tag{26}$$

$$1.00\,\text{Hexanoyl}-\text{CoA} \longrightarrow 0.17\,\text{NADH}_2 + 1.00\,\text{3-hydroxyhexanoate} \tag{27}$$

$$1.00\,\text{Butyryl}-\text{CoA} \longrightarrow 0.25\,\text{NADH}_2 + 1.00\,\text{3-hydroxybutanoate} \tag{28}$$

$$0.13\,\text{ATP} + 0.13\,\text{NADH}_2 + 1.00\,\text{3-hydroxyactoanoate} \longrightarrow 1.00\,\text{Octanoyl}-\text{CoA} \tag{29}$$

$$0.17\,\text{ATP} + 0.17\,\text{NADH}_2 + 1.00\,\text{3-hydroxyhexanoate} \longrightarrow 1.00\,\text{Hexanoyl}-\text{CoA} \tag{30}$$

$$0.25\,\text{ATP} + 0.25\,\text{NADH}_2 + 1.00\,\text{3-hydroxybutanoate} \longrightarrow 1.00\,\text{Butyryl}-\text{CoA} \tag{31}$$

The reactions of the model are represented by Figure 20, which can also be found in the introduction.

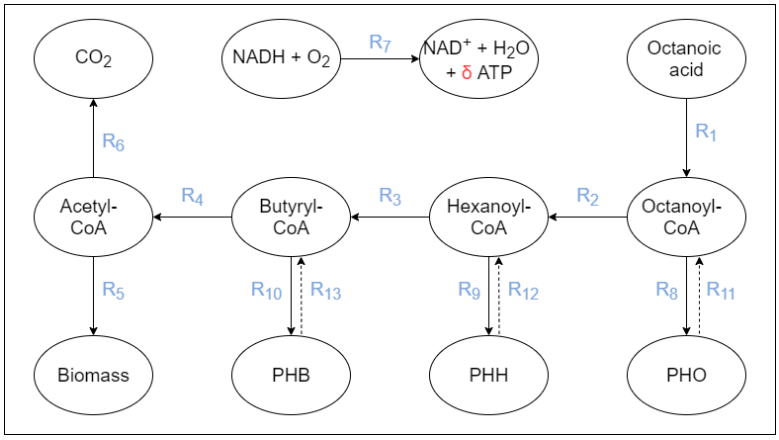

Figure 20: Overview of the considered reactions in the metabolic model. The degradation reactions are indicated with broken arrows.PHO = poly-hydroxy-octanoate, PHH = poly-hydroxy-hexanoate, PHB = poly-hydoxy-butyrate.

As described in the introduction, there are 5 phases for the metabolic model. The mathematical description for the determination of the variables which determine the yields is given by equation 32.

$$\begin{pmatrix} x_1 \\ x_2 \\ \vdots \\ x_M \end{pmatrix} = \begin{pmatrix} b_1 \\ b_2 \\ \vdots \\ b_M \end{pmatrix} \begin{pmatrix} A_{1,1} & A_{1,2} & \dots & A_{1,N} \\ A_{2,1} & A_{2,2} & \dots & A_{2,N} \\ \vdots & \vdots & \vdots & \vdots \\ A_{M,1} & A_{M,2} & \dots & A_{M,N} \end{pmatrix}^{-1} \tag{32}$$

The matrix A contains the conserved moieties of each reaction participating in each part. The conserved moieties are the rows of matrix A and the reactions are the columns of matrix A. The conserved moieties considered in this model are ATP, $NADH_2$, acetyl-CoA, butyryl-CoA, hexanoyl-CoA and octanoyl-CoA. The last row in the matrix A is always the bootstrap. The reactions vary per phase. The vector b contains the bootstrap reaction which ensures normalization of the reactions. The vector x contains the variables which will be used to calculate the yields.

The first phase, the growth in the feast phase, consists of 7 reactions. Those reactions are the uptake (equation 19), the production of hexanoyl-CoA (equation 20), the production of butyryl-CoA (equation 21), the production of acetyl-CoA (equation 22), the anabolism (equation 23), the catabolism (equation 24) and the oxidative phosphorylation (equation 25). The bootstrap in this equation is the uptake of octanoic acid (equation 19). Equation 33 shows the matrices involved in calculating the yields.

$$\begin{pmatrix} 1.00 \\ 1.00 \\ 1.00 \\ 1.00 \\ 6.45 \\ -0.17 \\ 8.46 \end{pmatrix} = \begin{pmatrix} -3 & 0 & 0 & 0 & -2 & 0 & 2 \\ 0 & 2 & 2 & 2 & 0 & 2 & -1 \\ 0 & 2 & 2 & 4 & -1 & -1 & 0 \\ 0 & 0 & 4 & -4 & 0 & 0 & 0 \\ 0 & 6 & -6 & 0 & 0 & 0 & 0 \\ 8 & -8 & 0 & 0 & 0 & 0 & 0 \\ 1 & 0 & 0 & 0 & 0 & 0 & 0 \end{pmatrix}^{-1} \begin{pmatrix} 0 \\ 0 \\ 0 \\ 0 \\ 0 \\ 0 \\ 0 \\ 1 \end{pmatrix} \tag{33}$$

The yields which will be calculated in this part are the yield of CO_2 over the biomass in the feast, yield of O_2 over the biomass in the feast, the yield of biomass over the substrate in the feast and the yield of the nitrogen source over the biomass. These yields are calculated by the general equation:

$$Y_{i,j} = \frac{\sum x_{phase} * i_{participating\ reactions}}{\sum x_{part} * j_{participating\ reactions}} \tag{34}$$

In words, the yield of compound i over compound j is the summation of the product of the vector with the variables for each phase by the compound i for the reactions participating in the phase over the the summation of the product of the vector with the variables for each phase by the compound j for the reactions participating in the phase.

The second phase, storage compound production in feast phase, consists of 7 reactions. Those reactions are the uptake (equation 19), the production of hexanoyl-CoA (equation 21), the production of butyryl-CoA (equation 21), the production of acetyl-CoA (equation 22), the catabolism (equation 24), the oxidative phosphorylation (equation 25) and the production of one of the storage compounds, either PHB (equation 28), PHH (equation 27) or PHO (equation 26). The bootstrap in this equation is the uptake of octanoic acid (equation 19). Equations 35, 36 and 37 show the matrices involved in calculating the yields..

Equation 35 shows the matrices for the production of PHB in the feast.

$$\begin{pmatrix} 1.00 \\ 1.00 \\ 1.00 \\ -1.28 \\ -1.11 \\ 1.50 \\ 2.28 \end{pmatrix} = \begin{pmatrix} -3 & 0 & 0 & 0 & 0 & 2 & 0 \\ 0 & 2 & 2 & 2 & 2 & -1 & 1 \\ 0 & 2 & 2 & 4 & -1 & 0 & 0 \\ 0 & 0 & 4 & -4 & 0 & 0 & -4 \\ 0 & 6 & -6 & 0 & 0 & 0 & 0 \\ 8 & -8 & 0 & 0 & 0 & 0 & 0 \\ 1 & 0 & 0 & 0 & 0 & 0 & 0 \end{pmatrix}^{-1} \begin{pmatrix} 0 \\ 0 \\ 0 \\ 0 \\ 0 \\ 0 \\ 0 \\ 1 \end{pmatrix} \tag{35}$$

Equation 36 shows the matrices for the production of PHH in the feast.

$$\begin{pmatrix} 1.00 \\ 1.00 \\ -0.37 \\ -0.37 \\ -0.20 \\ 1.50 \\ 1.37 \end{pmatrix} = \begin{pmatrix} -3 & 0 & 0 & 0 & 0 & 2 & 0 \\ 0 & 2 & 2 & 2 & 2 & -1 & 1 \\ 0 & 2 & 2 & 4 & -1 & 0 & 0 \\ 0 & 0 & 4 & -4 & 0 & 0 & 0 \\ 0 & 6 & -6 & 0 & 0 & 0 & -6 \\ 8 & -8 & 0 & 0 & 0 & 0 & 0 \\ 1 & 0 & 0 & 0 & 0 & 0 & 0 \end{pmatrix}^{-1} \begin{pmatrix} 0 \\ 0 \\ 0 \\ 0 \\ 0 \\ 0 \\ 0 \\ 1 \end{pmatrix} \tag{36}$$

Equation 37 shows the matrices for the production of PHO in the feast.

$$\begin{pmatrix} 1.00 \\ 0.02 \\ 0.02 \\ 0.023 \\ 0.19 \\ 1.50 \\ 0.98 \end{pmatrix} = \begin{pmatrix} -3 & 0 & 0 & 0 & 0 & 2 & 0 \\ 0 & 2 & 2 & 2 & 2 & -1 & 1 \\ 0 & 2 & 2 & 4 & -1 & 0 & 0 \\ 0 & 0 & 4 & -4 & 0 & 0 & 0 \\ 0 & 6 & -6 & 0 & 0 & 0 & 0 \\ 8 & -8 & 0 & 0 & 0 & 0 & -8 \\ 1 & 0 & 0 & 0 & 0 & 0 & 0 \end{pmatrix}^{-1} \begin{pmatrix} 0 \\ 0 \\ 0 \\ 0 \\ 0 \\ 0 \\ 1 \end{pmatrix} \tag{37}$$

The yields which will be calculated in the second phase are the yield of CO_2 over the PHA in the feast, yield of O_2 over the PHA in the feast and the yield of PHA over the substrate in the feast. For each storage compound, their respective matrices as described above will be used.

The third phase, the catabolism in the feast, consists of 6 reactions. Those reactions are the uptake (equation 19), the production of octanoyl-CoA (equation 20), the production of hexanoyl-CoA (equation 21), the production of butyryl-CoA (equation 22), the production of acetyl-CoA (equation 23), the catabolism (equation 24) and the oxidative phosphorylation (equation 25). The bootstrap in this equation is the uptake of octanoic acid (equation 19). In this reaction, ATP is not considered a conserved moiety.

$$\begin{pmatrix} 1.00 \\ 1.00 \\ 1.00 \\ 1.00 \\ 8 \\ 22 \end{pmatrix} = \begin{pmatrix} 0 & 2 & 2 & 2 & 2 & -1 \\ 0 & 2 & 2 & 4 & -1 & 0 \\ 0 & 0 & 4 & -4 & 0 & 0 \\ 0 & 6 & -6 & 0 & 0 & 0 \\ 8 & -8 & 0 & 0 & 0 & 0 \\ 1 & 0 & 0 & 0 & 0 & 0 \end{pmatrix}^{-1} \begin{pmatrix} 0 \\ 0 \\ 0 \\ 0 \\ 0 \\ 1 \end{pmatrix} \tag{38}$$

The yields which will be calculated in the third phase are the yield of CO_2 over the substrate in the feast, yield of O_2 over the substrate in the feast and the yield of ATP over the substrate in the feast.

The fourth phase, the growth during famine phase, consists of 7 reactions. Those reactions are the production of hexanoyl-CoA (equation 20), the production of butyryl-CoA (equation 21), the production of acetyl-CoA (equation 22), the anabolism (equation 23), the catabolism (equation 24), the oxidative phosphorylation (equation 25) and the degradation of one of the storage compounds, either PHB (equation 31), PHH (equation 30) or PHO (equation 29). The bootstrap in this equation is the degradation of one of the storage compounds (equation 31, 30 or 29).

Equation 39 shows the matrices for the degradation of PHB in the famine.

$$\begin{pmatrix} 0.00 \\ 0.00 \\ 1.00 \\ 2.67 \\ 0.61 \\ 3.39 \\ 1.00 \end{pmatrix} = \begin{pmatrix} 0 & 0 & 0 & -2.16 & 0 & 2 & -1 \\ 2 & 2 & 2 & 0.434 & 2 & -1 & -1 \\ 2 & 2 & 4 & -1.267 & -1 & 0 & 0 \\ 0 & 4 & -4 & 0 & 0 & 0 & 4 \\ 6 & -6 & 0 & 0 & 0 & 0 & 0 \\ -8 & 0 & 0 & 0 & 0 & 0 & 0 \\ 0 & 0 & 0 & 0 & 0 & 0 & 1 \end{pmatrix}^{-1} \begin{pmatrix} 0 \\ 0 \\ 0 \\ 0 \\ 0 \\ 0 \\ 1 \end{pmatrix} \tag{39}$$

Equation 40 shows the matrices for the degradation of PHH in the famine.

$$\begin{pmatrix} 0.00 \\ 1.00 \\ 1.00 \\ 4.56 \\ 0.22 \\ 5.42 \\ 1.00 \end{pmatrix} = \begin{pmatrix} 0 & 0 & 0 & -2.16 & 0 & 2 & -1 \\ 2 & 2 & 2 & 0.434 & 2 & -1 & -1 \\ 2 & 2 & 4 & -1.267 & -1 & 0 & 0 \\ 0 & 4 & -4 & 0 & 0 & 0 & 0 \\ 6 & -6 & 0 & 0 & 0 & 0 & 6 \\ -8 & 0 & 0 & 0 & 0 & 0 & 0 \\ 0 & 0 & 0 & 0 & 0 & 0 & 1 \end{pmatrix}^{-1} \begin{pmatrix} 0 \\ 0 \\ 0 \\ 0 \\ 0 \\ 0 \\ 1 \end{pmatrix} \tag{40}$$

Equation 41 shows the matrices for the degradation of PHO in the famine.

$$\begin{pmatrix} 1.00 \\ 1.00 \\ 1.00 \\ 6.45 \\ -0.17 \\ 7.46 \\ 1.00 \end{pmatrix} = \begin{pmatrix} 0 & 0 & 0 & -2.16 & 0 & 2 & -1 \\ 2 & 2 & 2 & 0.434 & 2 & -1 & -1 \\ 2 & 2 & 4 & -1.267 & -1 & 0 & 0 \\ 0 & 4 & -4 & 0 & 0 & 0 & 0 \\ 6 & -6 & 0 & 0 & 0 & 0 & 0 \\ -8 & 0 & 0 & 0 & 0 & 0 & 8 \\ 0 & 0 & 0 & 0 & 0 & 0 & 1 \end{pmatrix}^{-1} \begin{pmatrix} 0 \\ 0 \\ 0 \\ 0 \\ 0 \\ 0 \\ 1 \end{pmatrix} \tag{41}$$

The yields which will be calculated in the fourth phase are the yield of the nitrogen source over the biomass in the famine, the yield of CO_2 over the biomass in the famine, yield of O_2 over the substrate in the famine and the yield of biomass over the storage compounds in the famine. For each storage compound, their respective matrices as described above will be used.

The fifth and final part, the catabolism during the famine phase, consists of 6 reactions. Those reactions are the production of hexanoyl-CoA (equation 20), the production of butyryl-CoA (equation 21), the production of acetyl-CoA (equation 22), the catabolism (equation 24), the oxidative phosphorylation (equation 25) and the degradation of one of the storage compounds, either PHB (equation 31), PHH (equation 30) or PHO (equation 29). The bootstrap in this equation is the degradation of one of the storage compounds (equation 31, 30 or 29). ATP is not considered a conserved moiety in these reactions.

Equation 42 shows the matrices for the catabolism with the degradation of PHB in the famine.

$$\begin{pmatrix} 0.00 \\ 0.00 \\ 1.00 \\ 4.00 \\ 9.00 \\ 1.00 \end{pmatrix} = \begin{pmatrix} 2 & 2 & 2 & 2 & -1 & -1 \\ 2 & 2 & 4 & -1 & 0 & 0 \\ 0 & 4 & -4 & 0 & 0 & 4 \\ 6 & -6 & 0 & 0 & 0 & 0 \\ -8 & 0 & 0 & 0 & 0 & 0 \\ 0 & 0 & 0 & 0 & 0 & 1 \end{pmatrix}^{-1} \begin{pmatrix} 0 \\ 0 \\ 0 \\ 0 \\ 0 \\ 1 \end{pmatrix} \tag{42}$$

Equation 43 shows the matrices for the catabolism with the degradation of PHH in the famine.

$$\begin{pmatrix} 0.00 \\ 1.00 \\ 1.00 \\ 6.00 \\ 15.00 \\ 1.00 \end{pmatrix} = \begin{pmatrix} 2 & 2 & 2 & 2 & -1 & -1 \\ 2 & 2 & 4 & -1 & 0 & 0 \\ 0 & 4 & -4 & 0 & 0 & 0 \\ 6 & -6 & 0 & 0 & 0 & 6 \\ -8 & 0 & 0 & 0 & 0 & 0 \\ 0 & 0 & 0 & 0 & 0 & 1 \end{pmatrix}^{-1} \begin{pmatrix} 0 \\ 0 \\ 0 \\ 0 \\ 0 \\ 1 \end{pmatrix} \tag{43}$$

Equation 44 shows the matrices for the catabolism with the degradation of PHO in the famine.

$$\begin{pmatrix} 1.00 \\ 1.00 \\ 1.00 \\ 8.00 \\ 21.00 \\ 1.00 \end{pmatrix} = \begin{pmatrix} 2 & 2 & 2 & 2 & -1 & -1 \\ 2 & 2 & 4 & -1 & 0 & 0 \\ 0 & 4 & -4 & 0 & 0 & 0 \\ 6 & -6 & 0 & 0 & 0 & 0 \\ -8 & 0 & 0 & 0 & 0 & 8 \\ 0 & 0 & 0 & 0 & 0 & 1 \end{pmatrix}^{-1} \begin{pmatrix} 0 \\ 0 \\ 0 \\ 0 \\ 0 \\ 1 \end{pmatrix} \tag{44}$$

The yields which will be calculated in the fifth phase are the yield of CO_2 over the storage compound in the famine, yield of O_2 over the storage compound in the famine and the yield of ATP over the storage compounds in the famine. For each storage compound, their respective matrices as described above will be used.

A.4 Kinetic model

The kinetic model is based on the Herbert-Pirt kinetics and consists of the following parts:

- Substrate uptake for PHA
- The maintenance on external substrate
- Growth on external substrate
- Production of the PHA's
- Consumption of the PHA's
- Maintenance on the internal substrates, the PHA's
- Growth on PHA

The substrate uptake for the various PHA's is given by equation 45 to 48. The total substrate uptake is calculated by adding the individual substrate uptakes multiplied by the ratio of the specific PHA by the total PHA.

$$\text{Substrate uptake PHB: } q_{s,PHB} = q_s^{max} * \frac{[S]}{K_s + [S]} * \left(1 - \left(\frac{\frac{[PHB]}{X}}{f_{PHB}^{max}}\right)^{\alpha}\right) \tag{45}$$

$$\text{Substrate uptake PHH: } q_{s,PHH} = q_s^{max} * \frac{[S]}{K_s + [S]} * \left(1 - \left(\frac{\frac{[PHH]}{X}}{f_{PHH}^{max}}\right)^{\alpha}\right) \tag{46}$$

$$\text{Substrate uptake PHO: } q_{s,PHO} = q_s^{max} * \frac{[S]}{K_s + [S]} * \left(1 - \left(\frac{\frac{[PHO]}{X}}{f_{PHO}^{max}}\right)^{\alpha}\right) \tag{47}$$

$$\text{Substrate uptake: } q_s = \frac{f_{PHB}}{f_{PHA}} * q_{s,PHB} + \frac{f_{PHH}}{f_{PHA}} * q_{s,PHH} + \frac{f_{PHO}}{f_{PHA}} * q_{s,PHA} \tag{48}$$

The maintenance on external substrate is given by equation 49.

$$\text{Maintenance on external substrate: } m_s = \frac{m_{ATP}}{Y_{ATP/S}^{feast}} \tag{49}$$

The growth on external substrate is given by equation 50.

$$\text{Growth on external substrate: } q_{x/s} = q_x^{max} * \frac{[NH_4^+]}{K_N + [NH_4^+]} * \frac{[S]}{K_s + [S]} \tag{50}$$

The production of the various PHA's is given by the equations 51 to 53.

$$\text{PHB production: } q_{PHB}^{prod} = Y_{PHB/s}^{feast} * \left(q_s + \frac{q_{x/s}}{Y_{x/s}^{feast}} + m_s\right) \tag{51}$$

$$\text{PHH production: } q_{PHH}^{prod} = Y_{PHH/s}^{feast} * \left(q_s + \frac{q_{x/s}}{Y_{x/s}^{feast}} + m_s\right) \tag{52}$$

$$\text{PHO production: } q_{PHO}^{prod} = Y_{PHO/s}^{feast} * \left(q_s + \frac{q_{x/s}}{Y_{x/s}^{feast}} + m_s\right) \tag{53}$$

The consumption of the various PHA's is given by the equations 54 to 56.

$$\text{PHB consumption: } q_{PHB}^{con} = k_{PHB} * \left(\frac{[PHB]}{X}\right)^{2/3} * \frac{[NH_4^+]}{K_N + [NH_4^+]} * \left(1 - \frac{[S]}{K_s + [S]}\right) \tag{54}$$

$$\text{PHH consumption: } q_{PHH}^{con} = k_{PHH} * \left(\frac{[PHH]}{X}\right)^{2/3} * \frac{[NH_4^+]}{K_N + [NH_4^+]} * \left(1 - \frac{[S]}{K_s + [S]}\right) \tag{55}$$

$$\text{PHO consumption: } q_{PHO}^{con} = k_{PHO} * \left(\frac{[PHO]}{X}\right)^{2/3} * \frac{[NH_4^+]}{K_N + [NH_4^+]} * \left(1 - \frac{[S]}{K_s + [S]}\right) \tag{56}$$

The maintenance on the individual external substrates is given by equation 57 to 59.

$$\text{Maintenance on PHB: } m_{PHB} = m_{ATP} * Y_{X/PHB}^{feast} \tag{57}$$

$$\text{Maintenance on PHH: } m_{PHH} = m_{ATP} * Y_{X/PHH}^{feast} \tag{58}$$

$$\text{Maintenance on PHO: } m_{PHO} = m_{ATP} * Y_{X/PHO}^{feast} \tag{59}$$

The growth on the individual PHA's is given by equations 60 to 62, with the overall growth as seen in equation 63 calculated by adding the growth rates multiplied by the ratio of the specific PHA over the total PHA.

$$\text{Growth on PHB: } q_{X/PHB} = Y_{X/PHB}^{famine} * (q_{PHB}^{con} + m_{PHB}) \tag{60}$$

$$\text{Growth on PHH: } q_{X/PHH} = Y_{X/PHH}^{famine} * (q_{PHH}^{con} + m_{PHH}) \tag{61}$$

$$\text{Growth on PHO: } q_{X/PHO} = Y_{X/PHO}^{famine} * (q_{PHO}^{con} + m_{PHO}) \tag{62}$$

$$\text{Growth on PHA: } q_{X/PHA} = \frac{f_{PHB}}{f_{PHA}} * q_{X/PHB} + \frac{f_{PHH}}{f_{PHA}} * q_{X/PHH} + \frac{f_{PHO}}{f_{PHA}} * q_{X/PHO} \tag{63}$$

A.5 Evolution feast times

Figure 21 shows the evolution of the end of feast times during enrichment 1. There is a clear decline in the time needed for the feast.

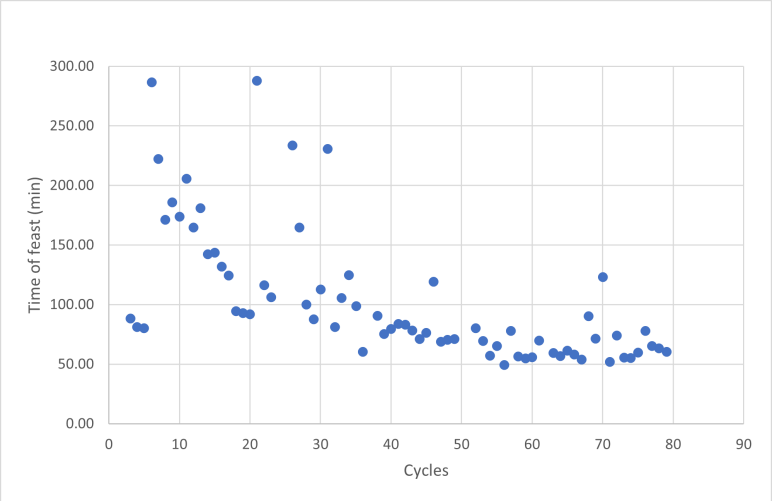

Figure 21: Evolution of the end of feast times during enrichment 1.

Figure 22 shows the evolution of the end of feast times during enrichment 2. The end of the feast time was relatively stable during the second enrichment except the cycles after a computer crash, which caused the organisms to be starved for one day.

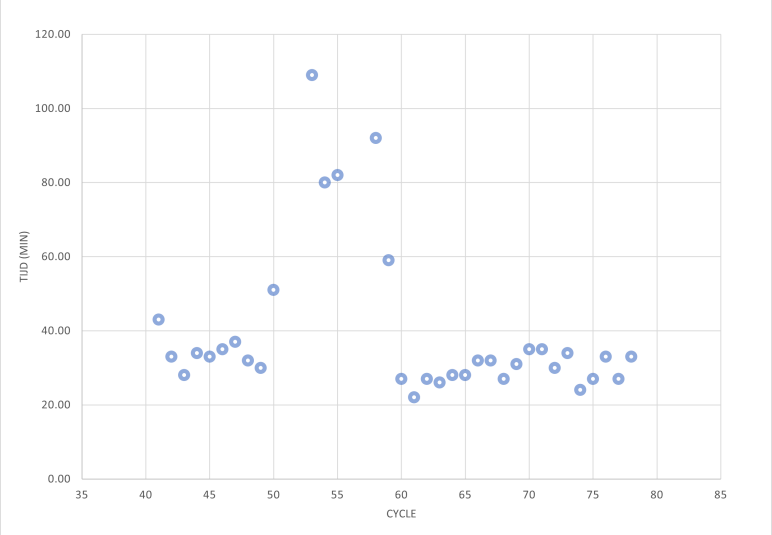

Figure 22: Evolution of the end of feast times during enrichment 2.

A.6 Original cycle analysis and accumulation of enrichment 2

The evolution of the most important compounds and the PHA content can be seen in Figure 23.

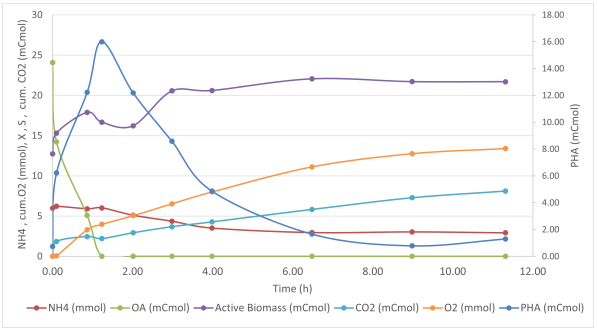

(a) Evolution of compounds during the cycle of the original second enrichment

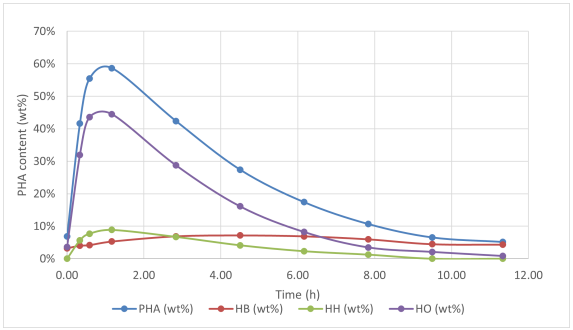

(b) Evolution of the PHA content during the cycle of the original second enrichment

Figure 23: Evolution of the PHA content and the important compounds during the cycle of the original second enrichment

During the cycle analysis, the maximum concentration of PHA was 16.95 mCmol. This corresponds with a weight percentage of 48 wt% PHO, with a total PHA yield of 62 wt%. PHB and PHH had weight percentages of 5 wt% and 8 wt% at their peaks respectively. This is the highest obtained weight percentage of mcl-PHA during the enrichment. During the cycle analysis of this enrichment, the biomass remained relatively constant during the famine. This is a notable improvement compared to the first cycle analysis. The substrate was consumed after 0.87 hours. During the cycle, the ammonia was not depleted. Only 9% of the ammonia was used during the feast and the other 91% was consumed during the famine. However, this was likely due to a measuring error of the first sample since the second sample had a higher ammonium content despite the second sample being taken 37 minutes after the nutrient addition while the first sample was taken 17 minutes after nutrient addition. The ratio of oxygen consumed in the feast to oxygen consumed in the famine was equal to 0.118. Neither the carbon nor the electron balance for the data closed, with a carbon balance off by 26% and the electron balance off by 38%. This is likely due to the assumed ash content of the biomass.

The model for this cycle analysis can be found in Appendix A.9.

Figure 24 shows the evolution of the PHA content during the original accumulation of the second enrichment.

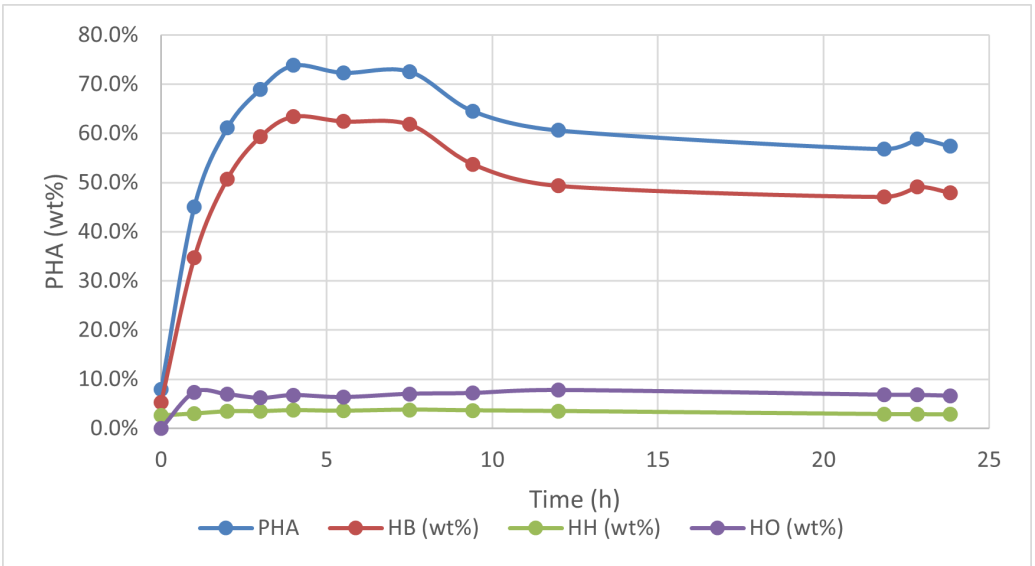

Figure 24: PHA content during the original accumulation of the second enrichment

As can be seen, the PHO content is significantly lower than the ones observed during the second enrichment. On the other hand, the PHB content is much higher. This is likely due to system failure in the weeks leading up to the accumulation.

A.7 Description and comparison of oxygen profiles

For the oxygen profiles, the end of feast was determined using the acid/base profiles. It should be noted that not all samples were taken at the optimal moment and should therefore be considered indicative and not absolute.

The gas profiles of enrichment 1 can be seen in Figure 25.

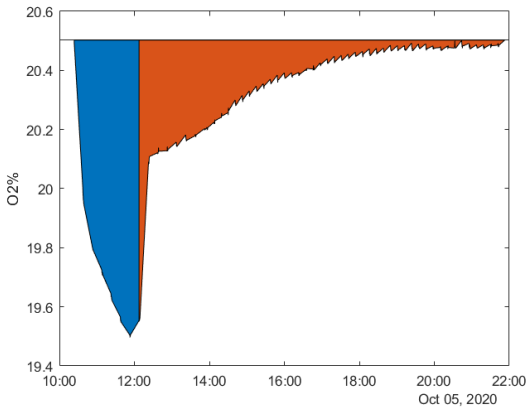

(a) Gas profile begin enrichment 1. In blue, the feast is shown and in orange, the famine is shown. The end of feast was at 12:07 (1h43 after C-addition), with an oxygen consumption of 49% in the feast.

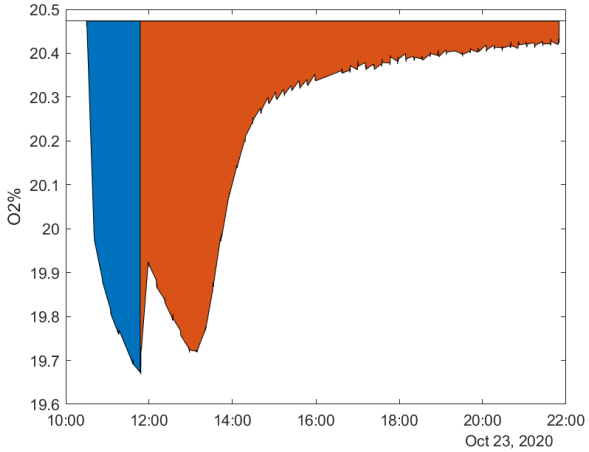

(b) Gas profile end of enrichment 1. In blue, the feast is shown and in orange, the famine is shown. The end of feast was at 11:46 (1h32 after C-addition), with an oxygen consumption of 26% in the feast.

Figure 25: Evolution of the gas profiles during the first enrichment.

As can be seen, over the course of the enrichment a camel-like profile is obtained. In this first enrichment, this corresponds with a higher PHO and PHH content. At the beginning of the enrichment, the PHO content was 1 wt%, the PHH content was 1 wt% and the PHB content was equal to 34 wt%, for a total PHA content of 34 wt%. At the end of the enrichment, the PHO content was 28 wt%, the PHH content was 8 wt% and the PHB content was 10 wt%, for a total PHA content of 46 wt%. On top of that, the ratio of oygen consumed in the feast over oxygen consumed in the famine is lowered through out the enrichment: at the beginning, 49% of oxygen is consumed in the feast and at the end 26% of oxygen is consumed in the feast. The end of feast remained stable throughout this enrichment, at around 1h10 after adding carbon.

Two gas profiles from during the second enrichment can be seen in Figure 26.

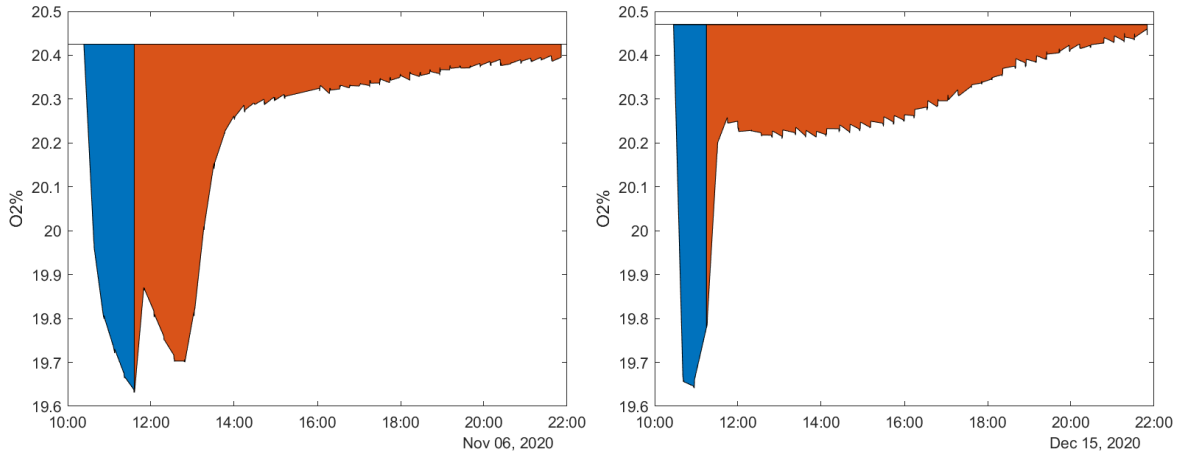

(a) Gas profile begin enrichment 2. In blue, the feast is shown and in orange, the famine is shown. The end of feast was at 11:35 (1h12 after C-addition), with an oxygen consumption of 27% in the feast.

(b) Gas profile end of enrichment 2. In blue, the feast is shown and in orange, the famine is shown. The end of feast was at 11:08 (0h47 after C-addition), with an oxygen consumption of 23% in the feast.

Figure 26: Evolution of the gas profiles during the second enrichment.

During the second enrichment, the characteristic camel-like profile which indicated high mcl-PHA content was slowly replaced by a very thin oxygen peak followed by a wave-like profile in the famine. At the beginning of the second enrichment, the PHO content was 17 wt%, the PHH content was 6 wt% and the PHB content was equal to 10 wt%, for a total PHA content of 33 wt%. At the end of the second enrichment the PHO content was 41 wt%, the PHH content was 7 wt% and the PHB content was 4 wt%, for a total PHA content of 52 wt%. The oxygen consumed in the feast was decreased even further from the first enrichment, with 27% at the beginning of the second enrichment and 23% at the end of the second enrichment. The end of feast time also decreased, from 1h15 minutes since the addition of carbon to 47 minutes since the addition of carbon.

Figure 27 shows the evolution of the gas profile of the third enrichment.

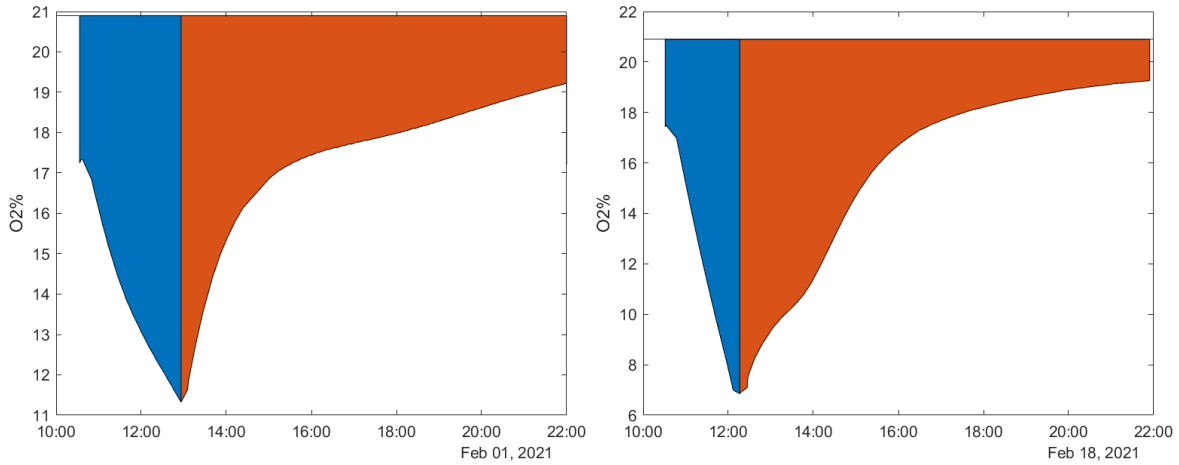

(a) Gas profile begin enrichment 3. In blue, the feast is shown and in orange, the famine is shown. The end of feast was at 12:56 (2h23 after C-addition), with an oxygen consumption of 43% in the feast.

(b) Gas profile mid enrichment 3. In blue, the feast is shown and in orange, the famine is shown. The end of feast was at 12:16 (1h45 after C-addition), with an oxygen consumption of 28% in the feast.

Figure 27: Evolution of the gas profiles during the third enrichment.

During the third enrichment, the community slowly adapted to the lowered oxygen flow rate. At the 10th cycle of the third enrichment, the PHO content was 20 wt%, the PHH content was 7 wt% and the PHB content was 34%, for a total PHA content of 62 wt%. At the 44th cycle of the third enrichment, the PHO content was 26 wt%, the PHH content was 7 wt% and the PHB content was 17 wt%, for a total PHA content of 49 wt%.

This was not the end of the enrichment, but later cycles had struggles with the data of the MS and therefore presented a distorted view of the cycle. The oxygen consumption in the feast decreased during this enrichment, from 43% at the beginning to 28% at the 44th cycle. This is similar to the oxygen consumption in the feast from the second enrichment, despite the lower mcl-PHA content. However, the ratio of mcl-PHA over total PHA content is similar at the end of the second enrichment to the middle of the third enrichment. The decrease in oxygen consumption in the feast does indicate that perhaps a longer enrichment or a more optimized oxygen gas flow could have resulted in higher mcl-PHA content. Similarly to the first and second enrichment, the end of feast became faster during the enrichment but due to the low gas flow rate, it is longer than the first or second enrichment.

Figure 16 shows a representative gas profile of the fourth enrichment. Since the fourth enrichment only ran for 26 cycles, no evolution was shown.

Figure 28 shows the consumption of the oxygen in the feast over the famine plotted against the mcl-PHA content over PHA content for enrichments with octanoic acid and hexanoic acid.

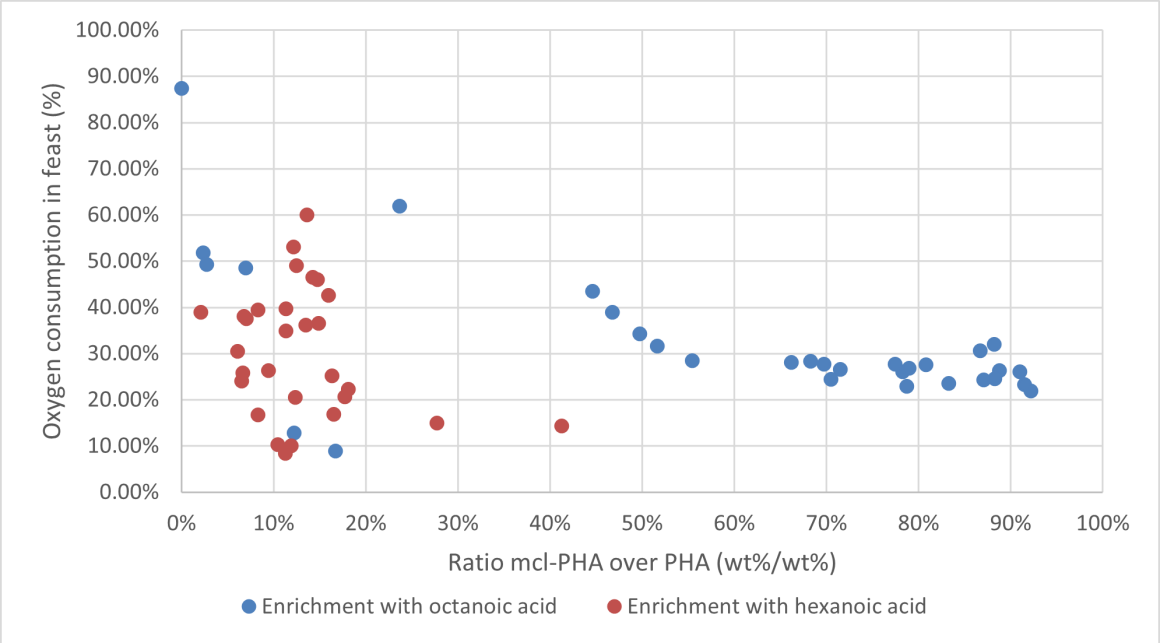

Figure 28: Oxygen consumption in the feast over oxygen consumption in the famine plotted against the mcl-PHA production over PHA production for enrichments with octanoic acid and hexanoic acid.

While the enrichments with octanoic acid show a clear trend, with low oxygen ratio's indicating high mcl-PHA content, the enrichments with hexanoic acid do not show such a trend. This could be due to the low mcl-PHA content, making it harder to distinguish the trends. For a more thorough understanding of the enrichments with hexanoic acid, please refer to [47].

Similar to Figure 17 and 28, Figure 29 shows the oxygen consumption in the feast over the total mcl-PHA production. For octanoic acid, this is the sum of the PHH and the PHO content in wt%. For hexanoic acid, this is solely the PHH content.

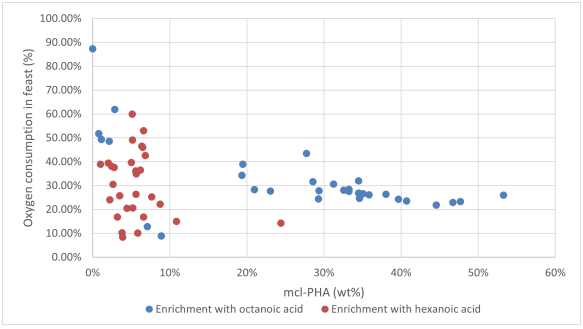

(a) Oxygen consumption in the feast over total oxygen consumption in the cycle plotted against the mcl-PHA production for the enrichments with octanoic acid and hexanoic acid.

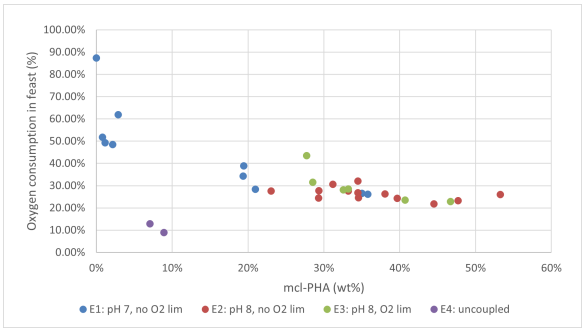

(b) Oxygen consumption in the feast over total oxygen consumption in the cycle plotted against the mcl-PHA production for each enrichment with octanoic acid.

Figure 29: Oxygen consumption in the feast over total oxygen consumption in the cycle plotted against the mcl-PHA production for the enrichments with octanoic acid and hexanoic acid.

A.8 Oxygen consumption rates

A.8.1 Cycles

Figure 30 shows the oxygen consumption rate during the cycle analysis of the first enrichment.

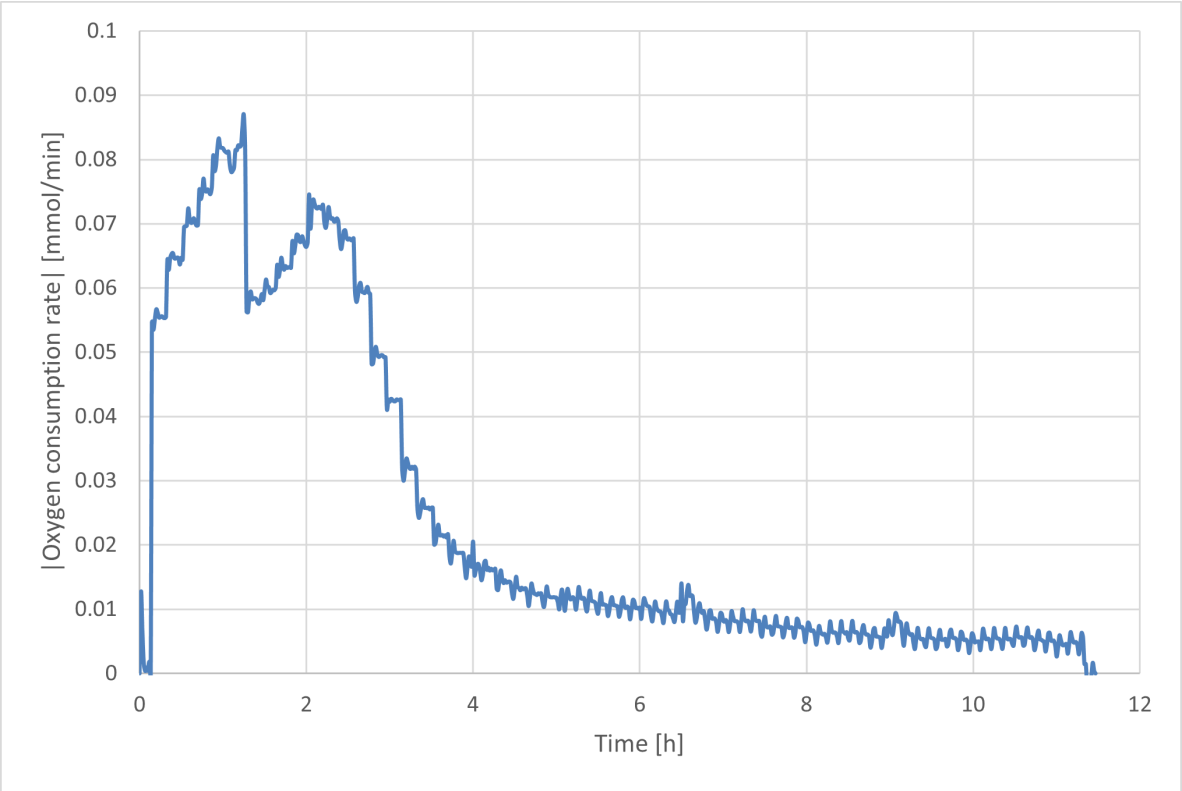

Figure 30: Oxygen consumption during the cycle analysis enrichment 1

As can be seen, 1 hour after the addition of the carbon source, the oxygen consumption rates drops before climbing up again for another hour. This camel-like profile can also be seen in the oxygen profile during the enrichment. After around 4 hours, the oxygen consumption rate declines until reaching almost 0 mmol/min at the end of the cycle.

Figure 31 and 32 show the cycle analysis' during the second enrichment.

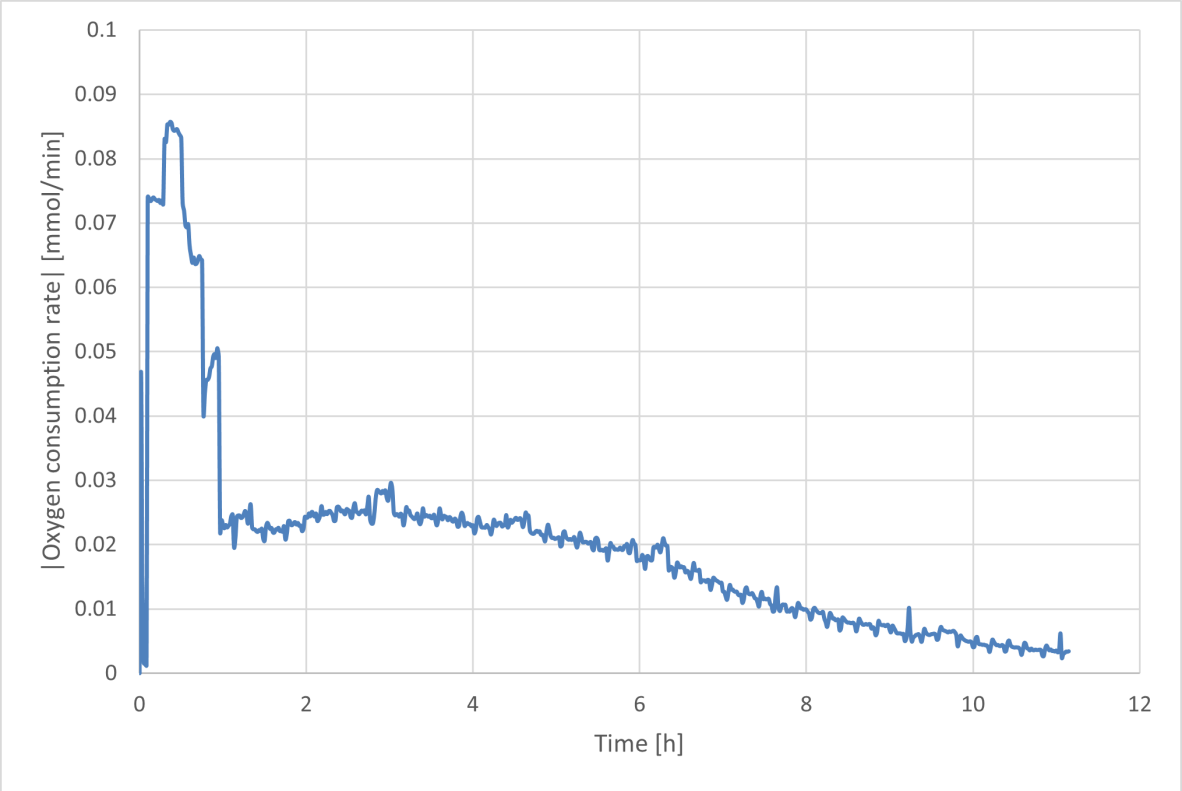

Figure 31: Oxygen consumption during the original cycle analysis enrichment 2

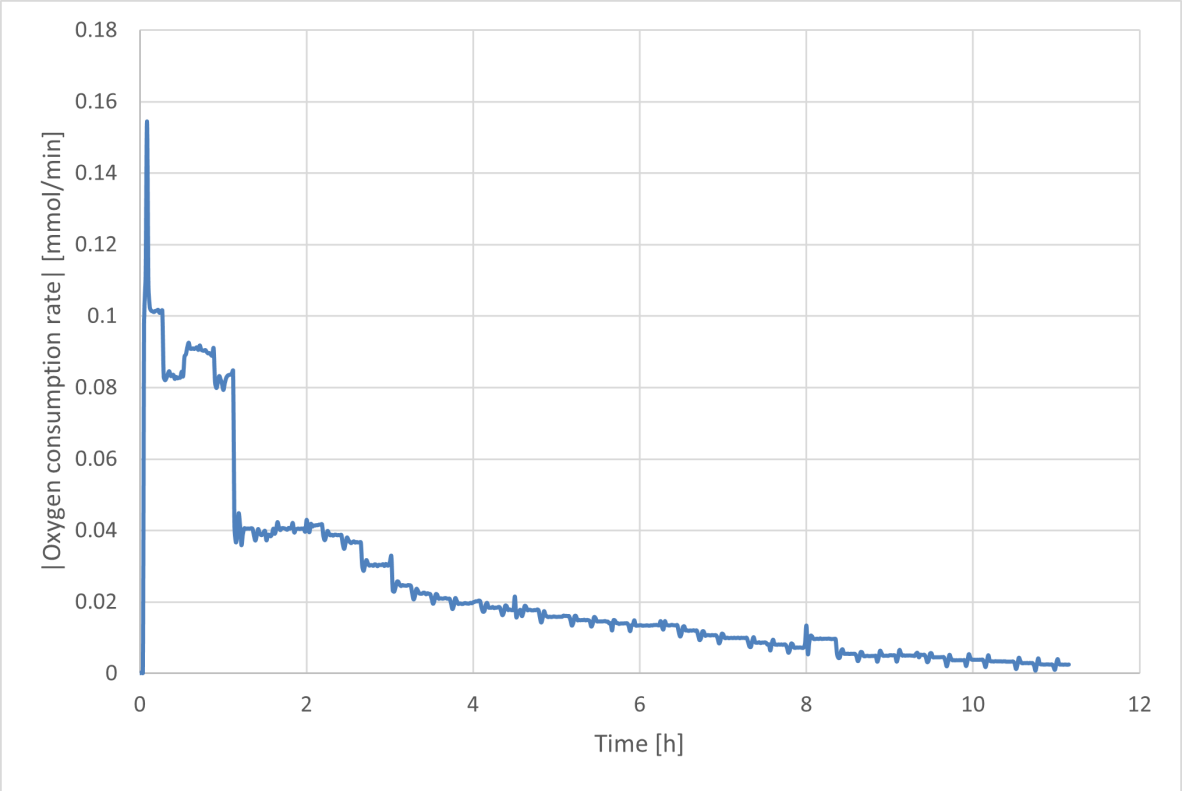

Figure 32: Oxygen consumption during the re-done cycle analysis enrichment 2

The profiles of the second enrichment are similar to one another, which is a good thing. However, the wave in the re-done cycle analysis is higher but shorter. After 3 hours, the decline in the oxygen consumption rate becomes

more more similar to a linear function than a second degree polynomial, which is not the case in the original cycle analysis. In the original cycle analysis, it takes around 6 hours for the second degree polynomial-like shape to turn into a linear function.

A.8.2 Accumulations

Figure 33 shows the oxygen consumption rate during the accumulation of the first enrichment.

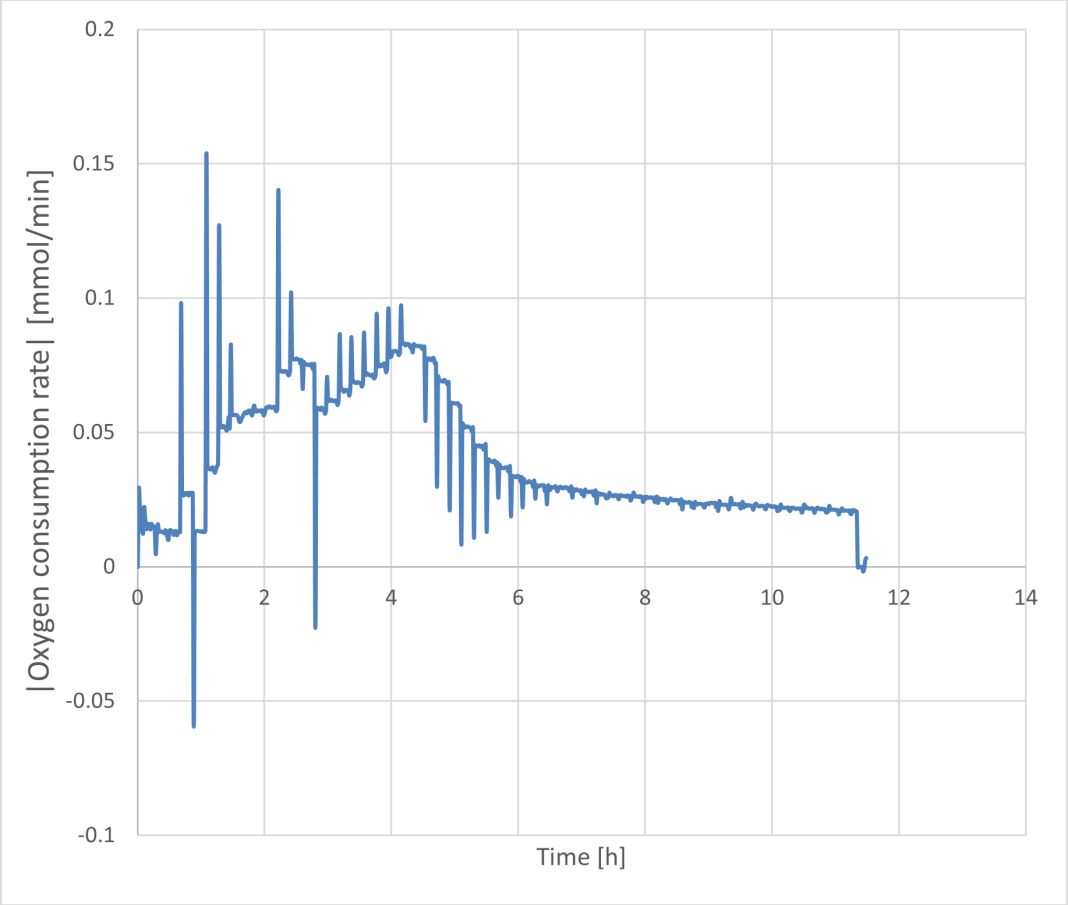

Figure 33: Oxygen consumption during the accumulation enrichment 1

As can be seen in the figure, there are many outliers in this profile. This is an effect of the assumed in-flow of the gas. The general shape of the figure is a peak at around 4 hours, with after 4 hours a sharp decline in the oxygen consumption rate and a stable oxyhen consumption after about 6 hours. During the accumulation, the oxygen consumption rate does not reach 0 mmol/min.

Figure 34 shows the oxygen consumption rate during the re-done accumulation with octanoic acid for the second enrichment.

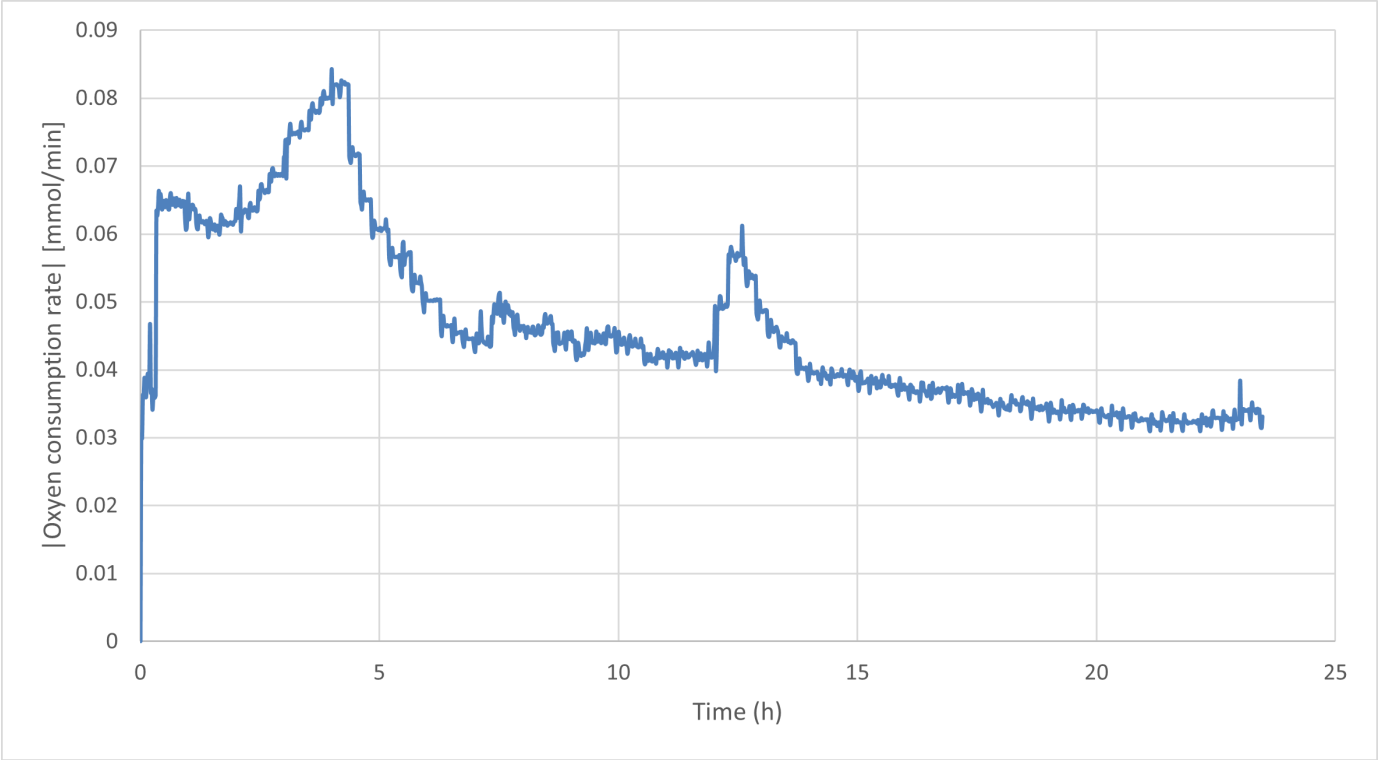

Figure 34: Oxygen consumption during the re-done accumulation enrichment 2 with octanoic acid

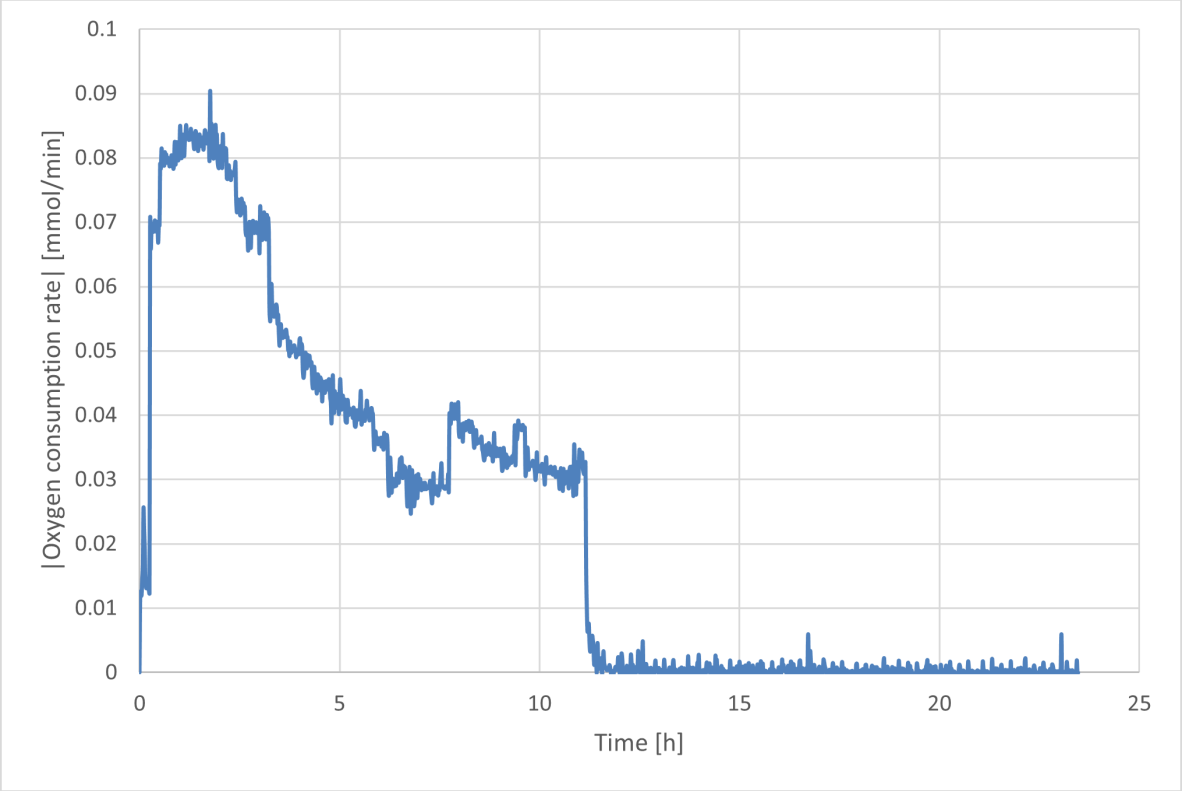

Figure 35: Oxygen consumption during the accumulation enrichment 2 with hexanoic acid

The accumulations with octanoic acid and hexanoic acid do not resemble each other. For the accumulation with hexanoic acid, a peak is observed in the first 3 hours, after which the oxygen consumption rate drops drastically. After 11 hours, the oxygen consumption rates stays close to 0 mmol/min. On the other hand, the

oxygen consumption rate for the accumulation with octanoic acid is high during the first 4.5 hours and then drops. It does not reach 0 mmol/min during the whole accumulation.

A.9 Model

The overview of the parameters of the models can be seen in Figure A.6.

Table 10: Overview of all relevant parameters for the models for each cycle analysis.

Variable	Unit|	Enrichment 1	Enrichment 2a	Enrichment 2b
q_{PHA}^{max}	[Cmmol/Cmmol/h]	1.70	3.40	2.00
p		1.50	1.20	1.25
q_S^{max}	[Cmmol/Cmmol/h]	-2.30	-1.50	-2.50
μ^{max}	[Cmmol/Cmmol/h]	0.59	0.40	0.09
K_S	[mCmol/L]	0.30	0.30	0.30
m_{ATP}	[mol/Cmol/h]	0.16	0.15	0.09
m_S		-0.03	-0.03	-0.02
f_{PHO}^{max}	[Cmol/Cmol]	10.20	16.81	12.47
f_{PHH}^{max}	[Cmol/Cmol]	1.42	2.51	1.98
f_{PHB}^{max}	[Cmol/Cmol]	1.70	1.35	2.27
f_{PHA}^{max}	[Cmol/Cmol]	7.26	13.30	8.54
K_{NH4+}	[mmol/L]	0.00	0.00	0.00
k	$[(Cmol/Cmol)^{1/3}/h]$	-0.45	-0.19	-0.15
n		0.60	1.10	1.00

A.9.1 Enrichment 1

Figure 36 shows the model for the cycle analysis of the first enrichment.

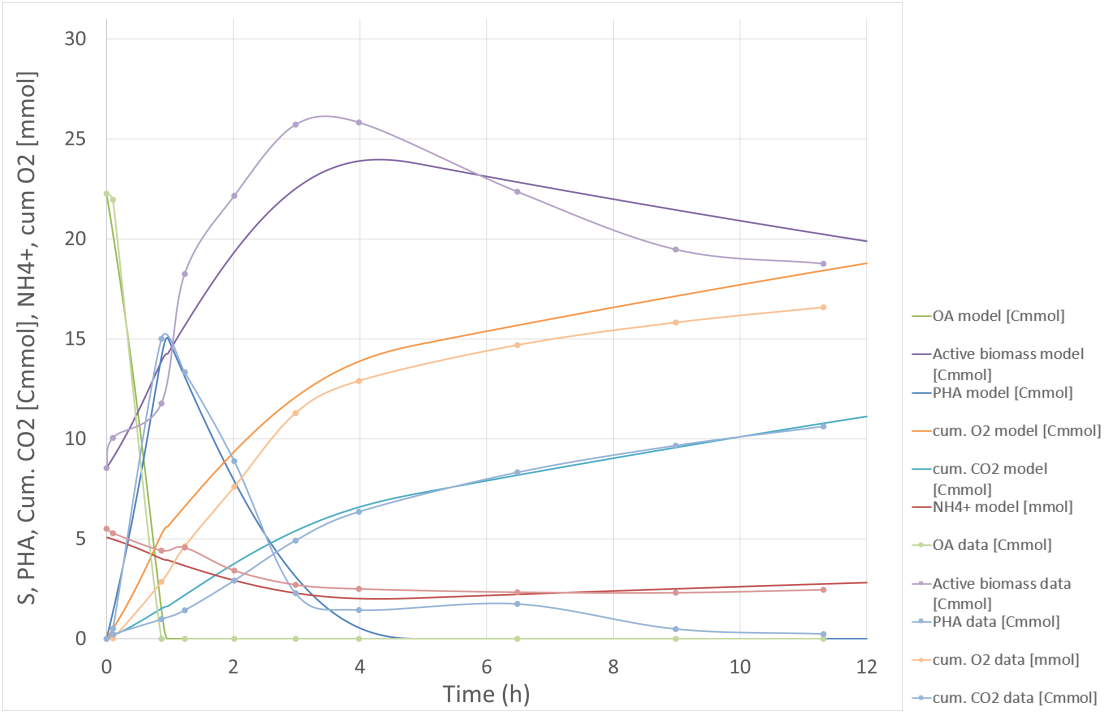

(a) Cycle model (b) Legend

Figure 36: Model for the cycle of the first enrichment

All compounds except for the biomass fit well to the model.

A.9.2 Enrichment 2

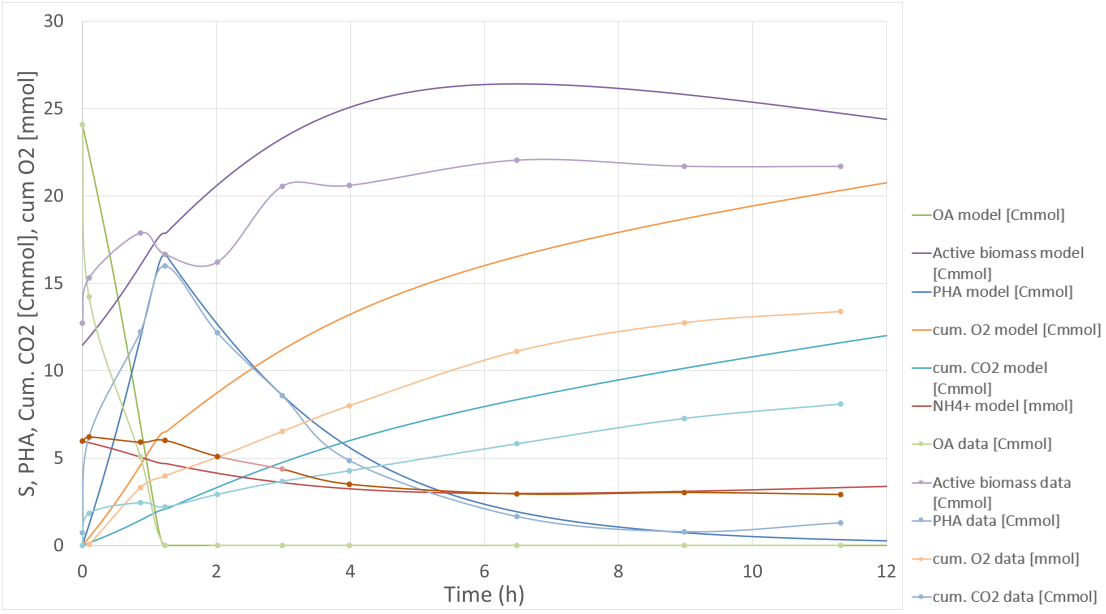

(a) Cycle model (b) Legend

Figure 37: Model for the cycle of the second enrichment

The model does not fit properly to the data set for the biomass, the consumed oxygen and the produced CO_2. However, the model does fit the data for the octanoic acid, the PHA and the ammonia. Since the ammonia directly has an influence on the biomass, the fact that the ammonia fits but the biomass does not indicates that there is an issue met the biomass. This is most likely due to the fact that an estimate was made about the ash content and the TSS content of the sample. That the biomass does not fit is also reflected in the balances for the data: the carbon is 26.8% off and the electron balance is 38.8% off. The fact that the electron balance is so far off could also indicate that the oxygen is too little. Unfortunately, both the data set of the gas and the biomass have their own issues. The biomass data is obtained by taking the pellet out of its container, measuring the pellet and then make an assumption of the TSS content and the ash content based on previously obtained TGA data. This has two weak points: it is first of all possible that some of the biomass was discarded and second of all, it is possible that there were errors in the measured biomass due to the fact that the measured quantities were very small. For the gas data, the inflow of the gas was only measured once every hour. This could lead to a skewed perception of the gas data.

The re-done cycle analysis can be seen in Figure 38.

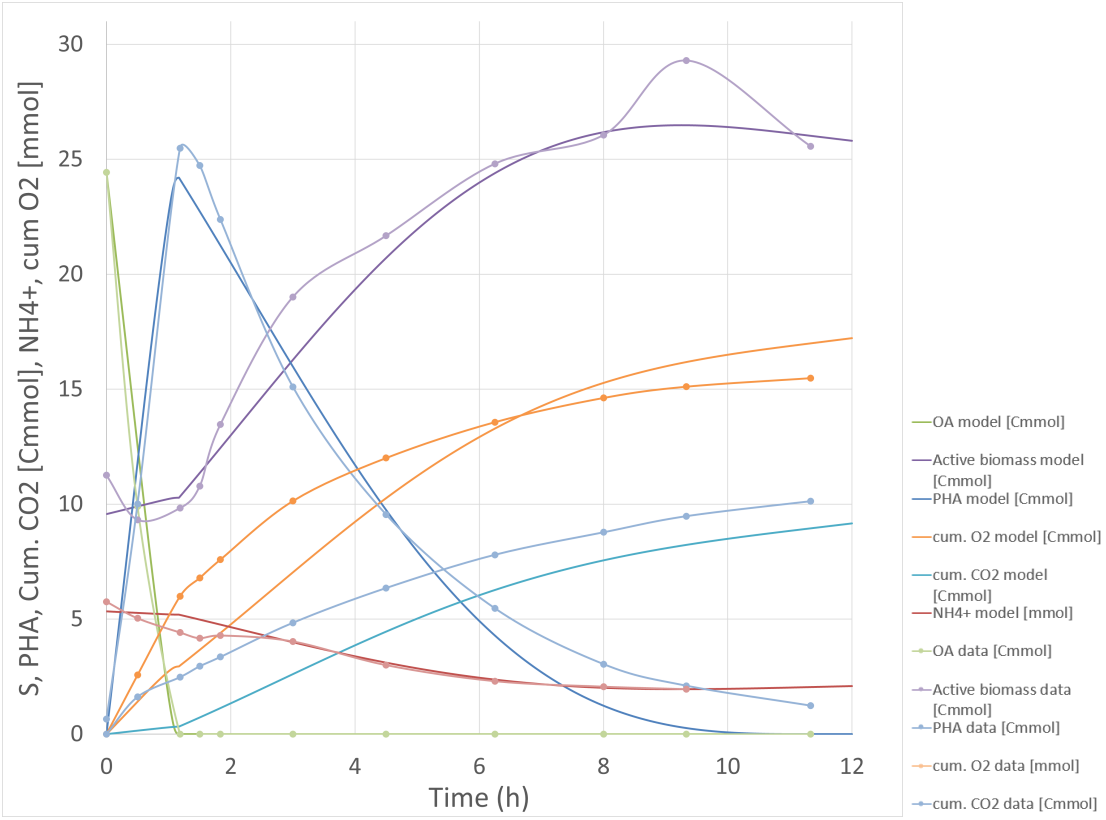

(a) Cycle model (b) Legend

Figure 38: Model for the cycle of the second enrichment

This model fits the data much better for all compounds. Despite the fact that the oxygen and CO_2 still does not fit perfectly, the biomass, the ammonia, the PHA and the octanoic acid fit quite well. The balances for this data set are also less off than the one for the original cycle analysis of the second enrichment: the carbon balance is -2.45% off and the electron balance is 9.5% off.